



DIPARTIMENTO SCIENZE DELLA VITA

**DOTTORATO DI RICERCA IN SCIENZE DELLA VITA  
LIFE SCIENCES**

CICLO XXXVI

COORDINATRICE Prof.ssa Simona Maccherini

Development of murine B cell platform for the isolation and characterization of mAbs  
against gonococcal antigens

SETTORE SCIENTIFICO-DISCIPLINARE: BIO/11

TUTOR: Prof.ssa Cosima Baldari

DOTTORANDA: Dr.ssa Francesca Papi

TUTOR aziendale: Dr.ssa Elisabetta Frigimelica  
(GSK, Siena)

A.A. 2022-2023

# Index

## Contents

ABSTRACT .....	3
1 INTRODUCTION: .....	4
1.1 <i>Neisseria gonorrhoeae</i> multi-drug resistance and public health threat: disease and epidemiology .....	4
1.2 Ng growth and metabolism and genetics.....	5
1.3 Pathogenesis and infection dynamics: colonization, invasion, and immune evasion.....	6
1.4 Colonization determinants .....	9
1.5 Opacity (Opa) proteins: an important family of adhesins and invasins .....	12
1.6 Single B Cell Technologies for Monoclonal Antibody Discovery .....	18
2 AIM AND STRATEGY OF THE PROJECT .....	21
3 MATERIALS AND METHODS.....	22
3.1 Sorting of Ng OMVs specific Memory B Cells (MBCs) from mouse splenocytes.....	22
3.2 Analysis of Raw Supernatants from MBCs through Luminex 3D in two independent assays: IgG detection and binding specificity .....	23
3.3 Recovery of full-length paired VH/VL genes of Ag-specific MBCs.....	25
3.4 Expression of recombinant monoclonal antibodies in Expi293 mammalian expression system....	30
3.5 Recombinant mAbs purification with protein G/A.....	31
3.6 Gonococcal growth conditions.....	31
3.7 Western Blot with Ng lysates .....	31
3.8 Dot Blot with Ng Opacity associated proteins (Opa) constructs .....	32
3.9 Serum bactericidal activity with exogenous human complement (hSBA) .....	32
3.10 Protein array protocol .....	33
4 RESULTS .....	34
4.1 Strategy for the isolation and expression of specific Ag+ mAbs against gonococcus .....	34
4.2 Results from sorting of Ng OMV-specific Memory B cells (MBCs) from mouse splenocytes with single-cell FACS sorting.....	34
4.3 Results from Luminex assays: IgG detection and Binding Specificity.....	36
4.4 Isolation and Next Generation Sequencing (NGS) of Binding positive mAbs.....	38
4.5 Transfection of VH/VL expression plasmids in mammalian cells .....	42
4.6 Characterization of recombinant murine gonococcus mAbs .....	43
5 DISCUSSION .....	60
DECLARATION OF INTERESTS: .....	65
BIBLIOGRAPHY:.....	66

## ABSTRACT

In recent years, there has been the emergence of a number of single-B cell technologies that allow a direct sampling of the immune repertoire: these platforms retain the natural heavy and light chain pairing and avoid the inefficient hybridoma fusion step, enabling efficient mining of B cell population and allowing the discovery of rare antibodies.

The aim of this project was to develop an efficient mouse B-cell cloning and expression platform allowing the generation of large libraries of diverse mAbs sampling the B cell repertoire of antigen specific antibodies after immunization with gonococcal Outer Membrane Vesicles (OMVs).

A protocol for the isolation and characterization of mAbs derived from mouse Ag-specific single Memory B-cells (MBCs) was developed, leading to the generation of a large number of antigen-specific recombinant mAbs. We analyzed 816 OMV-specific MBC-derived supernatants for their binding to the main protein components of the bacterial surface (PorB and OpaB). Most mAbs (68%) recognized the major outer membrane protein PorB; 8.7% of mAbs were against OpaB; another group cross recognized PorB and OpaB (8.9 %), while the remaining mAbs (14.4 %) recognized other unknown antigens expressed on gonococcal surface. All tested mAbs were confirmed to bind one or more gonococcal strains, demonstrating their ability to recognize the native antigens on the surface of the bacterium. Through this approach a library of functional mAbs directed against key bacterial surface proteins of gonococcus has been generated and characterized. A total of 2 recombinant anti-OpaB mAbs, 2 anti-PorB and 2 mAbs with unknown target were fully characterized for their specificity against the antigen target through Luminex assay, Western Blot and Microarray, and for their functionality, with Serum Bactericidal Assay (SBA). This method could be easily exploited for the generation of large libraries of antibodies against diverse proteins of any pathogen.

# 1 INTRODUCTION:

## 1.1 *Neisseria gonorrhoeae* multi-drug resistance and public health threat: disease and epidemiology

*Neisseria gonorrhoeae* (Ng, also known as gonococcus) is the etiological agent of the sexual transmitted disease gonorrhea: it is an obligate human pathogen described for the first time by Albert Nesser in Gram-stained microscopy in 1879 (Quillin and Seifert., 2018).

Ng has a diplococcal shape, meaning that it is composed of two joined cells with the adjacent sites flattened appearing in a kidney or coffee bean shape in microscopy. Ng belongs to the bacterial class *Betaproteobacteria*, family *Neisseriaceae*, and has been co-evolving with its human host for centuries. The *Neisseria* genus includes at least 23 species, about half of which are human-restricted.

Genomically, morphologically and phenotypically it is closely related to the other pathogenic *Neisseria* species, such as *Neisseria meningitidis* often found as a commensal in the pharynx of 10-15% of the population but occasionally causing fatal septicaemia and meningitidis. Moreover, Ng is also related to several other commensal *Neisseria* species that normally reside in the pharynx: those species do not normally cause pathology, are unable to induce inflammation by polymorphonuclear leukocytes (PMNs) and lack additional factors and mechanisms for host cell interaction (Elias, J.F. & Vogel, U. ., 2019, Tønjum, T. & Van Putten., 2016, Johnson, A.P., 1983).

In 2016, the World Health Organization (WHO) estimated that the incidence of gonorrhea was 86,9 million cases per year (Rowley et al., 2019) and WHO global Gonococcal Antimicrobial Surveillance Program (GASP) has pointed the attention in the increase of multi-drug resistant gonococcal infections all around the world (Unemo et al., 2019). Ng has already become resistant to the first-line or second-line empirical antibiotic treatment (e.g., sulfonamides, penicillins, tetracyclines, fluoroquinolones, early generation macrolides such as erythromycin, and cephalosporins the most common used is the cefuroxime). Ng has acquired resistance via an accumulation of Antimicrobial Resistance (AMR) determinants, the majority of which does not seem to impact the bacterial fitness (Unemo, M., & Shafer, W. M., 2014), (Warner, D. M., Shafer, W. M., & Jerse, A. E., 2008). These AMR strains are considered a serious public health issue because they have become highly resistant to all previously recommended antibiotics, and they are extremely resistant not only to the current recommended extended spectrum cephalosporin (ESC), but also to ceftriaxone and macrolide azithromycin, the latter remaining option for empirical monotherapy. Those observations have been reported worldwide. The WHO estimates that global impact of gonorrhea, including its complications and sequelae, will augment and the number of AMR Ng strains will increase in the near future. As a result, improved global actions and research efforts to retain gonorrhea as a readily treatable infection are essential (Unemo et al., 2019).

Advancement in molecular diagnostics gives tools such as several Nucleic Acid Amplification Tests (NAATs), mostly RT-PCRs and/or Next Generation Sequencing (NGS), to detect AMR determinants and try to predict AMR in Ng. These tests should be cost-effective, and they could improve treatment and reduce AMR selection pressure (Golparian & Unemo., 2021). In the absence of a gonococcal vaccine, optimal public health control of gonorrhea will continue to rely on effective, accessible, affordable, and timely antimicrobial treatment in combination with prevention strategies, diagnostics (index cases and traced sexual contacts), and surveillance. Appropriate gonorrhea case management is essential to reduce unnecessary or incorrect antimicrobial treatment and development of AMR (Wi et al., 2017).

Ng mainly infects the epithelium of the urethra, endocervix, rectum, oropharynx, and conjunctivae. The mode of transmission occurs by direct inoculation of infected secretions from one mucosa to another (e.g., genital-urogenital, urogenital-anorectal, oro-urogenital, or oro-anal contact, or by mother-to child transmission at birth).

Regarding the clinical outcomes, symptoms and physical signs involve localized inflammation of infected mucosal surfaces in the urogenital tract, similarly to different other STIs causing comparable symptoms (Unemo et al., 2019), (Unemo et al., 2020).

In men, the predominant symptoms are the acute urethritis that led to urethral discharge (>80%) and dysuria (>50%), 2-8 days after first exposure, while asymptomatic infections are rare (<10%).

In women, endocervical and urethral infections lead to increased or altered vaginal discharge ( $\leq 50\%$ ), lower abdominal pain ( $\leq 25\%$ ), dysuria (10-15 %) and in some cases also menstrual bleeding or menorrhagia. Moreover, in women, endocervical infection is usually asymptomatic in  $\geq 50\%$  of cases (Unemo et al., 2019), (Unemo et al., 2020).

When untreated, if the Ng infection succeeds to ascend to the Upper Genital Tract (UGT) it can lead to complications and sequelae such as pelvic inflammatory disease (PID) in women, that could cause ectopic pregnancy and infertility, and epididymo-orchitis in men. The further severe complication could be Disseminated Gonococcal Infection (DGI), when the infection spreads through the bloodstream affecting various tissues and causing permanent damage, such as arthritis, endocarditis, and meningitis, although gonococcal bacteremia is generally rare (Unemo, M. et al., 2020).

## 1.2 Ng growth and metabolism and genetics

### *Growth and metabolism*

Ng is a fastidious organism that is not able to survive outside the human host, thus, it is sensitive to many environmental factors such as oxygen, non-physiological temperatures, and desiccation, and it is susceptible to toxic substances (e.g., fatty acids). The majority of the strains are unable to autonomously biosynthesize amino acids, supposedly because together with other fundamental nutrients these are taken from the host (Morse, S. A., 1979).

Ng must interact and compete with resident microbiota for available nutrients, and it needs to acquire iron, zinc and manganese limited by the human host as a defense against a bacterial pathogen in a process called nutritional immunity. Bacteria possess a series of membrane transport complexes and use them for the translocation of metals across the bacterial cell (Kehl-Fie, T. E., & Skaar, E. P., 2010). Indeed, iron, an essential factor for bacterial growth, is acquired from the host's iron-binding molecules such as transferrin, lactoferrin and hemoglobin through scavenging mechanisms (Rohde, K. H., & Dyer, D. W., 2003).

The bacteria seem to be well adapted to different oxygen conditions, being exposed to different oxygen levels within different niches of the male and female urogenital tract (Cole, J. A., 2012).

### *Genetics*

Ng harbors a circular chromosome containing between  $\sim 2.1$  and  $2.3$  mega base pairs ( $\sim 2200$ - $2500$  protein-coding sequences): the chromosome exists as diploid and homozygous chromosomes. Furthermore, the bacteria can acquire DNA through horizontal genetic transfer (HGT) that occurs mainly through type IV pilus-mediated DNA transformation (uptake of DNA from the environment and subsequent incorporation into the genome): transformation occurs at high frequency between

cells of Ng and with other *Neisseria* species. This efficient transformation is the reason why AMR determinants efficiently spread from cell to cell (Unemo et al., 2019).

Gonococcal strains also contain a plasmid encoding a penicillinase, resulting in high-level tetracycline resistance. Moreover, some strains contain conjugative plasmids, which sometimes carry the *tetM* gene causing high-level tetracycline resistance.

### 1.3 Pathogenesis and infection dynamics: colonization, invasion, and immune evasion

Ng usually colonizes the genital mucosa, but it has also been found in anal, nasopharyngeal, and ocular mucosa. The first step in the establishment of the infection is mediated through different bacterial surface structures, also named colonization determinants (discussed in detail in the next paragraph). These structures include Type IV pili (Tfp), opacity (Opa) proteins, the lipooligosaccharide (LOS), and the major Porin PorB (Quillin and Seifert., 2018), all exposed on the bacterial outer membrane (Fig 1.3.1).

During the initial stages of colonization, Ng uses Tfp to come in contact with the epithelial cell surface. This is followed by pilus retraction that allows gonococci to be in the close proximity to the cell surface and to start the secondary stages of adhesion (Morand et al., 2004). Once localized adherence is accomplished, bacteria proliferate in piliated microcolonies and probably compete with the resident microbiota. At this point Ng exploit the specialist outer membrane adhesins Opa, to start intimate adhesion and contact with host cells. Opa proteins can bind to different host cell receptors including carcinoembryonic antigen cell adhesion molecules (CEACAMs) and heparate sulphate proteoglycans (HSPGs) to promote intimate adherence (Virji, M. et al., 1996).

Intimate adherence and Pili retraction seems to contribute to extrusion of microvilli-like structures from the cell surface which protect bacteria from the shear stress connected with cell surface and moreover are associated with Ng invasion of host cells through transcytosis (Griffiss et al., 1999).

At this point, bacteria start to release peptidoglycans fragments, outer membrane vesicles (OMV) and LOS, causing the activation of Toll-like receptors (TLRs) and nucleotide-binding oligomerization domain-like receptor (NOD) signaling in epithelial cells, macrophages, and dendritic cells. NOD and TLR signaling leads to the activation of an inflammatory cascade: inflammatory transcription factors and the release of cytokines and chemokines (e.g., IL-1, IL-6, IL-8, IL-17, and TNF). These molecules attract Polymorphonuclear Leukocytes (PMNLs), and the influx of neutrophils causes a purulent exudate that facilitate transmission. (Unemo et al., 2019) (Quillin and Seifert., 2019).

In turn, the bacteria have evolved a number of defense mechanisms to overcome immune surveillance systems such as phagocytosis, antimicrobial factors released during degranulation and NETosis (i.e., cell's death caused by the release of neutrophils extracellular traps, NETs). For example, the bacteria are able to disrupt NET'S through a thermonuclease named Nuc that is able to degrade the NET DNA backbone. Another example of bacterial defense is against Neutrophil's antimicrobial content: Ng has a series of enzymes to counteract Reactive Oxygen Species (ROS), such as catalase, superoxide dismutase and repair enzymes against oxidative DNA damage (Palmer & Criss., 2018). The bacterium has also developed mechanisms to defend itself from complement killing as an example, the LOS can be modified by sialic acid scavenging the CMP-NANA (cytidine 5'-monophospho-n-acetylneuraminic acid) from the host, thus increasing complement resistance. Sialylated LOS binds C3b complement factor and promotes its inactivation via factor I, blocking the

complement cascade and subsequent killing mediated by the Membrane Attack Complex (MAC) formation (Mandrell, R. E. et al., 1990). Moreover, the outer membrane channel protein PorB binds to Factor H and Complement component C4b thus hiding the bacteria from complement recognition and evading killing by complement pathway (Ngampasutadol, J., 2005) (Figure 1.3.2).

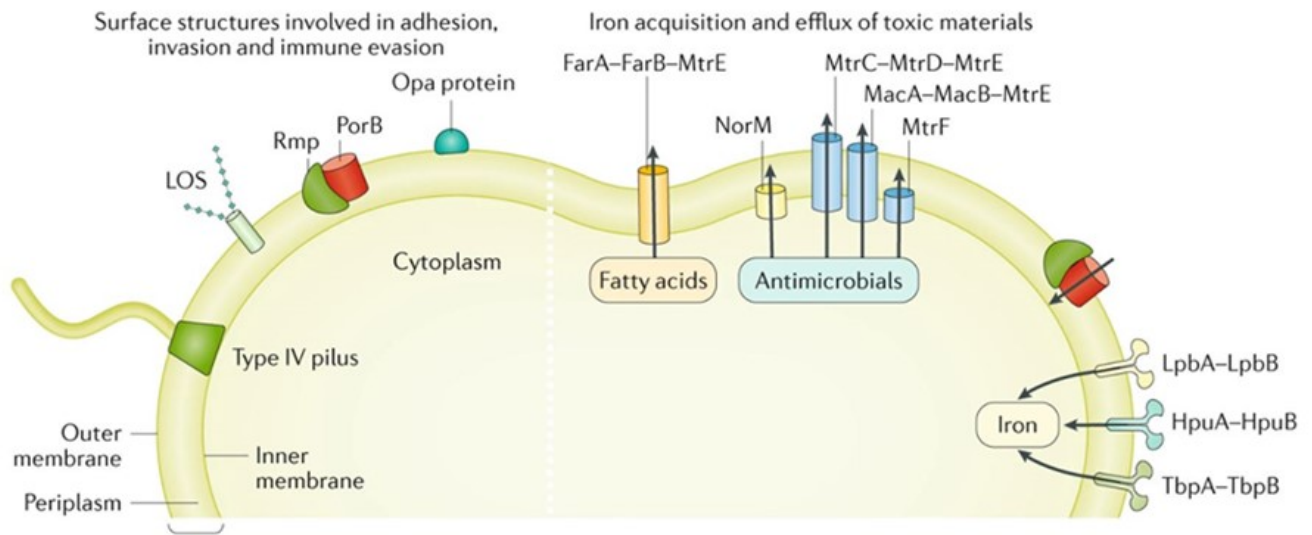


**Figure 1.3.1 : *Neisseria gonorrhoeae* cell envelop structure :** The cell envelope is composed by a cytoplasmic membrane (inner membrane), periplasmic space that harbour the peptidoglycan cell wall, outer membrane with Lipooligosaccharide LOS, type IV pilus, Opa proteins, the Porin. Moreover, the outer membrane contains the five efflux pump systems (FarA-FarB-MtrE, NorM, MtrC-MtrD-MtrE, MacA-MacB-MtrE and MtrF) used for toxic molecules removal and elimination of antimicrobials. Finally, the three iron-scavenging complexes (LpbA-LpbB, HpuA-HpuB and TbpA-TbpB) are necessary for iron sequestration from the host (Unemo et al., 2019), copyright authorization n°5581860871178.

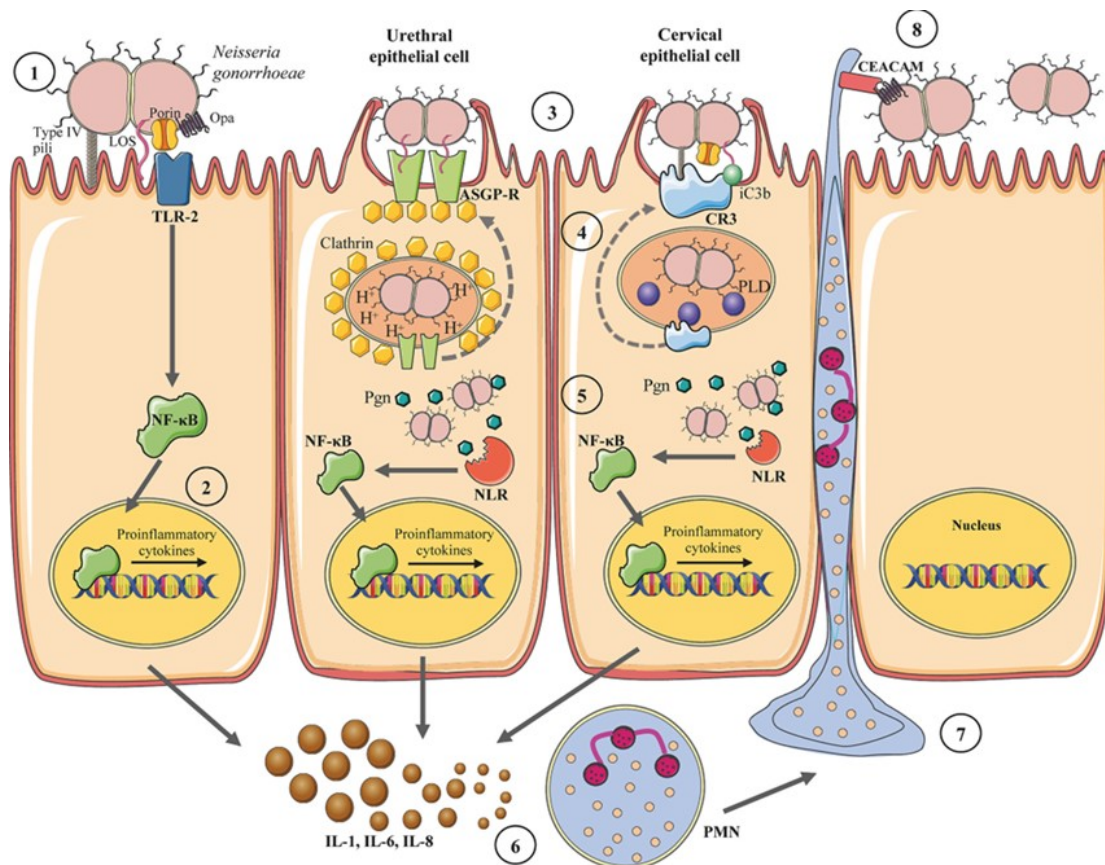


**Figure 1.3.2 : Ng mechanism of invasion** (Green et al., 2020, copyright authorization n°5581390196274):

- (1): After initial attachment of Ng through Type IV pili to urethral epithelial cells; Lipooligosaccharide (LOS), Porin and Opa activate Toll-like receptor 2
- (2) This binding causes the activation of NF-κB and production of pro-inflammatory cytokines
- (3) The phagocytosis in urethral epithelial cells is induced by LOS binding to asialoglycoprotein receptor (ASGP-R) whilst in cervical cells binding of type IV pili, Porin and complement iC3b to cervical complement receptor 3 (CR3)
- (4) In uroepithelial cells the engulfment occurs in a clathrin dependent way, whilst in cervical epithelial cells the internalization is clathrin-independent
- (5) NOD-like receptors (NLR) are activated by Ng development inside the cell, NLR in turn stimulates NF-κB and the production of pro-inflammatory cytokines (IL-1,IL-6,IL-8)
- (6-8): The pro-inflammatory cascade attracts PMNs to the infection site, at this point the bacteria bind to Carcinoembryonic antigen cell adhesion molecules (CEACAM) located on PMNs via Opa proteins

#### 1.4 Colonization determinants

Ng expresses a set of common virulence determinants that allow efficient colonization, immune evasion, and transmission. Due to their exquisite adaptation to humans these bacteria have evolved specialized mechanisms to promote growth and persistence in the host (Criss et al., 2012).

#### **Type IV pili (Tfp):**

Tfp are multimeric, filamentous structures which are peculiar for different bacterial processes including: initiate cellular adherence, twitching motility, natural transformation component and immune evasion (Craig et al., 2004).

Tfp are composed of multiple pilin proteins (PilE) arranged in a helical array, in which the variable carboxy-terminal globular domains decorate the outer shell while the hydrophobic amino-terminal  $\alpha$ -helix compose the backbone of the pilus resulting in a structure of different micrometers in length (Craig et al., 2019). The core of the Tfp machinery is composed by five essential components: PilF that is a cytoplasmic ATP-ase that powers assembly, PilQ an outer membrane secretin channel, PilG an inner membrane protein able to extrude the pilus through transduction of energy, PilE the mayor pilin subunit that forms the pilus filament which extends across the bacteria periplasm and across the secretin channel and is constructed by inner-membrane anchored pilin subunits and lastly PilT a retraction ATPase that catalyzes disassembly of the pilus. Different cytoplasmic, periplasmic, and inner membrane proteins form a complex that resemble a cage, this serves to connect the ATP-ases to secretin channel in order to keep the pilus aligned (Ayers et al., 2010). Ng moreover possess PilC protein, which is a pilus tip adhesin essential in the formation of the pilus, this protein is fundamental for pilus retraction, bacterial transformation, and adhesion to host cells (Rudel et al., 1995). PilC is encoded by two variant genes (*pilC1* and *pilC2*). The expression of the protein is controlled by frequent frameshift phase mutations within a polyguanine (G) tract located in the signal-peptide coding region (Jonsson et al., 1991).

During colonization and infection, Tfp are able to antigenically change to generate diversity and evade the host immune responses. A single gonococcal strain expressing one pilus type can generate isolates whose pili have undergone antigenic variation to express different pili (Hagblom et al., 1995). This antigenic variation occurs by non-reciprocal recombination events between the expressed *pilE* gene and one of the silent *PilS* loci (Haas, R., & Meyer, T. F., 1986). Tfp can undergo also to post translational decoration of the PilE subunits with glycans.

Human membrane co-factor protein CD46 and complement receptor 3 (CR3) have been identified as putative pilus receptors. Piliated gonococci can induce CD46 redistribution beneath bacteria, together with tyrosine phosphorylation of CD46 and release of CD46-enriched vesicles from host cells (Gill et al., 2005).

In addition, gonococcal Tfp associate with  $\beta$ 1 integrins comprising several I-domains (binding site for ligands of the abovementioned integrins), particularly complement receptor 3 on cervical epithelial cells (Edwards, J. L., & Apicella, M. A., 2005).

Tfp, after initial localized adherence to host cells, promote the formation of underlying cortical plaques beneath bacterial adhesion sites composed by some component of the cytoskeleton (e.g., ezrin and moesin) and a subset of membrane proteins (ICAM-1 and Erb-2). This is followed in turn by the activation of Rho and Cdc42 GTP-ases leading to cortical actin localized polymerization, the consequent cytoskeletal organization is fundamental for bacterial internalization (Corbett et al., 2004). Another mechanism of adhesion used by Ng is the association with microvilli-like protrusion

(containing large amount of cytoskeleton associated proteins) from the host cells associated with PilT-dependent pilus retraction. When intimate adherence occurs, gonococci lose their pili in a PilT dependent manner. This causes the disassociation of the formed microcolonies at the cell surface allowing the spreading across the cell leading to diffuse adherence (Pujol et al., 1999).

### **Porins:**

Porins are homotrimeric  $\beta$ -pleated barrels, each monomer is composed of 16 anti-parallel  $\beta$ -strands between 32-38 kDa and 8 surface-exposed loops (Chen & Seifert., 2013). Porins are able to selectively regulate the exchange of ions, cations and other solutes between the bacteria and the outside environment (Zeith et al., 2013). Gonococcal porins are present as either a Porin.1A (PI.A) or a Porin.1B (PI.B) isotypes). Porin B (PorB) is the most abundant gonococcal outer membrane protein (60 % of the total gonococcal surface (Zeith et al., 2013). The *porB* gene exists in two different alleles encoding for PorB.1A or PorB.1B. (Cannon et al., 1983). PorB molecules do not undergo high-frequency variation, clinical isolates exhibit antigenic differences in surface-exposed loops, probably because of low-frequency mutations or recombination events in the *porB* gene (Fudyk et al., 1999).

One of the major roles of the gonococcal PorB is to mask the bacteria by the innate immune system recognition: PorB can give serum resistance through the binding to specific negative regulators of the complement system: *N. gonorrhoeae* bind to the negative regulator C4BP through PorB, C4BP is a strong inhibitor of the classical and lectin pathways (Ram S., 2001).

In the cervical epithelium, Ng binds to the alternative complement pathway regulator Factor H (FH) via sialylated LOS and porin (Quillin and Seifert., 2018). The negative complement regulator FH recruitment via PorB is fundamental for bacterial survival, PorB binding to FH increase when sialylated lipo-oligosaccharide LOS is present. (Jones et al., 2023). Sialylation of the lacto-N-tetraose moiety on  $\alpha$  chain of LOS enhances FH deposition on porins, explaining in part the increased resistance of sialylated Ng to phagocytosis (Shaughnessy et al., 2016)

During the infection, PorB is recognized by Toll-like receptors (TLRs) present on the surface of the innate immune cells (e.g., Dendritic cells, macrophages) and also non-immune cells, like epithelial cells. TLRs are fundamental components of the immune system able to recognize pathogen-associated molecular patterns (PAMPs) (Kawasaki & Kawaki., 2014). In particular TLR2 is able to recognize PorB leading to a proinflammatory signaling cascade.

PorB is able to aid in the invasion and transcytosis of epithelial cells through the binding with a scavenger receptor on endothelial cells-1 (SREC-1) and human heat shock glycoprotein 86 (gp86) (Jones et al., 2023). PorB plays a role in the adhesion and invasion of epithelial cells altogether with Pili, Opacity associated protein (Opa) and LOS, all acting as adhesins and contributing to the bacterial interaction with different cell types (Van Putten et al., 1998).

The binding of Pili and the opsonin iC3b on the surface of gonococcus upon complement activation are fundamental for the binding of PorB to the complement receptor 3 (CR3) present on the female genital-tract epithelia (Edwards et al., 2002). Indeed, the bacteria exploit PorB for adherence to epithelial cells enabling invasion and intracellular survival (Jones et al., 2023).

Moreover, the bacteria develop the ability to survive within macrophages and hinder apoptosis, thus promoting intracellular survival (Château, A., & Seifert., 2016). PorB also targets host mitochondria in infections, the mechanism by which PorB translocate from the outer membrane to host mitochondria is not clear, seems that the bacteria use Outer Membrane Vesicles (OMVs) to

interact with macrophages and to deliver PorB to mitochondria. In OMV-treated cells and purified organelles PorB translocate to mitochondria causing the loss of membrane potential and apoptosis (Deo et al., 2018).

Ng also manipulate the neutrophils through PorB during infection into the genital tract, to ensure bacterial survival. The bacterium, in order to persist intracellularly, prolongs the survival of neutrophils impeding their apoptosis, using PorB for the inhibition of neutrophil killing mechanisms (Cho et al., 2020).

For example, experiments with purified gonococcal PorB, shown degranulation and ROS inhibition (Lorenzen et al., 2000). In Ng strains expressing the PorB.1B binding to C4BP, it has been demonstrated that recruitment of C4BP negative regulator diminishes the phagocytosis of bacteria by neutrophils altogether with suppression of ROS production (Werner et al., 2023). Another mechanism observed that decreases phagocytosis is the inhibition of actin polymerization through PorB.1B in activated neutrophils thereby reducing the expression of complement receptors (Bjerknes et al., 1995).

To summarize, PorB blocks the killing activity of neutrophils and macrophages, it is involved in immune evasion, aids in invasion of the host cells. There is a conflict in the induction and inhibition of apoptosis modulated by PorB in epithelial cells and macrophages, this could be due to the fact that specific cell types may influence the effects of PorB (Jones et al., 2023).

### **Lipooligosaccharide (LOS):**

Lipooligosaccharide (LOS) is abundant in Ng outer membranes: it is composed by three oligosaccharide chains attached to a lipid A core and lacking a repeating polysaccharide O-side chain (Edward and Apicella., 2004). The oligosaccharide chains branch from two heptose molecules attached to lipid A when one chain elongates from the first heptose (HepI) and chains 2 and 3 elongate from the second (HepII). The oligosaccharide chains can vary in number and length between different gonococcal strains or even within the same Ng population (Gulati et al., 2019).

Ng harbors the *lgt* genes: these genes encode for a series of glycosyl-transferases that control the synthesis of the oligosaccharides. *LgtF*, *E*, *A*, *B* and *D* are essential for the addition of hexose residues (hexosamine residues in the case of *LgtA* and *LgtD*) in a sequential manner to the oligosaccharide chain (Gotschlich, E.C., 1994).

Gonococcus has distinct LOS structures due to the phase variability of *lgt* genes: homopolymeric tracts of poly-guanine can be found in *lgtA*, *lgtC* and *lgtD*, while a poly-cytosine tract is present in *lgtG*, which can add a glucose to the HepII molecule on lipid A (Danaher et al., 1995).

At the level of translation there will be various truncated LOS structures at a frequency of  $10^{-2}$  to  $10^{-3}$  due to a slipped strand mispairing within these tracts. Several LOS oligosaccharide chains result in epitopes which resemble mammalian glycosphingolipids (Schneider et al., 1988). This is a mechanism of immune evasion through molecular mimicry, which allows bacteria to interact with host molecules. For example, the lacto-*N*-neotetraose (LNnT) epitope of LOS (four sugars extending from HepI) is identical to the LNnT of the human erythrocyte glycosphingolipid paragloboside. The immunochemical identity may indicate that the two glycolipids share epitopes, and both human and Ng cells could share the same antigenic structures (Mandrell et al., 1988). The asialoglycoprotein receptor (ASGP-R) recognizes, captures, and mediates endocytosis of galactose (Gal) and N-acetylgalactosamine (GalNAc) terminating glycoproteins and is responsible to maintain tissue physiology; the primary role may be the elimination of potentially dangerous glycoconjugates from

normal tissue turnover. It is usually expressed at high levels by the liver cells, but can be found also elsewhere, the role of the receptor at these extrahepatic sites is uncertain (Harris et al., 2012). The close association between the urethral epithelium and the bacteria seems to be accomplished through the interaction of the asialoglycoprotein receptor on the cell surface and gonococcal LOS: the LNnT moiety must be present in the oligosaccharide in order to achieve the association with the receptor (Harvey et al., 2001). This is confirmed by studies showing that gonococci with the LNnT moiety on their LOS structure have enhanced infectivity in humans (Schneider et al., 1991). In primary cell culture, this binding results in pedestal formation beneath the bacterium and F-actin polymerization leading to endocytosis, this is observed also in men with natural acquired infection (Harvey et al., 1997).

Endocytosis mediated by ASGP-R is dependent by actin-dependent and clathrin-dependent mechanisms: this led to endosomal fusion and acidification resulting in clathrin coat disassembly and uncoupling of the ASGP-R-ligand complex (Giardina et al., 1998), (Harvey et al., 1997). Once the bacteria are internalized, the ASGP-R is recycled to the urethral cell surface, where can bind more gonococci. However, the intracellular activity of the bacteria within the urethral epithelium is currently unclear, indeed it is thought that gonococcus utilize these cells as protective environment to survive and replicate (Harvey et al., 2001).

Moreover, the LNnT moiety can also be capped through sialylation using sialyltransferase present in the outer membrane and using as a suitable substrate from the host the exogenous cytidine monophospho-*N*-acetylneuraminic acid (CMP-NANA). LOS sialylation is fundamental for the bacterial pathogenesis: first at all it is able to inhibit all three complement pathways, reduce opsonic killing and lastly it is able to diminish Opa-mediated invasion of epithelial cell lines (Gulati et al., 2019).

Gonococci isolated from infected urethral epithelial cells possess the sialylated LNnT moiety highlighting its importance during the infection (Apicella et al., 1990).

### 1.5 Opacity (Opa) proteins: an important family of adhesins and invasins

The integral outer-membrane Opa proteins of Ng are encoded by a family of related genes (individual loci) disseminated throughout the genome: gonococci typically have 11 loci that encode for 7 to 9 unique Opa proteins (Bhat et al., 1991).

The name Opacity is derived from the fact that, when they are expressed by the bacteria, they give opaque colonies when viewed by a stereomicroscope, an effect attributed to differences in bacterial aggregation (Belland et al., 1997).

The *opa* genes are constitutively transcribed, but Opa expression undergoes regulation at the translational level called phase variation, a reversible way of gene regulation by which synthesis of specific proteins occurs in different levels within different part of bacterial population (Van der Wonde., 2011). *opa* loci contain a pentanucleotide repeat sequence within the coding region of the amino-terminal leader peptide (5'-CTCTT-3') and the number of these coding repeat (CR) units is variable. Since the number of repeats is fundamental for the correct reading frame, modulation of the repeat number by slipped-strand mispairing mechanism is believed to result in the frequent phase shifts in Opa protein expression (Stern, A., & Meyer, T. F., 1987), (Robertson, B. D., & Meyer, T. F., 1992). The result is that any given neisserial population should comprise a mixture of individual bacteria expressing either none, one or multiple Opa proteins (Kuespert et al., 2007).

Another mechanism of phase variation is achieved thanks to the presence of multiple *opa* genes that undergo genetic recombination between loci in the same chromosome and between different organisms: this recombination phenomenon allows the exchange of entire or partial *opa* genes, intra- and inter-genomic recombination events are much more common than mutations (Bilek et al., 2009).

The predicted structure of Opa proteins possesses eight membrane-spanning domains arranged as anti-parallel  $\beta$  strands, resulting in a membrane-embedded  $\beta$  barrel with four extracellular loops that differentiate in sequence (Malorny et al., 1998).

Sequence variation among Opa families is observed within the two central loops: hypervariable domain 1 (HV-1) and 2 (HV-2). New Opa proteins variants can occur due to point mutations within the two regions (HV-1/HV-2) and by modular exchange of domains among different Opa genes (Hauck et Mayer., 2003). The predicted structural model of the protein is reported in figure 1.5.1.

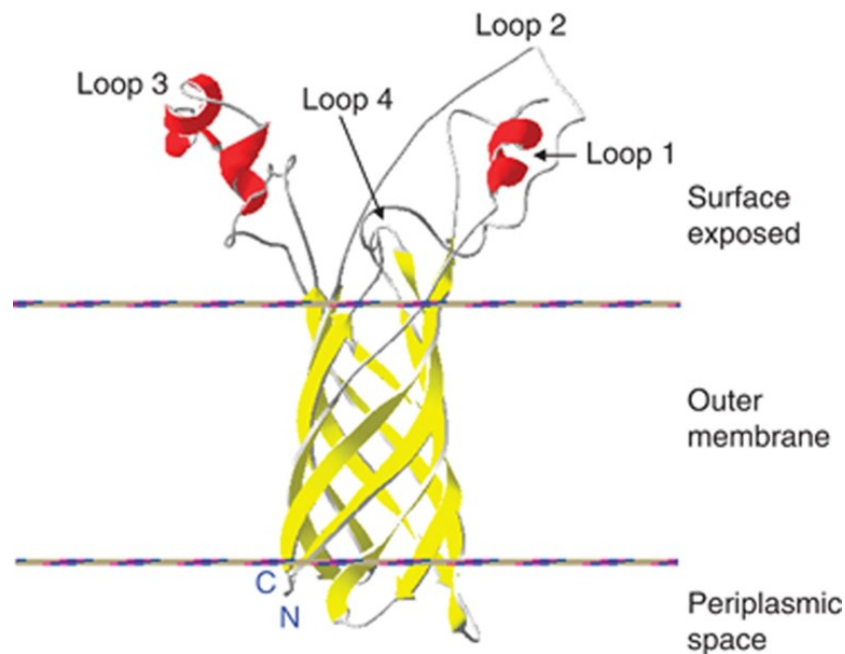


**Figure 1.5.1: Predicted 3D structure of Opa proteins:** eight-stranded  $\beta$ -barrel topology, linked by four putatively surface-exposed loops. A semivariable region (SV) is located in loop1, and hypervariable regions (HV1 and HV2) in loops 2 and 3, loop4 is the conserved one. The transmembrane region is highly conserved in primary sequence and predicted  $\beta$ -barrel structure, while the extracellular loops of other Opa variants may diverge remarkably depending on the length and primary sequence of the surface-exposed sequences. *FEMS Microbiol Rev*, Volume 35, Issue 3, May 2011, Pages 498–514, <https://doi.org/10.1111/j.1574-6976.2010.00260.x>, License authorization number: 5587080549656.

Opa proteins facilitate the interaction of Ng with different host cell types: epithelial cells on mucosal surfaces and various immune cells (Sadarangani et al., 2011). These adhesins appear to have tropism for human receptors, which can be broadly divided into two categories: the majority of the Opa proteins bind to members of the CEACAM receptor family, meanwhile a small subgroup binds to

HSPGs, integrins, ECM proteins (e.g., fibronectin and vitronectin) and saccharides (Hung, M. C., & Christodoulides, M., 2013).

The interaction of Opa proteins with all these different receptors has been attributed to the HV-1 and HV-2 regions. In particular, specific conformational interactions between the HV1 and HV2 regions within Opa loops seem to be necessary for binding to CEACAMs, since despite their high rate of sequence variation in Opa HV regions, the binding sites for CEACAM do show significant conservation (Hung et al., 2013), (Boss et al., 2002).

### **Opas and CEACAM human receptors on immune cells and epithelial cells:**

The CEACAM structure is composed of a single Immunoglobulin-variable (IgV)-like N-terminal domain which contains the portion recognized by different Opa proteins followed by up to 6 Ig-constant (IgC2)-like domains (Kuespert et al., 2006). CEACAMs are proteins with elevated levels of glycosylation and can be anchored to the cell membrane either by glycosylphosphatidylinositol (GPI) moieties or by transmembrane and cytoplasmic domains. For example, CEACAMs 5 and 6 are GPI-anchored with no cytoplasmic domain while CEACAM 1 and 3 are transmembrane proteins with cytosolic tails able to activate signaling pathways within the cell. In particular, the cytoplasmic tail of CEACAM1 contains an immunoreceptor tyrosine-based inhibitory motif (ITIM) motif that can inhibit signaling by activating the SH2 domain-containing nonreceptor tyrosine phosphatases SHP 1 and 2. On the contrary CEACAM3, which is only expressed by granulocytes, have a C-terminal immunoreceptor tyrosine-based activation motif (ITAM) that allows the recruitment of Src family and SyK tyrosine kinases allowing a signaling cascade that activate actin-dependent phagocytosis, release of neutrophils granules and production of reactive oxygen species (ROS) (Schitter et al., 2004), (McCaw et al., 2003).

The Opa proteins are able to bind to the non-glycosylated face of the IgV-like domain of CEACAMs, this is why they are also named Opa<sub>CEA</sub> (Hauck and Meyer., 2003). Opa-CEACAM interaction has been identified for 4 CEACAMs: CEACAM1, CEACAM3, CEA/CEACAM5 and CEACAM6 (Bos et al., 1997) (Figure 1.5.2). CEACAMs are expressed on different cell types involved in Ng infection: neutrophils, endothelial cells, and epithelial cells. Engagement of these receptors leads to differential bacterial fate. On human neutrophils, Opa proteins are able to bind to CEACAM1, 3, 6 but not 4 and 8. On epithelial cells instead, Opa proteins are able to bind to CEACAM1, 5 and 6 (Popp et al., 1999).

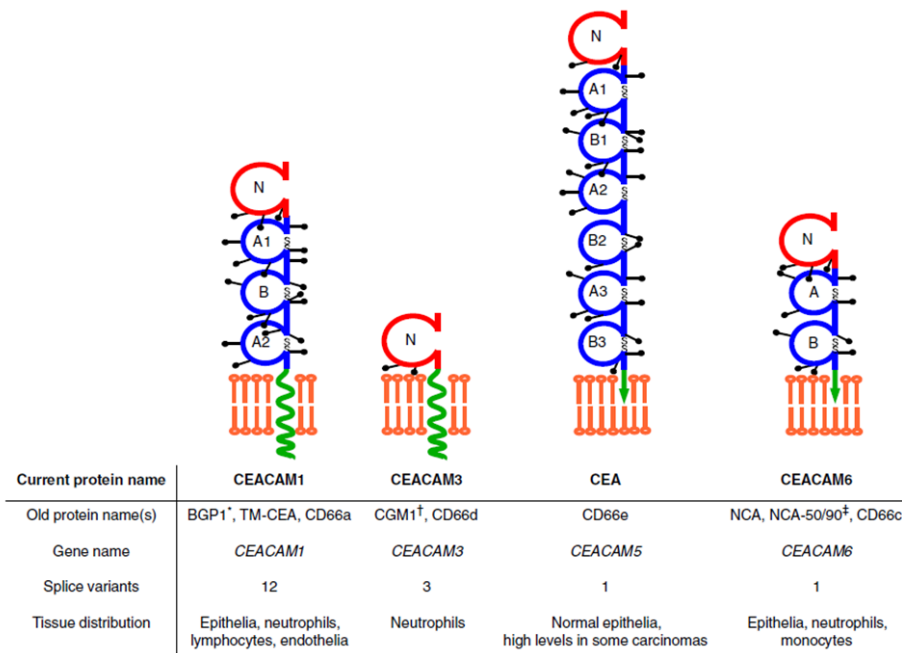


**Figure 1.5.2: Opa protein-binding receptors of the human CEACAM family.** Different CEACAM receptors consist of an immunoglobulin-like domain (in red) and variable numbers of domains homologous to the immunoglobulin-constant region of the C2 set (in blue). Two different types of membrane anchoring are present: a hydrophobic transmembrane domain followed by a cytoplasmic tail (CEACAM 1 and 3) or a glycosylphosphatidylinositol moiety (CEACAM 5 and 6). FEMS Microbiol Rev, Volume 35, Issue 3, May 2011, Pages 498-514, <https://doi.org/10.1111/j.1574-6976.2010.00260-x>, License authorization number: 5587080549656-

Human neutrophils, during infection, have a constitutive expression of CEACAM1, 3, 6, all the receptors possess good recognition and phagocytosis of Opa<sup>+</sup> Ng. Internalization via CEACAM1 and 6 undergoes without substantial neutrophil activation, neutrophils that by CEACAM 1 and 6 bind and engulf gonococci do not give rise to bacterial degranulation and oxidative burst response (Sarantis & Gray-Owen., 2012). On the contrary, CEACAM3, is exclusively expressed on granulocytes and neutrophils suggesting that the receptor seems to be evolved on primate neutrophils has evolutionary tactics to fight microorganisms that uses CEACAM1 as factor of colonization (Alcott et al., 2023). When Opa proteins bind to CEACAM3 through a pretty conserved extracellular domain located on the receptor, this lead to bacterial phagocytosis and activation of degranulation and oxidative burst that promote bacterial clearance (Criss, A. K., & Seifert, H. S., 2008),(Schmitter et al., 2004). Moreover, the neutrophils activate pro-inflammatory cytokine cascade upon CEACAM3 *de novo* transcription. *In vivo*, the binding of Ng to CEACAM3, recruits more neutrophils to the site of infection promoting the auto-inflammatory process associated with the disease (Sintsova et al., 2014). Epidemiologically, bacteria are under strong selective pressure in avoiding the binding to CEACAM3 while maintaining that to CEACAM1 and others that serves for bacterial colonization (Sintsova et al., 2015). Indeed, the peculiarity of Ng to avoid phagocytic killing is dependent on three factors: Opa expression status, the specific Opa protein expressed by the bacteria and the amount of the protein stably expressed on the bacterial surface (Alcott et al., 2022). Neutrophils with their phagocytic and antimicrobial activities push the bacteria to drive the selection of an Opa population less prone to CEACAM3 binding, the bacteria exploit recombination mutation and phase variation events to have a panel of adhesins in which some of them evade CEACAM3 binding, there is a

selection of Opa- bacteria after neutrophil exposure (Alcott et al., 2023). On their side, gonococci are able to limit neutrophil phagosome maturation, probably due to components on the surface of the bacteria that are in contact with the phagocytic receptors, to increase their chance of survival (Palmer and Criss., 2018). Inside neutrophils, phagosome maturation occurs by fusion with cytoplasmic granules each with different antimicrobial content. Primary granules contain antimicrobial proteins ( $\alpha$ -Difensins, Bactericidal/permeability-increasing protein, Azurocidin) that are the main anti-gonococcal agents. Opa- Gc are then internalized into immature phagosome (lack primary granule components), the bacterial viability inside the phagosome is increased (Criss et al., 2009). The hypothesis that unopsonized, Opa- bacteria evade delivery into phagolysosomes, is that phagocytosis needs opsonization or expression of Opa proteins (Alcott et al., 2022). On the contrary, Opa+ Ng that bind to CEACAM3 or bacteria IgG-opsonized that recruit Fc receptors, neutrophils internalize them in mature phagolysosomes (Palmer and Criss., 2018).

Attachment to mucosal epithelium represents the first step in Ng genital colonization. The female reproductive tract (FRT) is constituted by a long canal covered with a variety of epithelial cells. The mucosal surface of the human cervix is highly heterogeneous and is usually divided into three regions: the ectocervix composed by multilayered, non-polarized, stratified, squamous epithelial cells, the endocervix consisting of a single-layer of polarized, columnar cells and the Transformation zone (TZ) where epithelial cells change from stratified squamous to columnar cells (Hafez, E. S., & Kenemans, P., 2012). Epithelial cells express different CEACAMs isoforms: CEACAM1, CEACAM5 and CEACAM6. Different Opa isoforms are able to bind to a single CEACAM or a combination of these receptors to ensure tight bacterial association (Chen et al., 1997). Ng bacteria modify their infection strategy in relation to the type of epithelia that they may encounter, and they differentially modulate cell-cell junctions. Opa-CEACAM binding can resist the flow of the mucus and *in vitro* studies highlight that this interaction allows gonococcal engulfment and transcytosis across polarized epithelia (Wang et al., 1998). Moreover, Opa binding to CEACAM 1, 5 or 6 can activate intracellular signaling cascade pathways that stimulate integrin-mediated focal adhesions in epithelial cells, thus preventing the normal shedding of infected mucosal cells (Muenzner et al., 2010). CEACAM engagement by bacteria triggers enhanced host cell adhesion to the ECM, thereby abrogating cell detachment, which is an essential component of the exfoliation response (Muenzner et al., 2004).

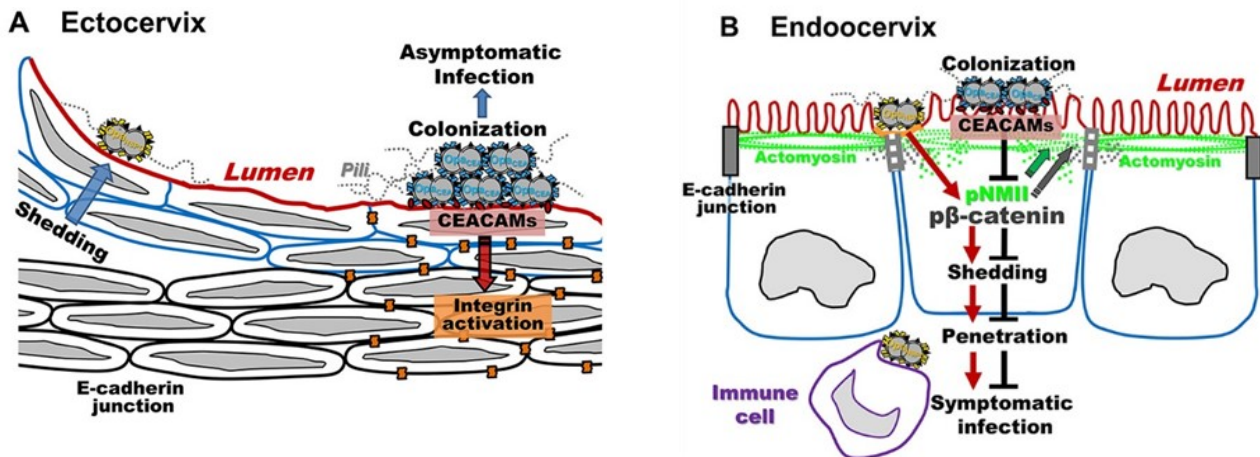


**Figure 1.5.3: Ng mechanism of colonization and invasion.** In the endocervix, the bacteria that penetrate the epithelia induce disassembly of cell-cell junctions; gonococcus can exploit essentially two distinct mechanisms: the first mechanism involves the phosphorylation of  $\beta$ -catenin, that functions as linker from the junctions to cell signaling and cytoskeleton, so phosphorylation cause the disassociation of the  $\beta$ -catenin leading to junction disassembly (Valenta et al., 2012). On the other side, in the ectocervix Opa<sub>CEA</sub> proteins, are able to interact with the high levels of CEACAMs expressed on the luminal surface of the cells, inducing the activation of integrin  $\beta_1$  but not  $\beta$ -catenin: this reduces the self-protective host mechanism of epithelial shedding without affecting E-cadherin-based cell-cell junctions. This mechanism enhances colonization inhibiting/reducing the epithelial shedding (Song et al., 2020).

Song W, Yu Q, Wang L-C, Stein DC. Adaptation of Neisseria gonorrhoeae to the Female Reproductive Tract. Microbiology Insights. 2020;13. doi:10.1177/1178636120947077, Permission is granted for use of content in doctoral dissertation.

## Opas and human Heparan Sulfate Proteoglycans (HSPGs) on endothelial and epithelial cells:

Heparansulphate proteoglycans (HSPGs) were identified as host cell binding sites “receptors” on human cells for Opa invasion (Van Putten, J. P., & Paul, S. M., 1995). HSPGs are membrane glycoproteins that can bind to different growth factors and extracellular matrix proteins and have the role of accessory molecules in cellular attachment, cell growth, signal transduction and cytoskeletal organization. The structure of HSPGs is organized in glycosaminoglycan sidechains with negatively charged heparansulphates and chondroitin sulphates (Hauck, C. R., & Meyer, T. F., 2003). The arrangement and number of positively charged aminoacids in HV-1 and HV-2 of Opa<sub>HS</sub> that confers recognition of the receptor (Grant et al., 1999). HSPGs can come either as glycosylphosphatidylinositol (GPI)-linked proteins (glypicans) or as transmembrane receptors (syndecans). Briefly, Ng recruit Opa<sub>HS</sub> to engage the glycosaminoglycan sidechain of HSPGs receptor; this contact in turn stimulates the activity of phosphatidylcholine-dependent phospholipase C (PC-PLC) and Acid sphingomyelinase (ASM): this activation is necessary to internalize microorganisms. PC-PLC and ASM in turn activate the second messengers diacylglycerol and ceramide respectively contributing to cytoskeletal rearrangement during gonococcal invasion (Keenan, C., & Kelleher, D., 1998), (Spiegel et al., 1996).

Moreover, localized PC-PLC and ASM activity could modify the lipid composition of the plasma membrane at the point of invasion, facilitating receptor clustering and bacterial internalization (Grassmé et al., 1997). Finally, transmembrane syndecan-type HSPGs connect to typical Protein

kinase C (PKC<sub>s</sub>) thus regulating the arrangement of cellular cytoskeleton and further contributing to bacterial engulfment.

In different epithelial cell lines, efficient bacterial internalization occurs through indirect interaction of Opa<sub>HS</sub> with Integrins, this is mediated by the extracellular matrix proteins (ECM) vitronectin or fibronectin: using these ligands as bridging molecules, Opa<sub>HS</sub> can indirectly recruit integrins  $\alpha_v\beta_3$  and  $\alpha_5\beta_1$  leading to uptake into epithelial cells. This interaction is sensitive to RGD (arginine-glycine-aspartic acid) peptides that imitate the binding site of ECM for integrins and in polarized epithelial cells occurs at the basolateral side. (Gomez et al., 1997). (Figure 1.5.4).

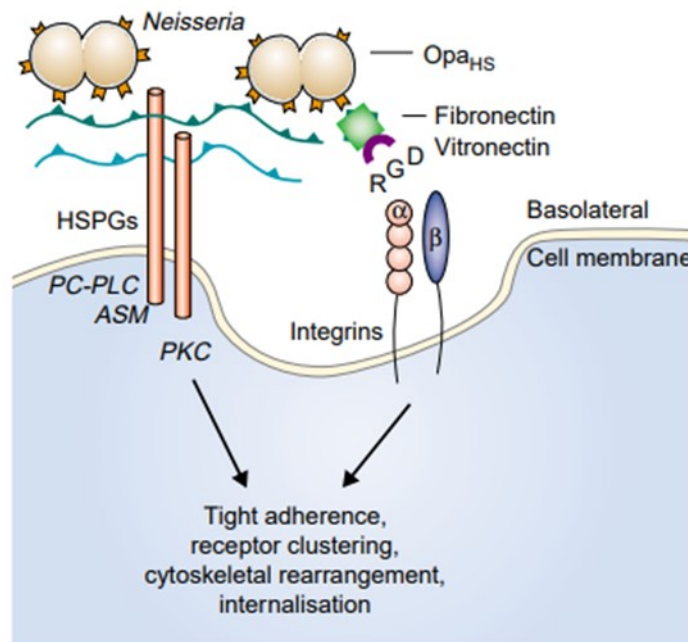


**Figure 1.5.4: OpaHS- mediated interactions with human epithelial cells:** Pathogenic *Neisseriae* uses OpaHS for binding to HSPGs, the binding trigger the activation of PC-PLC and ASM necessary for microorganisms internalization. For efficient internalization, OpaHS interact in indirect manner with integrins is facilitated by the ECM proteins vitronectin and fibronectin

[https://doi.org/10.1016/S1369-5274\(03\)00004-3](https://doi.org/10.1016/S1369-5274(03)00004-3), Current Opinion in Microbiology, Hauck, C. R., & Meyer, T. F., 2003, License authorization n°55870881388786

### 1.6 Single B Cell Technologies for Monoclonal Antibody Discovery

Antibodies, also known as immunoglobulins, are glycoproteins produced by B cells of eukaryotes. They are the major actors of the humoral response providing protection against invading pathogens. An antibody is composed by two structural components, the heavy and light chain; each heavy chain has one variable and three constant regions whilst the light chain possesses one variable and one constant region. It is the variable region that interacts with foreign pathogens and antigen recognition could be described as a lock and key system: each antibody has a paratope (lock) that bind a specific epitope (key). Based on their constant region, antibodies are grouped into five isotypes: IgM, IgG, IgA, IgD and IgE. The most abundant, with a long lifespan, permeable to extravascular spaces and with high therapeutical potential is the isotype IgG (Ma, H., & O’Kennedy, R. 2015).

Monoclonal antibodies (mAbs) are broadly used as essential tools for a variety of diagnostic applications, research investigations, and as therapeutics in the context of viral infections, metabolic diseases, neurological disorders and transplantation, up to date around 100 mAbs have been approved by the FDA (Pedrioli & Oxenius., 2021).

The first technology developed to isolate mAbs is the hybridoma technology, developed by Kohler and Milstein in 1975, that has revolutionized mAb discovery taking advantage of the natural ability of immunized animals to generate functional, highly specific, and high affinity mAbs (Zaroff & Tan., 2019). In this technology, hybridoma cells are generated through fusion of a short-lived-antibody-producing-B cell with an immortal myeloma cell, generating immortal clones whose supernatant can be screened for the presence of antigen-specific antibodies. Each hybridoma cell constitutively expresses a huge amount of one purely specific mAb.

Several mAbs are produced using this technology and used for diagnosis, prevention, and treatment of different diseases, often followed by chimerization or humanization processes to avoid human-anti-mouse antibody reactivity and *in vitro* affinity maturation (Parray et al., 2020), (Pedrioli, A., & Oxenius, A., 2021).

Although this method has revolutionized the use of mAbs, the technology is relatively inefficient for a comprehensive screening of large antibody repertoires due to highly selective and inefficient fusion and transformation events. It is a low-throughput and time-consuming technique, requiring around 4-6 months excluding the immunization of mice (Tiller., 2011) (Starkie et al., 2016)

Another technique to produce mAbs consists in the immortalization of human B-cells by their transformation with Epstein-Barr virus (EBV). As is the case for the hybridoma technology, this method allows the isolation of native mAbs preserving the natural VH/VL pairing (Tiller., 2011).

Alternative ways for creating and selecting mAbs include combinatorial display methodologies like phage and yeast display. Basically, in this case a large repertoire of antibody genes is subcloned into an *E. coli* expression vector, which is packaged into a filamentous phage. Upon production from host bacterial cells, these phage particles exhibit the antibody fragment on the surface as a fusion product with one of the viral coat proteins. The resulting library must be screened to isolate the phage antibodies of interest: to have a full representation of all Ig variants within the library, a larger number of phage particles is typically screened (Sheehan & Marasco., 2015). This technique has been successfully used in the screening of large antibody repertoires and the isolation of mAbs against any antigen (Tiller., 2011). One drawback is the random combination of antibody variable region genes that occurs during the construction of the library. This results in the loss of natural cognate heavy and light chain pairings, causing a loss of affinity for the target. The resulting antibodies usually require *in vitro* affinity maturation to produce molecules with an acceptable potency profile (Meijer et al., 2006).

In the recent years, a number of high through-put single-B cell technologies have been developed that allow the direct interrogation of the immune repertoire, allowing the maintenance of the original VH/VL pairings. The preservation of the natural heavy and light chain pairings during the cloning of the antibody genes allows the generation of recombinant antibodies with a profile affine, stable, and specific (Starkie et al., 2016).

The fluorescent foci method allows the identification and isolation of antigen-specific IgG-secreting cells, such as plasma cells, from heterogeneous bone marrow preparations. The technique uses standard microscope slides and a micromanipulator device to isolate single antigen-specific IgG-secreting cells from the bone marrow of immunized rabbits and rat. After isolation, heavy and light

chain variable region genes are recovered from each cell via single cell reverse-transcription (RT)-PCR and sequencing in order to recover the natural heavy and light chain cognate pairing (Clargo et al., 2014).

The high-throughput method named soft lithographic method for microengraving allows to screen up to one hundred thousand polyclonal B cells: first they are stimulated with a mitogen to give rise to antibody-secreting cells (ASCs) that are successively put individually into an array of microscale wells on a chip, thereafter this array is printed into a corresponding protein array. Whereby each element contains antibody secreted by one single B cells. The antigens used to screen the mAbs are fluorescently labeled and mapped to the corresponding cells, the cells are recovered from the wells by manual micromanipulation and processed for the amplification of the VH/VL genes. It is a high-throughput method to obtain specific B cells before cloning of the Ig gene (Tiller., 2011) (Love et al., 2006).

A similar method is the immunospot array assay on a chip (ISAAC) developed by the Muraguchis group, in which ASCs are spotted on a microwell chip with the surface coated with anti Ig-antibodies, so that the mAbs secreted by the ASC are captured on the surface around the well. The binding of biotinylated antigen to specific antibodies allows the detection with fluorescently-conjugated streptavidin. Those last two techniques have the advantage to obtain rapidly, from a polyclonal mixture, ASCs with high affinity for the antigen target of interest and to allow the simultaneous screening for multiple antigens (Jin et al., 2009).

In alternative, selection of antigen-specific B cells can be achieved using fluorochrome-labeled antigens via multi-parameter FACS, an approach that has been successfully used for the identification of antigen-specific memory B cells, expressing surface IgG as a part of the B cell receptor (Amanna et al., 2006).

The majority of the published works are focused on single cell sorting of antigen-specific B cells and plasmablasts from human samples, where a huge amount of blood is at disposal to conduct FACS sorting, while there are few published data of flow cytometric sorting of antigen-specific memory B cells from immunized animals aiming at mAbs discovery.

Starkie et al, published for the first time a multi-parameter flow cytometric single cell sorting technique protocol that allows the production of antigen-specific monoclonal antibodies from immunized mice and rabbits. The huge advantage of the FACS technology is that with the use of multi-parameter staining panel it is possible to accurately identify IgG+ antigen-specific MBCs in the flow cytometer. The RT-PCR can be used for the recovery of the unique paired VH/VL genes that can then be cloned into an expression vector and transfected on mammalian cell line to obtain the recombinant mAb of interest.

The available mAbs against the surface exposed antigens of the pathogen *Neisseria gonorrhoeae* are very few, and only obtained through hybridoma technology and ascitic fluid methodology (Nachamin et al., 1981), (Virji et al., 1985), (Virji et Heckles., 1988), (Rajasekariah G.R. et al., 1989), (Paz et al., 1995).

## 2 AIM AND STRATEGY OF THE PROJECT

Aim of this project was to isolate mouse mAbs against *Neisseria gonorrhoeae* PorB, OpaB, and unknown antigens to deconvolute the antigenicity of bacterial surface exposed antigens. To do so, an efficient mouse B-cell cloning, and expression platform was developed, that enables the generation of large library of diverse mAbs sampling the B cell repertoire of antigen specific antibodies after immunisation with an antigen/immunogen of choice. In order to elicit a library of antibodies to immunogenic surface antigens of gonococcus we used Ng outer membrane vesicles (OMV) as a surrogate for the bacterial surface, and the OMV were labelled and used as bait for sorting of OMV-specific memory B cells.

### 3 MATERIALS AND METHODS

#### 3.1 Sorting of Ng OMVs specific Memory B Cells (MBCs) from mouse splenocytes

##### **Feeder Preparation**

A vial of feeder cells (mouse fibroblast cell line that secretes mouse CD40L) was thawed and put in a 15ml Falcon tube with the addition of 7.5 ml of Iscove's Modified Dulbecco's Medium (IMDM) enriched with Benzonase at 37°C. The tube was centrifuged at 1200 rpm for 8 minutes at 4°C. At this point, the pellet was resuspended in 2 ml of IMDM media. To assess the viability of the cells, they were diluted 1 to 20 in PBS and counted through ViCell. The cells were resuspended to a final concentration of 200.000 cells/ml and 25uL/well were plated in 384well plates and incubated overnight at 37 °C, 5% CO<sub>2</sub>. The day after, 25 ul of IMDM media with IL2 (final concentration 100 U/ml) and IL-21 (final concentration 50 ng/ml) has been added in each well of the 384 well plates.

##### **Ng OMVs labelling with AlexaFluor488**

Ng OMVs were fluorescently labelled targeting lysine residues with AlexaFluor488 (AF488 carboxylic acid, succinimidyl ester, Invitrogen, A20000). AF488 dye dissolved in DMSO was added to the Ng OMVs sample (final concentration 1.5mg/mL) in a 1:20 w/w ratio. After 2 hours at room temperature in the dark with stirring, samples were purified through ultrafiltration with Amicon Ultra-4 100K using PBS 1X pH 7.2 for 30 washes. Labelled Ng OMVs were characterized by SE-HPLC (TSK gel 6000PW column). Fluorescence intensities were measured at 490/525 nm Ex/Em, where an increased signal intensity was observed confirming the successful labelling, while absence of unconjugated dye was also verified. Ng OMVs protein content was estimated through the Lowry method (Pierce Modified Lowry Protein Assay Kit, Thermo). Ng OMVs integrity after labelling was confirmed by Transmission Electron Microscopy (TEM).

##### **Single cell sorting:**

Female CD1 mice 7-week-old (10 animals/group) were injected intraperitoneally (IP) 3 times, 1 month apart with 10 µg of gonococcal OMVs adjuvanted with Aluminum Hydroxide (Alum). A group of mice immunized with the adjuvant alone was used as negative control. Fourteen days post 3<sup>rd</sup> immunization mice were euthanized, and spleens collected. All animal studies were ethically reviewed and carried out in accordance with European Directive 2010/63/EEC and the GSK policy on the Care, Welfare and Treatment of Animals.

Mouse spleens were smashed with a syringe plunger on filter in 50 ml falcon tubes, the cells were collected in a 15ml falcon tube and Hanks' Balanced salt solution (HBSS) was added to the cell suspension and centrifuged for 8 minutes at 1200 rpm at 18°.

For erythrocyte removal, lysis buffer was dispensed 2ml/spleen and left 2 minutes on ice and then HBSS was added to the cell suspension to block the lysis. After centrifugation, cells were resuspended in PBS and filtered with a filter of 70 µm in size. After the filtration, cells were counted through ViCell to assess their viability that was around 90 %.

In order to purify B cells from splenocytes, the B Cell Isolation kit MACS (Miltenyi Biotec) was used. Highly pure resting B cells are isolated by negative selection, with magnetic labeling and depletion of CD43-expressing B cells (activated B cells, plasma cells and CD5+ B-1a cells) and non-B cells. CD43+ B cells, T cells, NK cells, dendritic cells, macrophages, granulocytes, and erythroid cells are labeled with a cocktail of biotin-conjugated antibodies against CD43 (Ly-48), CD4 (L3T4), and Ter-119, followed by incubation with Anti-Biotin MicroBeads. The columns used for the purification

were the MS columns: for equilibration and wash, a cooled buffer was used (PBS/BSA 0.5 %/ 2mM EDTA). Cells coated with magnetic beads were held in the column by a magnet while non-coated B-cells were allowed to flow. After the procedure the B cell viability was again evaluated, cells were further processed when viability was higher than 90%.

A maximum of 10 million enriched B cells were used for each FACS condition. The Life/Dead Fixable Aqua Dead Cell stain kit (TermoFisher Scientific) diluted in PBS was added and the cells were incubated 20 minutes at Room Temperature (RT) in the dark. To remove the dye in excess the pellets were resuspended in PBS and centrifuged for 8 minutes at 1200 rpm. Finally, the samples were saturated via Fc block (diluted 1:50 in PBS/BSA 0.1 %) and incubated 10 minutes at 4°C and again washed with PBS. Then 10 µl of labeled OMVs and 50 µl of Abs mix composed by CD19 conjugated with Phycoerythrin (R-PE) dye, IgM conjugated with Brilliant Violet 421 dye (BV421) and IgD conjugated with Alexa700 dye were added to  $1 \times 10^7$  of purified B cells and incubated at 4°C for 60 minutes. After the incubation, cells were washed with FBS 1% and centrifuged for 8 minutes at 1200 rpm and finally resuspended in 300 µl of PBS/EDTA 2.5 mM.

At this point, the OMV-specific single cell sorting was carried out with BD FACSAria Cell Sorter in 384 well plates. In the end, the cells were incubated with the feeder cells at 37 °C, 5% CO<sub>2</sub> for 2 weeks to allow clonal expansion. After this incubation, supernatants were removed and transferred to a new 384 well plate for native mAbs characterization and cells were resuspended in 6 µL of lysis buffer (H<sub>2</sub>O + RNase Out+ BSA) and immediately frozen at -80°C to preserve mRNA for further sequencing steps.

### 3.2 Analysis of Raw Supernatants from MBCs through Luminex 3D in two independent assays: IgG detection and binding specificity

#### **Detection of IgG amount in supernatants of murine Memory B Cells (MBCs) using streptavidin magnetic beads**

For immunoglobulin detection in MBCs supernatants, a biotinylated antibody (antibody Biotin-SP (long spacer) AffiniPure Donkey Anti-Mouse IgG (H+L), Jackson ImmunoResearch, cod. 715-065-151) was conjugated to Streptavidin Magnetic Particles Radix HC (region 19) for a Luminex 3D (Luminex xMAP Technology) assay.

Beads were prepared as follows: 375 µl of PBS + 0.05% Tween were added to 100 µl of beads stock solution (corresponding to  $1.25 \times 10^6$  beads) and transferred in Low-binding tube to be magnetized to remove the supernatant. Beads were then washed 2 times with 500 µl of PBS + 0.05% Tween and resuspended in 500 µl of Storage Buffer (PBS + 0.5% BSA + 0.05% Tween).

Subsequently, 500 µl of diluted Biotin-SP antibody (2 µg/ml) were added to the beads, immediately vortexed for a few seconds and incubated for one hour at room temperature in the dark in a 360 degrees Vertical Rotor. After that, conjugated beads were washed 2 times with 500 µl of PBS + 0.05% Tween and vortexed for 20 seconds. After final magnetization, they were resuspended in 1 ml of Storage Buffer.

For the detection of the IgG amount in the MBCs supernatants, mouse IgGs (Sigma-Aldrich, I5381) were used as standards and serial dilutions were prepared to have the first concentration point at 10 µg/ml, followed by 12 3-fold dilution points, prepared by adding 15 µl of each solution to 30 µl of PBS + 1% BSA. St rept Radix HC beads were vortexed for 30 seconds, diluted 1:5 in PBS + 1% BSA and 5 µl were immediately dispensed in each well of a 384 well plate. 5 µl of the standard Mouse

IgGs or the MBCs supernatant were added to each well, the plate was incubated for 30 minutes at room temperature shaking in the dark. After the incubation, the plate was washed on Tecan HydroSpeed plate washer with PBS + 0.1 % Tween.

25  $\mu$ l of secondary Antibody R-Phycoerythrin AffiniPure F(ab')<sub>2</sub> Fragment Goat Anti-Mouse IgG, F(ab')<sub>2</sub> fragment (Jackson ImmunoResearch, Cat. 115-116-072), diluted 1:100 in PBS + 1% BSA, were dispensed in each well of the 384 well plate. After an incubation step of 15 minutes at 1100 rpm, with shaking in the dark, the plate was washed with PBS + 0.1% Tween on Tecan Hydrospeed. The beads were then resuspended in 80  $\mu$ l of PBS + 0.1% Tween, read at Luminex 3D and data were analyzed by Bioplex Manager Software 6.2 (BioRad).

### **Immunoassay procedure for determination of Ng antigens specific IgGs using MagPlex beads**

Ng rPorB, rOpaB protein antigens and OMVs derived from the strains FA1090, WHO-F, WHO-N, F62, BG27, MS11 were covalently conjugated to the free carboxyl groups on xMAP Multi-Analyte COOH Microspheres (Luminex Corporation, Austin, TX), respectively, using an N-hydroxysulfosuccinimide (sulfo-NHS)-enhanced carbodiimide-mediated conjugation chemistry.

Carboxylated microspheres were brought to room temperature and sonicated, followed by vortexing for approximately 1 min to obtain a homogeneous distribution of microspheres. An aliquot of  $1.25 \times 10^6$  microspheres from the stock vial was added to a clear 1.5-ml copolymer microcentrifuge tube and pelleted by centrifugation. Microspheres were then washed with 500  $\mu$ l of 0.1 M NaH<sub>2</sub>PO<sub>4</sub> (phosphate buffer) pH 6.2, suspended by sonication and then pelleted.

To activate the carboxyl sites on microspheres, 10  $\mu$ l of a 50 mg/ml solution of N-hydroxysulfosuccinimide (Pierce, Rockford, IL), 10  $\mu$ l of a 50 mg/ml solution of 1-ethyl-3-(3-dimethylaminopropyl)-carbodiimide hydrochloride (EDC; Pierce, Rockford) solution and 480  $\mu$ l of 0.1 M NaH<sub>2</sub>PO<sub>4</sub> were added to the microspheres. Tubes were incubated for 30 min at room temperature in the dark. Following activation, microspheres were washed with 500  $\mu$ l of 50 mM 2-(N-morpholino) ethane sulfonic acid buffer, pH 5.0 (MES; Sigma, St. Louis, MO) to remove residual EDC and sulfo-NHS.

After the conjugation reaction, a coupling confirmation was performed for each antigen-beads conjugation by testing serial dilutions of a murine hyperimmune serum or mAbs.

The following protocol was used to analyze the MBCs supernatants binding specificity against all antigens of interest in a single beads mix (Multiplexed assay). As positive control for each experiment, sera derived from mice immunized with the specific antigen target were used. Sera were pre-diluted in PBS + 0.05% Tween + 0.5% BSA (assay buffer) and then serial 3-fold dilutions were performed. MBC supernatants were tested undiluted.

Immediately before dispensing in plate, beads were vortex for approximately 20 seconds and an equal amount of each was added to a single solution for a final dilution of 1:8 each.

5 $\mu$ l of diluted beads were dispensed in a 384 wells plate and same volume of diluted sera or undiluted supernatants were added. The plate was incubated for 60 min at room temperature in the dark on a plate shaker at 1100 rpm and after incubation, unbound antibodies were removed by washing plates with PBS + 0.05% Tween wash buffer on Tecan HydroSpeed plate washer.

Secondary antibody R-Phycoerythrin-AffiniPure F(ab')<sub>2</sub> Fragment Goat Anti-Mouse IgG Fcy fragment specific (Jackson ImmunoResearch, cod. 115-116-071) was diluted 1:200 in PBS + 0.05% Tween + 0.5% BSA and 25  $\mu$ L were added to each well. The plate was incubated for 45 min at room temperature in the dark on a plate shaker at 1000 rpm and then washed on Tecan HydroSpeed plate

washer with PBS + 0.05% Tween wash buffer. The beads were then resuspended in 80  $\mu$ l of PBS + Tween 0.1 %, read at Luminex 3D and data were analyzed by Bioplex Manager Software 6.2 (BioRad).

### 3.3 Recovery of full-length paired VH/VL genes of Ag-specific MBCs

Reverse Transcriptase (RT) was carried out using the mRNA contained in the lysate of MBCs pellet as starting template and Gene Specific Primers (see table 3.3.1). The RT mix composition and the RT program are reported below (Table 3.3.2).

PRIMER NAME RT	SEQUENCE	REFERENCE
RT_mCH-IgG1+2A	AATTTTCTTGCCACCTTGGT	Jiang et al.
RT_mCH-IgG2B	AAGTTTTTTGTCCACCGTGGT	Jiang et al.
RT_mCH-IgG3	GATTCTCTTGATCAACTCAGT	Jiang et al.
RT_mCK	TTGTCGTTCACTGCCATCAATC	Meyer et al.
RT_mCL	GGGGTACCATCTACCTTCCAG	Meyer et al.

**Table 3.3.1.** Gene Specific Primers for RT.

Reagent	Final concentration	Volume $\mu$ l
dNTP(10mM) (ThermoFisher)	0.5mM	1.3
DTT(0.1M) (Invitrogen)	10mM	2.6
RnaseOUT (40U/ul) (Invitrogen)	2U/ul	0.8
5x First strand Buffer (Invitrogen)	1x	5.2
SuperScript IV (200U/ul) (Invitrogen)	4U/ul	0.52
RT primers mix VH (10uM) *	0.23 uM	0.6
RT primers mix VL (10uM) *	0.23 uM	0.6
RT primers mix VK (10uM) *	0.23 uM	0.6
lysis buffer with sorted cell		3 $\mu$ l/6 $\mu$ l
water DEPC (Ambion)		
total volume		26 $\mu$ l

RT program	
50°C	20 min
80°C	10 min
10°C	$\infty$

**Table 3.3.2.** RT-PCR: On the right is reported the RT program of the thermal-cycler, on the left the mix composition.

After the RT step, two subsequent nested PCRs were performed to recover full-length paired VH-VL genes and add at 5' and 3' all the sequences necessary for cloning in mammalian expression plasmids or direct sequencing with the Illumina platform. Forward primers of both PCR steps cover most of the murine heavy and light variable gene families; sequences and references are reported in Table 3.3.3 for the first PCR (PCR1) and 3.3.4 for the second PCR (PCR2). Forward primers of PCR1 anneal on the leader sequence whilst reverse primers on the CH/CK gene sequence; in PCR2 forward primers anneal from the first aminoacid of the VH/VL gene and reverse anneal at the beginning of the constant region. Forward and reverse primers of the second PCR were enriched with tails complementary to expression vectors for possible PIPE cloning or compatible with a following PCR step for direct HTS sequencing (Figure 3.3.1)

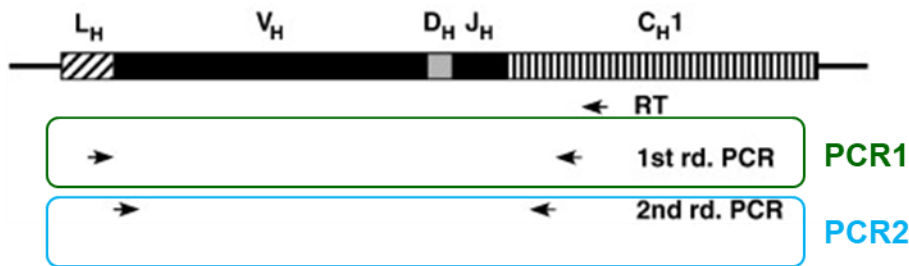


**Figure 3.3.1:** Schematic diagram outlining the nested (RT-)PCR based strategy used. Image adapted from Rohatgi et al., 2008, license authorization n° 5711461098297.

The programs of the amplification steps and the mix composition are reported below (see Table 3.3.5 for PCR1) and table 3.3.6 for PCR2. Amplified products after PCR2 were purified using ProNex Size-Selective Purification System (NG2002, Promega) with volumes ratio sample:beads=1:1,3; following the manufacturer's protocol set up on Hamilton StarPlus liquid handler to eliminate primers leftover.

Once purified, a following PCR step (HTS1) is performed to add Illumina compatible sequences to PCR2 5' and 3' tails for a direct High Throughput Sequencing (HTS) on Illumina Miseq Platform (see Tables 3.3.7 for the primer list and 3.3.8 for PCR mix and conditions).

The last PCR step (HTS2) to build an indexed Illumina library were performed with the commercial Illumina primer set for IDT (Primer sets codes in table 3.3.9) with PCR mix and conditions as in table 3.3.10. Illumina indexes are thus associated with each heavy and light chain amplified, allowing the correct association of reads to each sample during bioinformatic analysis.

ProNex Size-Selective Purification steps are performed after each HTS PCR as described above with volumes ratio sample:beads=1:0,9, to eliminate short fragments and primer dimers, and avoid interference with HTS run. In order to detect the fragment size and quality and to estimate the quantity of the obtained fragments, all samples were run using 2100-Bioanalyzer Instrument and the High Sensitivity DNA Kit (Agilent Technologies, High sensitivity DNA Chips cod. 5067-4626 and High sensitivity DNA reagents cod. 5067-4626) following the manufacturer's instructions.

Samples with expected size fragments (450-600bp) were normalized to 4 nM and pool together to reduce library bias and have a distributed read-count in Illumina multiplex run. The normalized pool of libraries was then denatured and diluted as in Denature and Dilute Libraries Guide Document (Illumina, cod. 15039740 v10). Denatured libraries were diluted to a final concentration of 7 pM with 10% of PhiX control v3 (Illumina, cod. 15017666) spike-in for sequencing to increases the nucleotide diversity and generate high-quality data.

Sample and PhiX mix were finally loaded on an Illumina MiSeq sequencer to perform HTS run using the 600-cycle MiSeq Reagent Kit v3 (Illumina, Cat. No. MS-102-1003) with paired-end reads of 300 base pairs (bp) (2 x 300).

Through an *ad hoc* developed pipeline of analysis, HTS data were analyzed to recover unique and paired VH:VL genes. Generated reads were demultiplexed to be correctly associated with each sample and an in-house modified pipeline, based on MiXCR tool and IMGT database as reference, allow the identification of VH and VL for each processed B-cell.

The recovered sequences were ordered as codon-optimized DNA cloned into pcDNA3.4 TOPO (Invitrogen cod.A14697) mammalian expression plasmid, containing the secretion leader sequence

and the constant region of murine IgG2a heavy chain and IgK light chain (Uniprot codes P01863 and P01837, respectively).

	1st PCR IgH	Primer sequence, primary mix	Reference
<b>Primer mix VH fw</b>	VH_I	AGGAACTGCAGGTGTCC	Bohemer et al
	VH_II	CAGCTACAGGTGTCCACTCC	
	VH_III	TGGCAGCARCAGCTACAGG	
	VH_IV	CTGCCTGGTGACATTCCCA	
	VH_V	CCAAGCTGTGTCTCTGTC	
	VH_VI	TTTTAAAAGGTGTCCAGKGT	
	VH_VII	CCTGTCAGTAACTRCAGGTGTCC	
	VH_VIII	TTTTAAAAGGGTCCAGTGT	
	VH_IX	CGTTCCTGGTATCCTGTCT	
	VH_X	ATGAAGTTGTGGYTRAACTGG	
	VH_XI	TGTTGGGGCTKAAGTGGG	
<b>Primer mix VH rv</b>	CH	GGGATCCAGAGTTCCAGGTC	Meyer et al
	CH3	CAGGTGCTGGAGGGTACAGTC	

	1st PCR IgK	Primer sequence, primary mix	Reference
<b>Primer mix VK fw</b>	VK_I	RGTGCAGATTTTCAGCTTCCTGCT	Bohemer et al
	VK_II	TGGACATGAGGGCYCCTGCTCAGT	
	VK_III	CTSTGGTTGTCTGGTGTGAYGGA	
	VK_IV	GTTGCTGCTGCTGTGGCTTACA	
	VK_V	GTATCTGGTACCTGTGG	
	VK_VI	TGCCTGTTAGGCTGTTGGTGCT	
	VK_VII	GCTCAGTTCCTTGGTCTCCTGTTGC	
	VK_VIII	TGGGTGCTGCTGCTCTGGGT	
	VK_IX	CAGTTCCTGTTTCTGTTARTGCTCTGG	
	VK_X	TGCTCTGTTATATGGTGCTGATGGG	
<b>Primer VK rv</b>	CK	ACATTGATGTCTTTGGGGTAGAAG	Meyer et al

**Table 3.3.3.** Forward primers anneal on leader sequences and reverse on constant region. Forward primer of each chain and reverse of heavy chain were pooled to perform a single PCR reaction per sample.

	Primer ID	Primer sequence
<u>Primers VH fw</u>	VH_I	CTGTTGCTCTGGGTTCCAGGATCTACAGGC <b>G</b> AWGTGCAGCTGGTGGAGTC
	VH_II	CTGTTGCTCTGGGTTCCAGGATCTACAGGC <b>C</b> AGGTGCAGCTGAAGSAGTC
	VH_III	CTGTTGCTCTGGGTTCCAGGATCTACAGGC <b>G</b> ARGTGAAGCTGGTGGARTC
	VH_IV	CTGTTGCTCTGGGTTCCAGGATCTACAGGC <b>C</b> AGGTCCAAGCTGCAGCAGCC
	VH_V	CTGTTGCTCTGGGTTCCAGGATCTACAGGC <b>S</b> AGGTYCAGCTGCARCAGTC
	VH_VI	CTGTTGCTCTGGGTTCCAGGATCTACAGGC <b>CA</b> AGTGCAGATGAAGGAGTC
	VH_VII	CTGTTGCTCTGGGTTCCAGGATCTACAGGC <b>C</b> AGATCCAGTTGGYGCAGTC
	VH_VIII	CTGTTGCTCTGGGTTCCAGGATCTACAGGC <b>C</b> AGGTCCAAGCTCCAGCAGCC
	VH_IX	CTGTTGCTCTGGGTTCCAGGATCTACAGGC <b>C</b> AGGTGCAACTGAAGCAGTC
<u>Primers VH rv</u>	CH_I	<b>GGGTACACGCTAGGGGCTGTTGTTTTGGC</b> GCTCGAGACGGTGACCGTGG
	CH_II	<b>GGGTACACGCTAGGGGCTGTTGTTTTGGC</b> GCTCGAGACTGTGAGAGTGG
	CH_III	<b>GGGTACACGCTAGGGGCTGTTGTTTTGGC</b> GCTCGAGACAGTGACCAGAG
	CH_IV	<b>GGGTACACGCTAGGGGCTGTTGTTTTGGC</b> GCTCGAGACGGTGACTGAGG
<u>Primers Vk fw</u>	VK_I	CTGTTGCTCTGGGTTCCAGGATCTACAGGC <b>G</b> AAAWTGTGCTCACCCAGTC
	VK_II	CTGTTGCTCTGGGTTCCAGGATCTACAGGC <b>CA</b> AATTGTTCTCACCCAGTC
	VK_III	CTGTTGCTCTGGGTTCCAGGATCTACAGGC <b>CR</b> ACATTGTGCTGACCCAATC
	VK_IV	CTGTTGCTCTGGGTTCCAGGATCTACAGGC <b>G</b> AAACAAGTGTGACCCAGTC
	VK_V	CTGTTGCTCTGGGTTCCAGGATCTACAGGC <b>G</b> GATATTGTGATGACSCAGGC
	VK_VI	CTGTTGCTCTGGGTTCCAGGATCTACAGGC <b>CR</b> RRTTGTGATGACCCARAC
	VK_VII	CTGTTGCTCTGGGTTCCAGGATCTACAGGC <b>G</b> GATATCCAGATGACACAGAC
	VK_VIII	CTGTTGCTCTGGGTTCCAGGATCTACAGGC <b>G</b> GACATTGTGATGACMCAGTC
	VK_IX	CTGTTGCTCTGGGTTCCAGGATCTACAGGC <b>G</b> GACATCCAGATGACHCAGTC
<u>Primers Vk rv</u>	CK_I	<b>GATGGACACGGTAGGAGCGGCGTCAGCTCT</b> TTTCAGCTCCAGCTTGGTCCC
	CK_II	<b>GATGGACACGGTAGGAGCGGCGTCAGCTCT</b> TTTTATTCCAGCTGGTCCC
	CK_III	<b>GATGGACACGGTAGGAGCGGCGTCAGCTCT</b> TTTKATTTCCARCTTKGTSCC

**Table 3.3.4:** In black, specific sequence for heavy and light variable region in forward primer and sequences annealing on constant chains for reverse primers. In red, tails compatible with the leader sequence of the expression plasmids and the primers for direct Illumina sequencing; in blue for heavy chain and violet for light kappa chain, sequences annealing with the constant regions of expression vectors and compatible the primers for direct Illumina sequencing.

Cycler program PCR1		
98°C	2 min	
98°C	10 sec	X 5
57°C	20 sec	
72°C	30 sec	
98°C	10 sec	X 30
60°C	20 sec	
72°C	30 sec	
72°C	2 min	
10°C	∞	

PCR1	
Reagent	Volume $\mu$ l
cDNA	2 $\mu$ l
primers mix for (5 $\mu$ M)	0,30 $\mu$ l
primers mix rev (10 $\mu$ M)	0,2 $\mu$ l
Q5 <sup>®</sup> High-Fidelity 2X MM (New England Biolabs)	10 $\mu$ l
Ultrapure Distilled Water (Invitrogen)	7,50 $\mu$ l
total volume	20 $\mu$ l

**Table 3.3.5:** Nested PCR: Cycler program of the first PCR/PCR1 on the left, mix composition of the PCR1 on the right

Cycler program PCR2		
98°C	2 min	
98°C	10 sec	x15
68°C (-0.5°C/cycle)	20 sec	
72°C	30 sec	
98°C	10 sec	x20
60°C	20 sec	
72°C	30 sec	
10°C	∞	

PCR2	
Reagent	Volume $\mu$ l
PCR1 not purified	2 $\mu$ l
primers mix for (10 $\mu$ M)	0,15 $\mu$ l
primers mix rev (10 $\mu$ M)	0,15 $\mu$ l
Q5 <sup>®</sup> High-Fidelity 2X MM (New England Biolabs)	10 $\mu$ l
Ultrapure Distilled Water (Invitrogen)	7,7 $\mu$ l
total volume	20 $\mu$ l

**Table 3.3.6:** Nested PCR: Cycler program of the second PCR/PCR2 on the left, mix composition of the PCR2 on the right

	Tail
VHL.fw	CTGTTGCTCTGGGTTCCAGGATCTACAGGC
CH.rv	GGGTACACGCTAGGGGCTGTTGTTTTGGC
CL.rv	GATGGACACGGTAGGAGCGGCGTCAGCTCT
	Illumina
Read 1 5'	TCGTCGGCAGCGTCAGATGTGTATAAGAGACAG
Read 2 5'	GTCTCGTGGGCTCGGAGATGTGTATAAGAGACAG
	<b>HTS primers</b>
VHL.fw	TCGTCGGCAGCGTCAGATGTGTATAAGAGACAGCTGTTGCTCTGGGTTCCAGGATCTACAGGC
CH.rv	GTCTCGTGGGCTCGGAGATGTGTATAAGAGACAGGGGTACACGCTAGGGGCTGTTGTTTTGGC
CL.rv	GTCTCGTGGGCTCGGAGATGTGTATAAGAGACAGGATGGACACGGTAGGAGCGGCGTCAGCTCT

**Table 3.3.7:** HTS1 primers: Illumina compatible sequences to PCR2 5' and 3' tails

Cycler program HTS1			HTS1	
			Reagent	Volume $\mu$ l
98°C	2 min	x10	PCR2 purified	3 $\mu$ l
98°C	10 sec		primer for (10 $\mu$ M)	0,2 $\mu$ l
62°C	20 sec		primer mix rev (10 $\mu$ M)	0,2 $\mu$ l
72°C	30 sec		Q5® High-Fidelity 2X MM (New England Biolabs)	12,5 $\mu$ l
98°C	10 sec	x15	Ultrapure Distilled Water (Invitrogen)	9,1 $\mu$ l
72°C	40 sec		total volume	25 $\mu$ l
72°C	3 min			
10°C	$\infty$			

**Table 3.3.8:** HTS1: Cycler program conditions on the left , mix composition on the right

HTS Illumina indexed primer*	Illumina cod.
IDT® for Illumina® DNA/RNA UD Indexes <b>Set A</b> , Tagmentation (96 Indexes, 96 Samples)	20027213
IDT® for Illumina® DNA/RNA UD Indexes <b>Set B</b> , Tagmentation (96 Indexes, 96 Samples)	20027214
IDT® for Illumina Nextera DNA Unique Dual Indexes <b>Set C</b> (96 Indexes, 96 Samples)	20027215
IDT® for Illumina Nextera DNA Unique Dual Indexes <b>Set D</b> (96 Indexes, 96 Samples)	20027216

**Table 3.3.9:** Commercial Illumina primer set

Cycler program HTS2			HTS2	
			Reagent	Volume $\mu$ l
98°C	2 min	x5	Q5® High-Fidelity 2X MM (New England Biolabs)	12,5
98°C	10 sec		Ultrapure Distilled Water (Invitrogen)	3,5
62°C	20 sec		Final volume	16
72°C	30 sec		<b>And in each reaction:</b>	
98°C	10 sec	x15	HTS2 Illumina indexed primer*	3
72°C	30 sec		Template 3 $\mu$ l VH + 3 $\mu$ l VL of <b>HTS1 dil.</b>	6
72°C	3 min		Final volume	9
10°C	$\infty$			

**Table 3.3.10:** HTS2: Cycler program conditions on left, mix composition on the right

### 3.4 Expression of recombinant monoclonal antibodies in Expi293 mammalian expression system

To produce recombinant murine monoclonal antibodies, the mammalian Expi293 cell line was transfected with a mixture of plasmids encoding for the heavy and light chain on each mAb. Two similar protocols were followed, for small scale expression (24 deep-well, triplicate 3 ml of each mAb) and large-scale expression (Erlenmeyer flask, in 30 or 60 ml), according to the manufacturer's instructions (Gibco, catalogue number A14635). Expi293 cells were diluted to the cellular density required for the Transfection ( $3 \times 10^6$  viable cells/mL) in Expi293 Expression Medium (Gibco, cod.

A1435101) and incubated at 37°C, CO<sub>2</sub> 8% and 100rpm shaking. The VH and VK purified expression plasmids were used as transfecting DNA in 1:2 ratio: 1 µg of total plasmid DNA per mL of culture volume to transfect was diluted with Opti-Plex Complexation Buffer (Gibco cod. A4096801), mixed by inversion and incubated 5 minutes at Room Temperature. ExpiFectamine 293 reagent (in ExpiFectamine 293 Transfection Kit, Gibco, cod. A14524) was diluted in Opti-Plex Complexation Buffer and mixed by swirling or inversion and incubated for 5 minutes at Room Temperature. After the incubation, the diluted ExpiFectamine Reagent was combined with the diluted plasmid DNA and then mixed by swirling or inversion. The Expifectamine/plasmid DNA complexes were incubated at Room Temperature for 20 minutes. Immediately after, the complexes were added to the cells, swirling the flask gently during addition (in the case of 24 well plate no swirling is necessary), then the cells were incubated in a 37°C incubator with > 80 % relative humidity and 8% CO<sub>2</sub> on an orbital shaker. 18-22 hours post-transfection, ExpiFectamine™ 293 Transfection Enhancer 1 and Expifectamine™ 293 Met (-) Enhancer 2 (in ExpiFectamine™ 293 Transfection Kit, Gibco, cod. A14524) were added to the flask or 24 deep-well plate. After 5/7 days post-transfection cells were removed by centrifugation and the supernatants containing the secreted mAbs were collected.

### 3.5 Recombinant mAbs purification with protein G/A

Purification of mAbs was carried out using a Protein G microplate (Cytiva) for antibody capture from cellular supernatants. The supernatants, approximately 10 mL for each mAb, were added onto the protein G resin equilibrated with buffer A (PBS). After column washing with 10 volumes of buffer A, bound antibodies were eluted with buffer B (0,1 M Glycine-HCl, pH 2,6). To neutralize the pH of the eluted antibodies, collection plate wells contained 10% of the final volume per fraction of 1 M Tris-HCl buffer, pH 9. Collected mAbs were buffer exchanged in PBS with a desalting plate (Thermo), according to the manufacturer's protocol. Purified mAbs quantity was measured using a NanoDrop8000 spectrophotometer (Thermo Scientific) and an internal IgG reference, while mAb monomer purity was characterized by analyzing absorbance at 215 nm in SE-UPLC after resolution on Superdex 200 increase 5/150 GL column (PBS).

### 3.6 Gonococcal growth conditions

Fresh cultures of Ng strains were prepared from frozen stocks by streaking bacteria onto gonococcal agar (GCA), consisting of agar base supplemented with 1% v/v IsoVitalex, and incubating the plate ON at 37°C, 5 % CO<sub>2</sub>. On the following day, bacteria were inoculated in in GC liquid medium supplemented with 1% Isovitalax at OD<sub>600</sub>=0.1 and grown at 37°C until mid-exponential phase (i.e., OD<sub>600</sub> = 0.5).

### 3.7 Western Blot with Ng lysates

The pellet of different Ng strains stored at -20°C were resuspended with 200 µl of PBS; the samples were lysed with three steps of freeze (dry-ice) and thaw (water 37°C). Thereafter a BCA assay was carried out to define the protein concentration of each sample. The concentration was defined using GraphPad Prism 7.0 and the function Interpolation linear regression to a standard curve.

The samples for western blot (WB) were prepared at a final concentration of 100 µg of total protein content corresponding to different volume depending on the strain, these volumes were put in a new tube with 50 µl of Sample Buffer 4X (Thermo Fisher Scientific), reducing buffer (10x) (Thermo Fisher Scientific) and H<sub>2</sub>O to reach the final volume of 200 µl. Samples were then boiled for 10 min at 100°C and 20 µl of each sample (correspond to 10 µg total protein content) were loaded into a NuPAGE™ 4-12 % Bis-Tris Gel. The gel was run for 40 minutes at 180 V in MES buffer. The gel was

then transferred with iblot (Invitrogen) using iblot Transfer Stacks Nitrocellulose Mini (Invitrogen) for 5 min. The membrane was blocked with 10 ml of BioRad Blocking Buffer for 5 min. The primary mAb (Final concentration 1 µg/ml) was added to the blocking solution and incubated for 1 hour at room temperature. After the incubation, the membrane was washed 3 times with PBS + 0.25 % Tween and incubated with secondary anti-mouse Ab HRP-conjugated diluted 1:10,000 in blocking buffer and incubated 30 minutes at RT. After 3 washes with PBS + 0.25 % Tween, the membrane was revealed using SuperSignal West Pico PLUS Chemiluminescent Substrate (Thermo Fisher Scientific) and the signal detected with the Chemidoc touch instrument (Bio-Rad).

### 3.8 Dot Blot with Ng Opacity associated proteins (Opa) constructs

#### **Cloning, expression, and purification of recombinant proteins**

Recombinant proteins used in this PhD thesis were previously generated in the lab as described by Cappelli et al., 2024. The OpaB-loop3a recombinant construct containing a longer OpaB-loop3 (HVRHSIDSTKKITGTLTAYPSDADA AVTVYPDGHQKNTYQKSNSSR) has been generated using the same protocol described in the paper. The plasmid encoding for D3-OpaB loop3 was purchased from Twist Bioscience. The expression plasmids (pET29b+) encoding for designed molecules were synthesized by Twist bioscience optimizing the codon usage for expression in the *E. coli* and adding an His-tag at the N-terminus for the protein purification.

Protein expression was performed using *E. coli* BL21(DE3) t1r strain (New England Biolabs). After 8h preculture in LB-PTK medium + 50ug/mL kanamycin at 37°C shaking, the cells were diluted in 500 mL of HTMC media (Glycerol 15 g/L; Yeast Extract 30 g/L; MgSO<sub>4</sub> x7H<sub>2</sub>O 0.5 g/L; KH<sub>2</sub>PO<sub>4</sub> 5 g/L; K<sub>2</sub>HPO<sub>4</sub> 20 g/L; KOH 1 M to pH final 7.35±0.1), and further incubated with shaking (160 rpm) at 20°C for 16-18h, followed by induction with 1mM IPTG and incubation for additional 24h at 20°C. Soluble proteins were extracted from bacteria by lysis with cell lytic express. The protein purification was performed with immobilized metal affinity chromatography (IMAC) using Ni-NTA agarose resin (Thermo Fisher Scientific), two wash steps with 20 mM imidazole in PBS buffer and an elution buffer (PBS + 350mM imidazole). Fractions containing the target protein were collected and buffer exchange was performed in PBS buffer, with PD10 column. SDS-PAGE analysis was performed to check protein purity and the concentration was determined by UV-Vis absorbance at 280nm (Nanodrop device).

#### **Dot blot**

5 µg of proteins were spotted on a nitrocellulose membrane and let dry for 10 minutes. The membrane was then blocked with PBS + 3% milk + 0.1% Tween. The binding with primary antibody (diluted 1:1000 in PBS + 3% milk) was allowed for 1h at room temperature with shaking, then the membrane was washed three times for 5 minutes with 10mL of PBS + 0.1% Tween. The secondary anti-mouse antibody conjugated with horseradish peroxidase (HRP) was then added (diluted 1:1000 in PBS + 3% milk) to the membrane for 1h. Three additional washing steps were performed, as above, before adding the chromogenic substrate 4-chloro-1-naphthol. The signal was acquired using GelDoc XR+ imaging system (Bio-Rad).

### 3.9 Serum bactericidal activity with exogenous human complement (hSBA)

Functional characterization of murine mAbs was performed by serum bactericidal assay (SBA) against 5 different Ng strains: FA1090, MS11, WHO-M, F62 and WHO-N. Human serum obtained from volunteer donors with no detectable intrinsic bactericidal activity was used as complement source. Fresh cultures of Ng strains were prepared from frozen stocks by streaking bacteria onto gonococcal agar (GCA), consisting of agar base supplemented with 1% v/v IsoVitaleX, and incubating the plate ON at 37°C , 5 % CO<sub>2</sub>. On the following day, bacteria were inoculated in in GC liquid

medium supplemented with 1% Isovitalax at OD<sub>600</sub>=0.1 and grown at 37°C until mid-exponential phase (i.e., OD<sub>600</sub> = 0.5). FA1090, F62, MS11, WHO-M growth was also supplemented with 1 µg/ml, 0.1 µg/ml, 0.2 µg/ml, 0.2 µg/ml respectively, of CMP-NANA (Cytidine-5'-MonoPhospho-N-Acetyl 915 NeurAminic acid sodium salt). Bacteria were then diluted in PBS + 0.1% glucose + 1% BSA to a working dilution of 10x10<sup>3</sup> CFU/mL. Subsequently, bacteria were two-fold diluted and incubated with 10% human complement and murine mAbs at different concentrations for 1h at 37°C. After the incubation, 100 µL of GC medium plus 0.5% of Bacto Agar, were added to the reaction mixture and incubated ON at 37°C with 5% CO<sub>2</sub>. The day after, plate well images were automatically acquired with a high throughput image analysis system and the Colony Forming Units (CFUs) were automatically counted for each well by an internal customized colony counting software. Bactericidal titers were defined as the monoclonal antibody concentration giving 50% decrease in CFU number compared to the reaction mixture, in the absence of antibodies.

### 3.10 Protein array protocol

Protein microarrays were generated and printed as described previously (Viviani et al., 2023). All the recombinant antigens were spotted at 0.5 mg/ml in 40% glycerol, while the vesicles at 0.25 mg/ml in 20% glycerol. Controls consisted of 8 serial two-fold dilutions of human IgG (from 0.5 mg/ml to 0.004 mg/ml in 40% glycerol) as well as PBS + 40% glycerol spots. All samples were printed in replicates randomly onto nitrocellulose-coated glass slides (FAST slides; Maine Manufacturing). The ink-jet spotter Marathon Argus (Arrayjet) (200 pl each spot) was used for printing at controlled temperature and humidity (18 °C and 50–55%, respectively). Preliminary experiments with mAbs showed that a range in concentration of 0,5 -1 µg/ml of mAbs corresponded to the best signal to noise ratio. Sera profiling experiments were performed as described Viviani et al., 2023 with few modifications. Each array was saturated with 500 µl of BlockIt blocking buffer (BKT; ArrayIt) and incubated for 1 hour at RT in a dark humid chamber. After this incubation, 300 µl of BlockIt blocking buffer with diluted Ab (0,5 or 1 µg/ml) of interest were added on the mini-array and incubated for 1 hour at RT in the dark humid chamber. Slides were washed 3 times with PBS + 0,1% Tween (5 minutes for each wash) and 300 µl of AlexaFluor647 AffiniPure rabbit anti-mouse IgG, Fc fragment specific (cod: 115-605-174) diluted 1:800 in BlockIt blocking buffer were added for 1 hour at RT in the dark humid chamber. Slides were washed 2 times with PBS + 0,1% Tween, followed by 2 washes in milliQ water. Slides were dried with compressed nitrogen flow, then the image was acquired with InnoScan 710-AL (Innopsys LifeSciences). Spot fluorescence intensities (FI) were calculated using ImaGene 9.0 software (Biodiscovery Inc.) and data analysis was performed using in-house developed R scripts. For each protein, the FI of the replicates was subtracted by local background values surrounding each spot and averaged, resulting in a single data point per sample named Mean Fluorescence Intensity (MFI). All obtained MFI scores were then ranked in four categories: (1) high reactivity; MFI ≥ 30,000; (2) medium reactivity; 15,000 ≤ MFI ≤ 29,999; (3) low reactivity; 6000 ≤ MFI ≤ 14,999; (4) no reactivity; MFI ≤ 5,999.

## 4 RESULTS

### 4.1 Strategy for the isolation and expression of specific Ag<sup>+</sup> mAbs against gonococcus

In order to isolate gonococcus-specific monoclonal antibodies, we set-up a workflow from the immunization of animals with OMVs, used as surrogate of the bacterial outer membrane, to the isolation of antigen-specific memory B-cells (MBCs) to the production of recombinant mAbs, as represented in Figure 4.1.1. In brief, mice were immunized 3 times with OMVs obtained by gonococcal strain FA1090. Two weeks after the third immunization mice were sacrificed, the spleens were collected, and Ag-specific single MBCs were isolated by FACS against the target antigen of interest. Cells were then incubated in 384 well plates with feeder cells and in presence of stimuli (IL-2 and IL-21) to allow their clonal expansion and the production of natural mAbs in the supernatants. Raw supernatants were analyzed by Luminex in two independent assays to detect IgG amount and binding specificity against the antigens of interest. Based on the Luminex results, the cell pellets of interest were lysed, retrotranscribed and processed through PCRs and sequencing to recover the paired VH:VL regions of the positive mAbs. At this point, expression plasmids containing the genes of interest fused to the constant regions of murine IgG2a and IgK, were used to transfect mammalian cell line Expi293: the recombinant mAbs secreted in the supernatants were purified for further characterization.

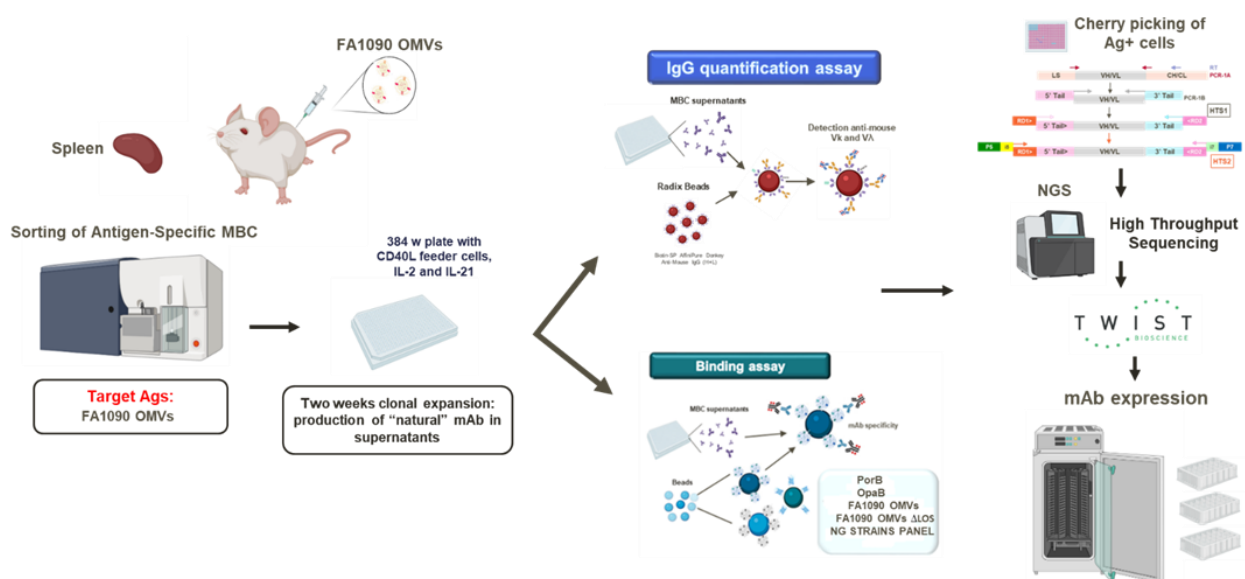


**Figure 4.1.1:** Overview of the murine single B-cell platform as tool to isolate Ag-specific single MBCs-derived mAbs from immunized mice (Image generated with BioRender).

### 4.2 Results from sorting of Ng OMV-specific Memory B cells (MBCs) from mouse splenocytes with single-cell FACS sorting

As extensively reported in literature, reactive or B-cell memory is the rapid recall or anamnestic response on re-encounter with antigens that is mediated by memory B cells residing in the spleen and other lymphoid organs and circulating in the blood (Stanley, M., 2010). To isolate the Memory B cells, CD1 mice at 7 weeks of age were immunized 3 times with gonococcal OMVs and 15 days after 3<sup>rd</sup> immunization, spleens were collected, and Ag-specific single B-cells isolated by FACS Aria Cell Sorter in 384 well plates. A Gating strategy was applied to isolate the specific population of interest: first of all, live cells were selected with Live-Dead fluorophore, which is able to permeate

the nuclei of dead cells. Cells were then evaluated for their morphology and the typical lymphocyte population was selected, then duplets were excluded, and single cells were examined for the presence of specific marker CD19, typically expressed on the surface of the B cells. We then selected the switched population negative for IgD and IgM: in this population of MBCs the Ag+ B cells to be sorted are present. The cells were previously incubated with the target antigen, Ng FA1090 OMVs, marked with AlexaFluor488, so the final gate for sorting was done on AlexaFluor488-positive MBCs. In Fig. 4.2.1 it is reported a representative gating strategy with all the subsequent selection gates previously described. In panels C1 and C2, the OMV+ MBCs of immunized spleen vs Negative control are reported. The number of Ag-specific cells selected in the final gate (N) is reported in the figure and highlights how the animals immunized with Ng OMVs responded one hundred times more respect to the negative control animals which received the adjuvant alone (Figure 4.2.1).

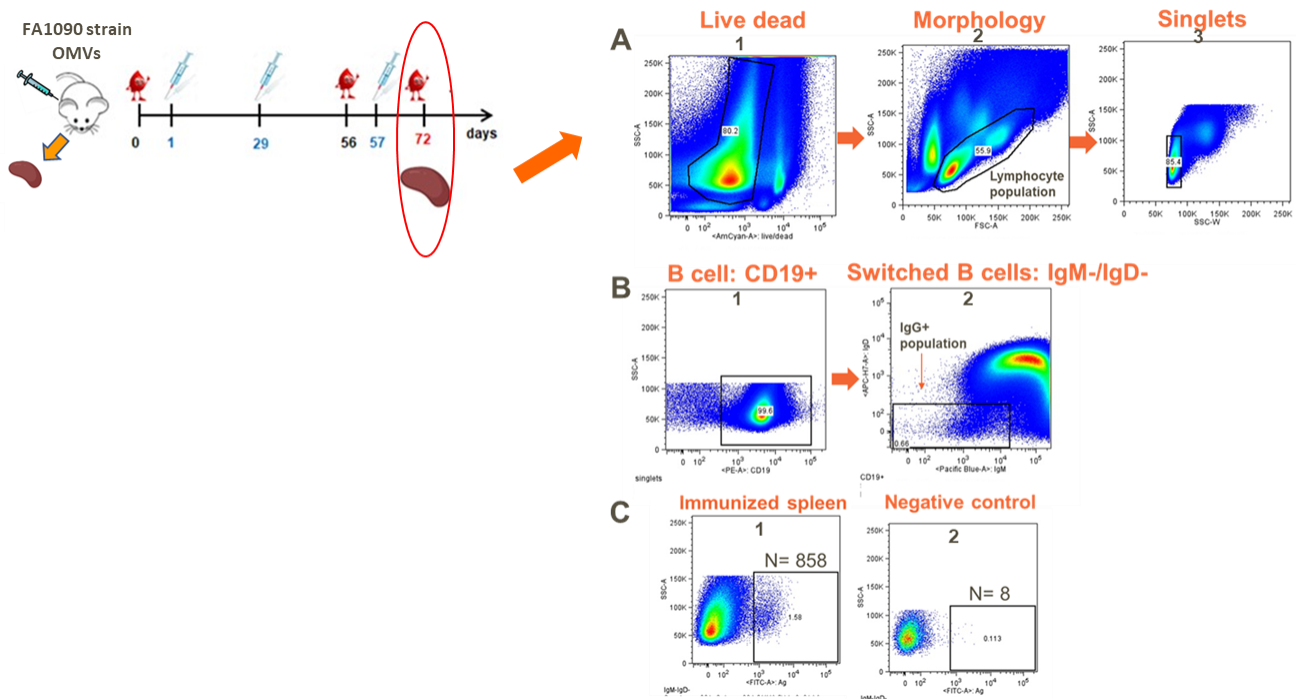


**Figure 4.2.1: FACS Aria gating strategy:** Live cells were selected with Live-Dead fluorophore (A1) and based on their morphology (A2), single cells (A3) were examined for the presence/absence of specific markers (CD19+) (B1), to select the MBCs negative to IgM and IgD (B2). In the last two panels are reported the OMV+ MBCs versus negative control (C1) and (C2). N=Ag specific MBC on 1 million singlets.

The selected population, able to bind the fluorescently labelled OMVs, was single-cell sorted in 384 well plates with CD40L-expressing feeder cells and medium containing IL-2 and IL-21 stimuli; to allow clonal expansion (cellular replication and release of natural mAbs in the supernatants), the plates were incubated at 37°C for two weeks. After two weeks, cell supernatants (SN) were transferred in a new 384 well plate for IgG analysis (first plate) while lysis buffer was immediately added to cells pellet and plate frozen (second plate) (Figure 4.2.2). A total of 3 spleens from OMV

immunized mice was processed and 816 MBCs were isolated as OMV-specific and further characterized.

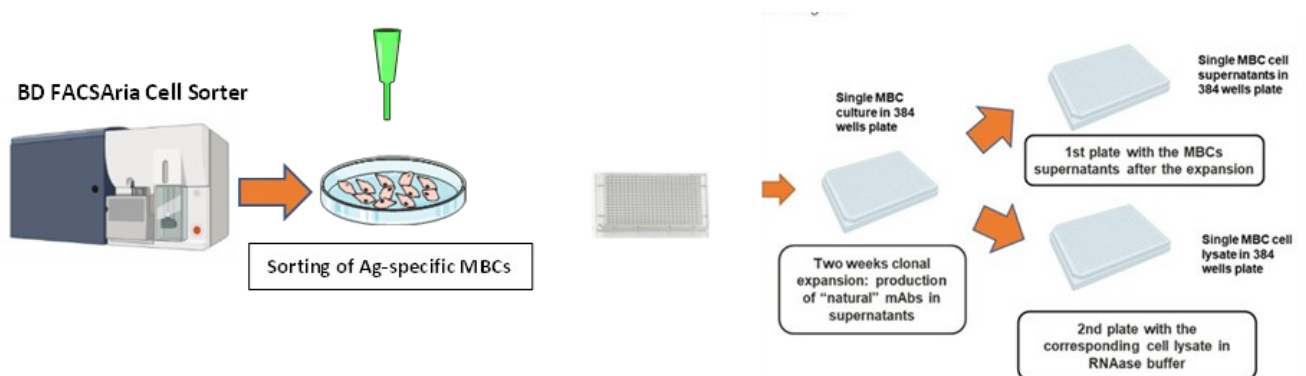


**Figure 4.2.2:** Schematic representation of the workflow after single-cell sorting (Image generated with Biorender).

#### 4.3 Results from Luminex assays: IgG detection and Binding Specificity

A total of 816 raw supernatants were analyzed through Luminex FlexMap Instrument System in 384 well plates to quantify the secreted mAbs. The analysis was performed using Streptavidin magnetic beads conjugated with Biotin anti Mouse IgG: the binding occurs through the biotin present in the anti-IgG antibody, which interacts with the Streptadivin on the beads. The analysis was performed to detect IgG in the cells supernatants after the two weeks of clonal expansion, the table below summarizes the number of samples analyzed and the number of positive IgG in the samples obtained: tested supernatants were positive for IgG in a range going from 60 to 70%, confirming a good viability and clonal expansion of sorted cells (Table 4.3.1)

Sample	Sorted cell number	IgG+ supernatants number
Spleen 1	308	239
Spleen 2	288	192
Spleen 3	220	134

**Table 4.3.1:** On a total of 816 derived MBCs supernatants, 69 % were positive to IgG binding.

Luminex technology depend on the use of magnetic fluorophore-coded beads, each one coated with different analytes that can be used to screen in parallel multiple conditions of interest. We wanted to dissect the recognition pattern of mAbs induced in mice upon vaccination with gonococcal OMVs, so the advantage of this technology was given by the possibility to perform multiplexing and test each single mAb against a panel of different antigens.

Binding between antigens coated on beads and mAbs present in raw supernatants was performed in a well of 384 well plate that allows the use of a very small amount of material and high throughput

analysis and then a phycoerythrinated (PE) Ab specific for mouse Fc fragment is added to the mixture to reveal the signal. Beads were read on a dual-laser flow-based detection instrument, the FlexMap® analyzer: one laser classified the beads, allowing the determination of the analyte that is being detected. The second laser determines the magnitude of the PE-derived signal, which is in direct proportion to the amount of mAb bound to a specific bead.

The IgG+ supernatants were subsequently subjected to a second analysis conducted to establish the binding specificity of the mAb produced through Luminex FlexMap: we aimed at confirming the specificity of the secreted mAbs to the target antigen FA1090 OMVs, used as a bait for the sorting. This step is needed to avoid the further analysis of false-positive samples. The graph below reports the summary of the overall numbers obtained from the two Luminex analysis of the 816 supernatants, with the percentage of IgG+ positive supernatants versus the positivity of the secreted mAbs against the target antigen. From a total of 816 supernatants, 565 (69%) were positive to IgG detection, while 251 (31%) were IgG negative. The IgG positive samples had positive binding to Ng OMVs in 471 samples (83%) highlighting high binding specificity of the sorted cells (Figure 4.3.1).

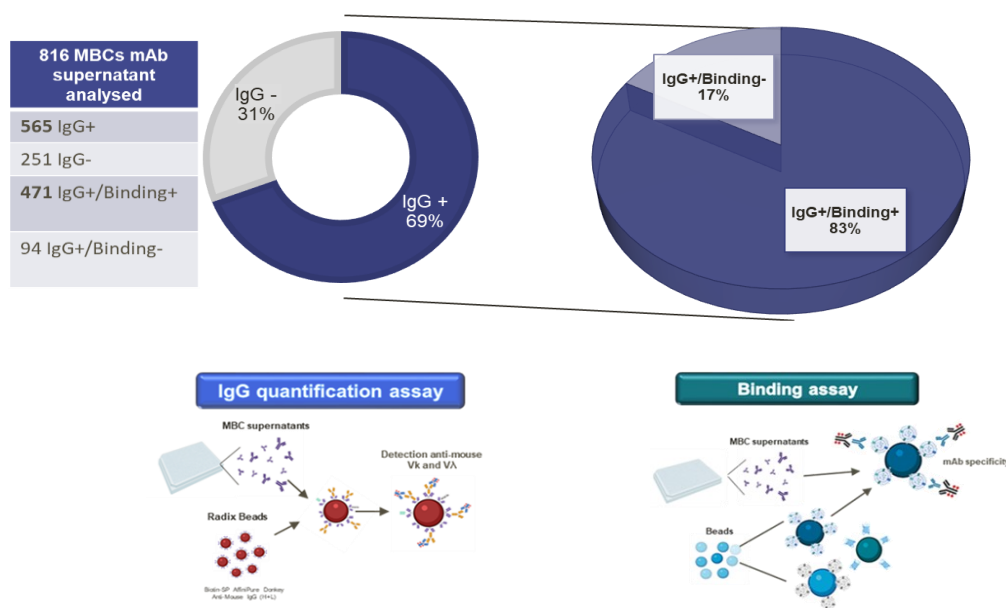


**Figure 4.3.1:** A total of 816 supernatants were analyzed to verify the presence of IgG in the samples and to define the binding specificity of the mAbs produced: 69 % of the MBCs supernatants generated IgG (IgG+)and moreover 83 % of them interact at least with Ng OMVs (IgG+/Binding+) demonstrating high binding specificity. Overall, the analysis shows high recovery from the FACS sorting.

Also, to discriminate the mAb specificity against the surface exposed antigens of the bacteria, magnetic beads were covalently coupled with the major surface exposed antigens of gonococcus: Porin B (PorB) and the Opacity associated protein (OpaB). Both antigens were produced as recombinant proteins in *E.coli*.

The results of the analysis are reported in Figure 4.3.2. It was observed that the majority of the mAbs with an identified target (68%) were specific for PorB, confirming it as the most abundant and immunogenic protein on the bacterial surface; 8.7% of mAbs were positive to OpaB; 8.9% of mAbs

showed a peculiar cross recognition for both PorB and OpaB; the remaining 14.4% of mAbs, categorized as LOS & others, are mAbs that do not show recognition neither for PorB antigen nor for OpaB but they are able to bind the positive control, Ng OMV. These mAbs probably interact with other antigens expressed on gonococcal surface or with the LOS component of the bacterial surface that are not present in our Luminex multiplexing assay.

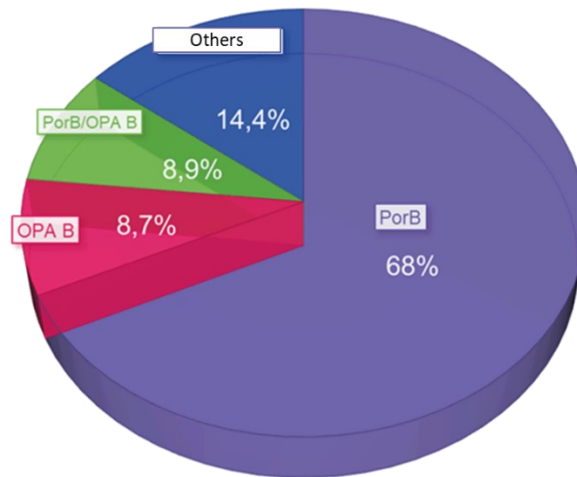


**Figure 4.3.2:** Pie chart representing the percentage of mAbs belonging to the clusters identified with the Luminex Binding Assay: the majority of the mAbs identified are specific against PorB (68%), the 8.7 % are specific for OpaB, the 8.9 % shows cross-recognition of both PorB and OpaB, the remaining 14.4% interact with other antigens expressed on Ng OMV surface.

#### 4.4 Isolation and Next Generation Sequencing (NGS) of Binding positive mAbs

Based on Luminex results, a cherry picking of Ag+ cells (frozen in lysis buffer to avoid RNA degradation) was conducted to recover full length VH:VL genes. For each isolated cell, antibody-encoding cDNA was generated using cell lysate as source of template mRNA in a RT reaction with Gene Specific Primers (GSPs). The cDNA was then used as template to specifically amplify the variable regions of the heavy and light chain of each antibody, as they represent the determinants of each specific binding to Ags. The variable heavy- and light-chains domains were amplified by two subsequent nested PCRs. The first PCR uses a mix of forward primers annealing across the leader sequence and the N-terminus of the V(D)J region, while the reverse primers anneal in the constant region of the immunoglobulins. The second PCR is carried out with primers strictly annealing to the 5' end of the variable region (V genes) and to the N-terminus part of the immunoglobulin constant region (all the primers used are listed in M&M section). All the primers of the second PCR were carrying at the 5' and 3' end tails compatible with cloning in plasmids expression vectors or following PCRs step to build an indexed Illumina library ready for HTS.

For the High Throughput Sequencing of these amplicons, an additional PCR step was performed to elongate VH and VL with Illumina universal tails (HTS1) and obtain the template for the last PCR step (HTS2). In this PCR, amplified heavy and light chains were mixed and Illumina dual indexed primers were added to the amplicons to allow the binding to the NGS flow cell and the association of each sample to specific indexes for the VH:VL discrimination during data analysis (demultiplexing) (Figure 4.4.1).

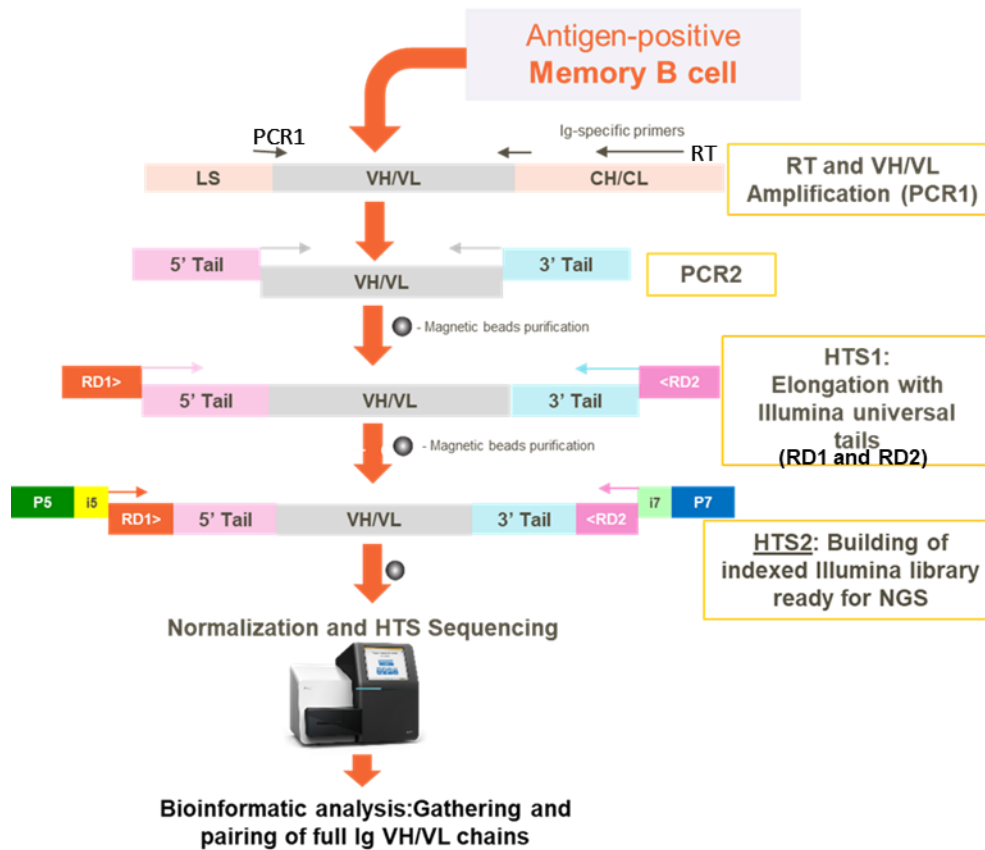


**Figure 4.4.1:** mAb platform from cell to sequence: schematic representation of the High throughput system for the recovery of full-length IgG VH/VL chains

Magnetic beads purification steps are necessary after PCR2, HTS1 and HTS2 to cut off primers leftover and avoid background in consecutive amplifications and MiSeq Illumina run. After the second PCR, samples were run on a 2% agarose precast gel (Invitrogen, cod n°GB00802) to verify the presence and the length (expected around 400-500 bp) of the PCR products (Figure 4.4.2).

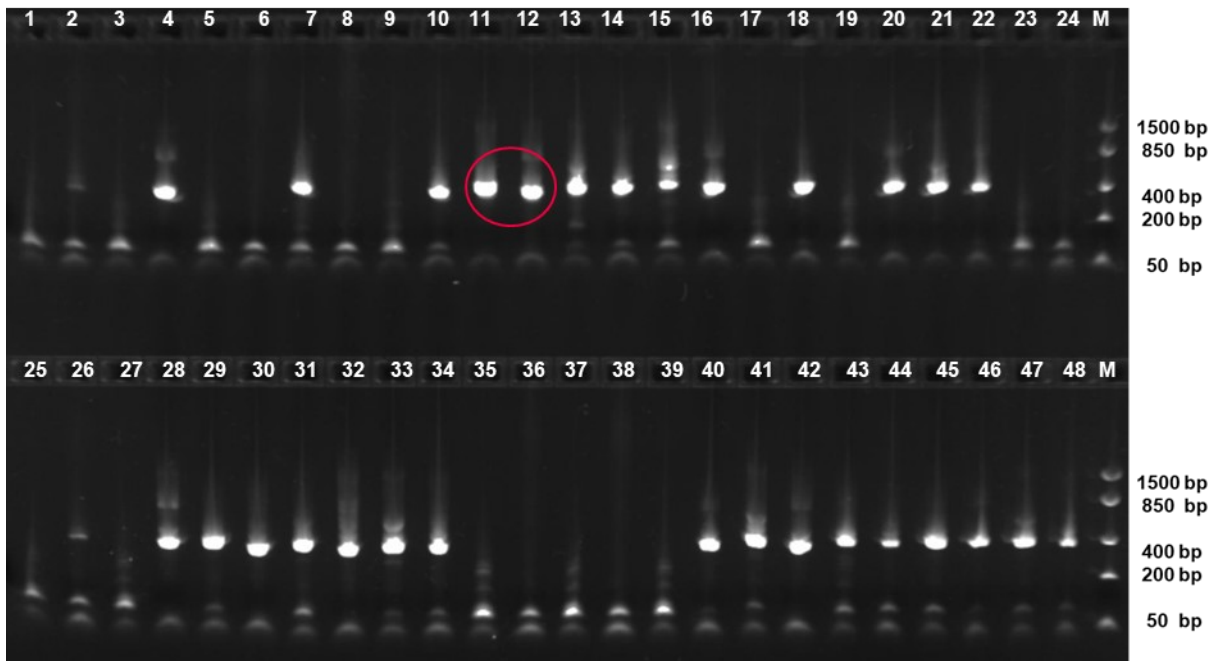


**Figure 4.4.2 Representative example of PCR2 products on gel:** Three  $\mu\text{L}$  of PCR products corresponding to the variable regions of the heavy and light chain of mAbs were loaded on a 48 wells precast gel and run for 30/35 minutes at 120V. Detection and acquisition was performed with GelDoc (BioRad) instrument. Above a representative gel: FastRuler Low Range DNA Ladder (Thermo Scientificc, cod. SM1103) was run on the right side of the gel (well M). The corresponding VH and VL fragments of each mAb were loaded in pairs: odd wells VH chain, even well VK chain of the same sample (the red circle represents an example of one sample positive both for H and L chain, expected size 400-500bp). The faint, low molecular weight bands visible in all samples, show primer mix leftover and relative by products which are removed by magnetic beads purification before proceeding with HTS PCR step, to favor the re-amplification of the correct PCR product.

To confirm the success of last HTS1 PCR, another 2% agarose gel was run before the purification step, as detailed in Figure 4.4.3. From agarose gel controls, on a total of 230 OMVs positive samples processed by RT and PCR steps, the recovery efficiencies are: VH about 52% (120 positive samples), VK about 61% (141 positive samples), but the VH+VK efficiency (samples showing both H and L product) is about 37% (86 positive samples).

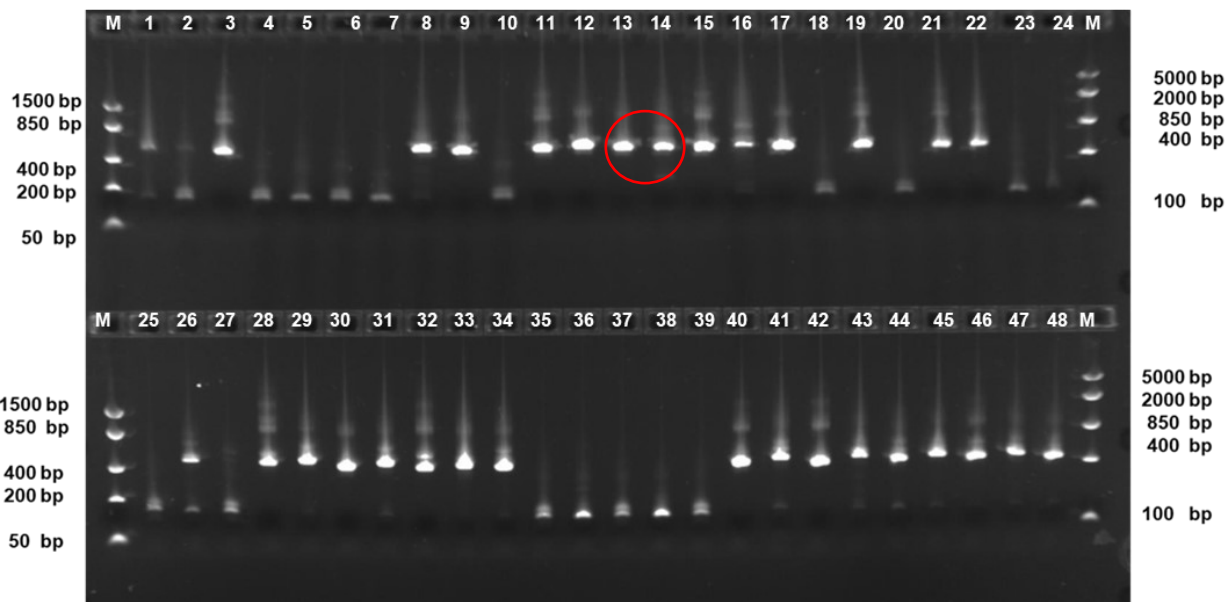


**Figure 4.4.3 HTS1 products on gel:** Three  $\mu$ L of PCR products corresponding to the variable regions of the heavy and light chain of mAbs enriched with Illumina universal tails were load on 48-well precast gel and run for 30/35 minutes at 120V. Detection and acquisition was performed with GelDoc (BioRad) instrument. Above a representative gel: FastRuler Middle Range DNA Ladder (Thermo Scientificc, cod. SM1113) was run on the left and right side of the gel (wells M). The corresponding VH and VL fragments of each mAb were loaded in pairs: odd wells VH chain, even well VK chain of the same sample (the red circle represents an example of one sample positive both for H and L chain, expected size 450-550bp). The faint, low molecular weight bands visible in all samples, show primer mix leftover and relative by products which are removed by magnetic beads purification before proceeding with HTS2 PCR step, to favor the re-amplification of the correct PCR product.

The successful incorporation of the Illumina universal tails in the VH/Vk amplicons, necessary for the further addition of Illumina indexes, is demonstrated by the slight increase in size of the HTS products, running now above 400 bp. HTS1 products were purified before the final addition of the Illumina Indexed Primers to build a library ready for NGS (HTS2 step). After HTS2 and Indexes incorporation, samples were then sequenced through Illumina MiSeq Platform and HTS data were analyzed by an in house developed pipeline to recover paired, unique full Ig VH:VL sequences. A total of 177 samples, showing an indexed amplification products from 450 to 600 bp, were included in the Illumina MiSeq run. After bioinformatic data analysis, 87 paired and unique VH:VL were identified and ordered as DNA codon-optimized in plasmids with murine IgG2a and IgK constant region, for transient expression in Expi293 cell lines.

#### 4.5 Transfection of VH/VL expression plasmids in mammalian cells

To express and test the recombinant mAbs of interest, we used the human cell line Expi293F. Expi293 Expression System are human cells derived from the HEK (Human Embryonic Kidney ) cell line and adapted to grow at high density in suspension culture. They are highly transfectable and able to generate optimal protein yields. To express recombinant mAbs, cells were co-transfected in 24-deep well plates with plasmids encoding paired VH and VL regions. Culture supernatants containing the secreted mAbs were harvested 6 days post-transfection. Raw culture supernatants were screened for the presence of mAbs by SDS-PAGE followed by Coomassie proteins staining. As reported in Figure 4.5.1, in the majority of supernatants a protein band at 150 KDa was visible, corresponding to the molecular weight of a correctly assembled mAb. Overall, we could observe successful mAb expression in 76% of the transfections.

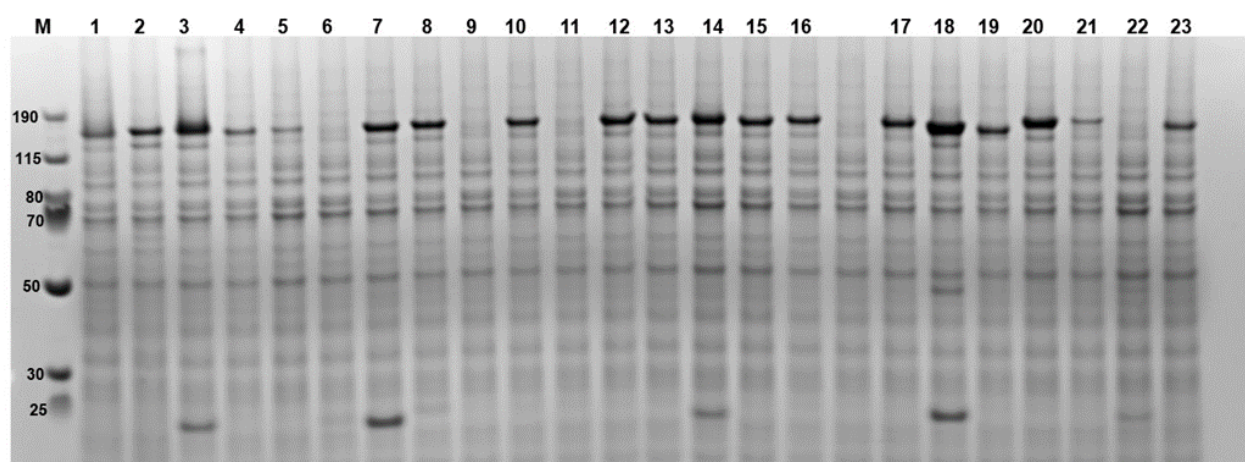


**Figure 4.5.1:** Raw supernatants from transfected Expi293 cells were run for 30 minutes at 180V; this gel corresponds to not reducing condition in which the expected size of the assembled mAb should be at expected molecular weight (MW) of 150 KDa . Representative plate of the mammalian transfection.

Despite the fact that the transfection conditions used were the same for all the constructs, we observed some variability in the expression level of the different mAbs. This might be dependent on the sequence of the different VH and VL chain. The mAbs were purified from the raw supernatants using protein-G resin for antibody capture and characterized with Size Exclusion Ultra Performance Liquid Chromatography (SE-UPLC). The results of this analysis showed monomer purity above 90 % for nearly all purified mAbs (data not shown). At the end of the process, we successfully purified 66 monomeric unique mAbs.

#### 4.6 Characterization of recombinant murine gonococcus mAbs

##### Overall results: from Ag specific-MBCs to recombinant mAbs

From a total of 816 sorted MBCs, 230 OMV-positive samples were selected and through RT and PCRs 177 paired VH:VL products were obtained: after HTS sequencing and NGS analysis 87 paired and unique sequences were retrieved and used to transfect mammalian cell line. 66 recombinant mAbs were successfully expressed and purified and 6 of them (2 anti-PorB, 2 anti-OpaB and 2 mAbs with unknown target) were selected for further functional characterization.

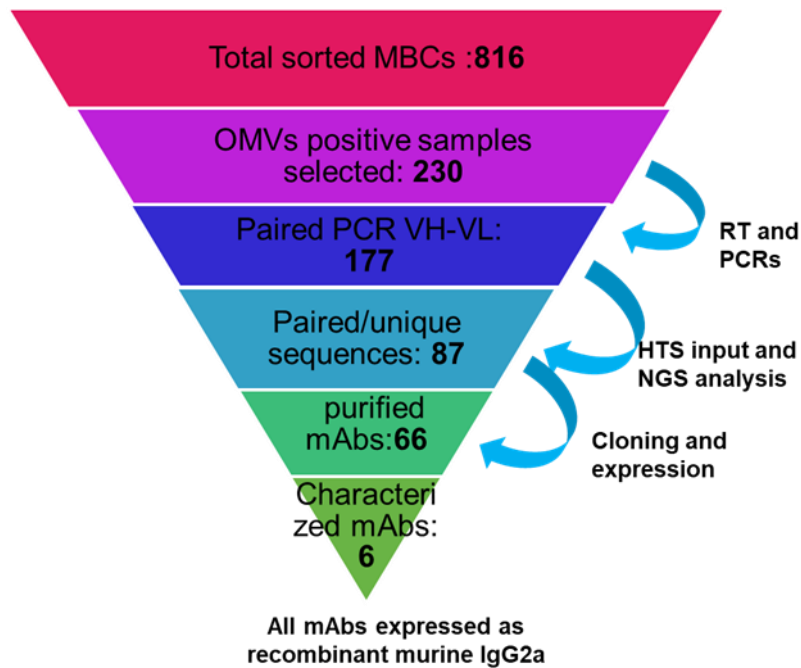


**Figure 4.6.1:** Pyramid shows the overall number obtained from a total of MBCs analyzed to the recombinant mAbs obtained, a panel of 6 mAbs were chosen to be further analyzed in specificity and functionality. The characterization of the other mAbs is ongoing.

##### Workflow used for characterization of recombinant murine Gono mAbs

In order to determine the specificity, cross-reactivity, cross-coverage, and functionality of mAbs, we set-up an analytical workflow. As represented in figure 4.6.2, a panel of six mAbs (2 anti-PorB, 2 anti-OpaB and 2 mAbs with unknown target) derived from mice MBCs sorted with gonococcal FA1090 OMVs, four different assays were carried out: Luminex assay was performed to confirm the specificity and assess cross-binding of the mAbs on a small number of strains, Western Blot was performed to assess protein recognition in a total bacterial extract, human Serum Bactericidal Assay (hSBA) to examine the functionality of the mAbs and protein microarray technology was used to evaluate mAb specificity and cross-reactivity on a large panel of strains.

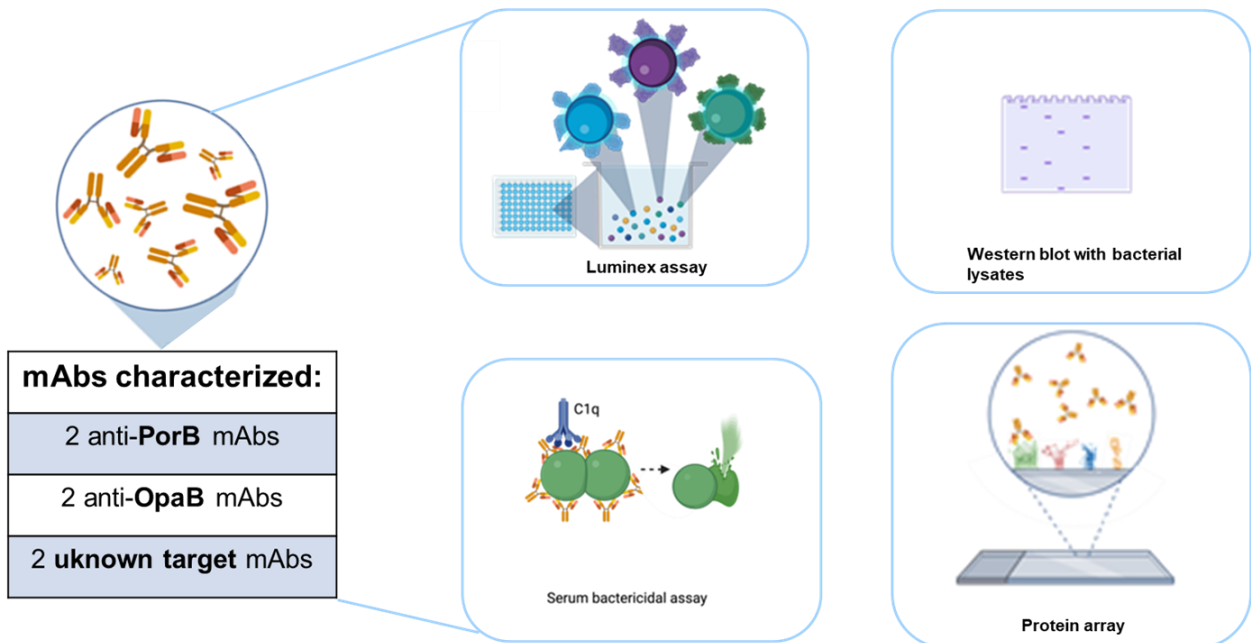
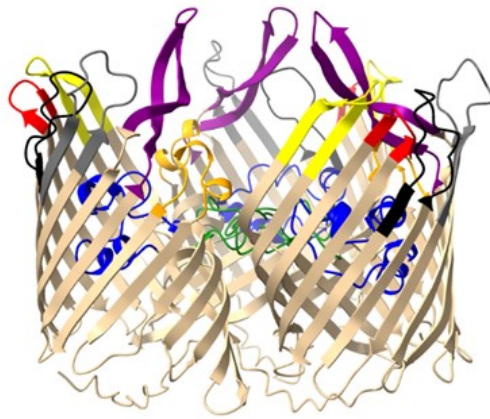


**Figure 4.6.2:** mAbs were evaluated through four different assays: Luminex multiplex assay to characterize cross-binding (A), WB to assess protein recognition from a total of bacterial extract (B), hSBA using human serum as source of complement to evaluate complement-mediated functional activity of mAbs (C), Protein chip array (D) to evaluate mAb specificity and cross-reactivity. Image created from BioRender.com

### Characterization of murine recombinant IgG2a mAbs specific for PorB

Porin B, the most abundant protein on the bacteria membrane of *N. gonorrhoeae*, representing approximately the 50% of the total membrane protein content (Guerrant et al., 2011). PorB is organized in the membrane as an homotrimeric  $\beta$ -pleated barrel with 8 surface exposed loops (Figure 4.6.3). Bacteria are able to express one of the two isoforms of the protein, namely Por1a and Por1b, sharing 80 % of sequence similarity at the nucleotide level (Chen and Seifert., 2013). In the table below the laboratory strains used for the assays are reported together with the relative isoform expressed (internal characterization, data not shown), the protein structure can be appreciated on the left.



NG strain	Isoforms
FA1090	Porb 1b
WHO-M	Porb 1b
WHO-F	Porb 1a
WHO-N	Porb 1a
MS11	Porb 1b
SK92-679	Porb 1a
F62	Porb 1b
BG27	Porb 1b

**Figure 4.6.3.:** On the left side is reported the homotrimeric model of the *Neisseria gonorrhoeae* Porb1b, on the right side the table of the NG laboratory strains used for the assays and the relative isoform of the protein expressed (80 % nucleotidic sequence similarity). Model generated with Alphaphold2; image elaborated with Pymol.

### Luminex binding assay

A Luminex multiplex binding assay was carried out to assess the binding properties of the two anti-PorB recombinant mAbs selected for further characterization. Luminex beads were coupled with the recombinant protein rPorB to confirm the specificity of the mAbs, with FA1090 OMVs as positive control and with a panel of OMVs derived from Ng laboratory strains (WHO-F, SK92-679, WHO-N, BG27, MS11 and F62) to assess the cross-reactivity of the 2 mAbs on different gonococcal strains. As reported in Figure 4.6.4, both mAbs recognized with high affinity the rPorB protein and the OMVs of FA1090, moreover they are slightly cross-reactive with the OMVs derived from the heterologous strain MS11, while none of them is able to react with OMVs derived from the other strains tested.

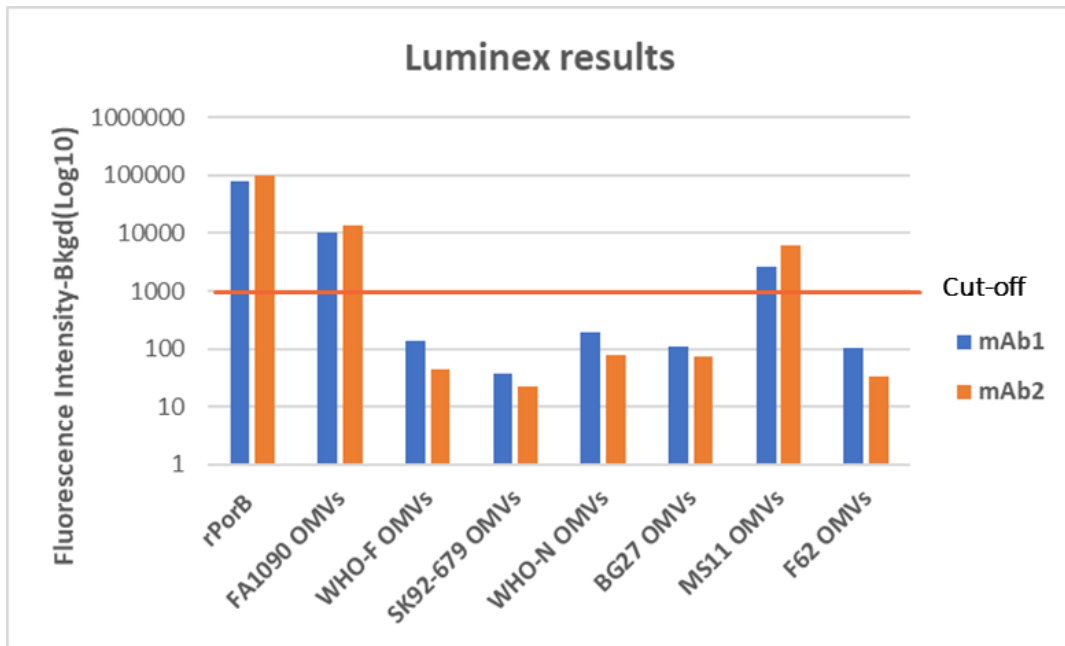


**Figure 4.6.4:** On the left axis is reported the mean fluorescence intensity (FI) measured with the Luminex, subtracted of the background in Log10 scale. A 1000 MFI was fixed as threshold to consider positive the binding of the mAbs above this value. The FI value reported correspond to a mAb concentration of 100 ng/μl.

### Western blot

To confirm the identity of the protein recognized on the bacterial surface, the two mAbs were tested in WB on Ng bacterial total extracts, using the homologous strain FA1090 and a panel of laboratory heterologous Ng strains (WHO-M, MS11, WHO-N, SK92-679, F62 and BG27) (Figure 4.6.5). Both mAbs recognized a band at the expected molecular weight of PorB (~35 kDa) in the homologous strain FA1090, moreover mAb2 showed recognition of a protein of the same size in the heterologous strain MS11. This is in line with the Luminex results where the two mAbs are specific for the rPorB, recognize the OMVs derived from the homologous strain FA1090 and have slightly cross-binding with the OMVs of the heterologous strain MS11.



**Figure 4.6.5:** WB using a total extract of Ng different laboratory strains.

## Serum bactericidal activity (hSBA)

In order to verify if our PorB-specific mAbs were able to kill gonococcus strains, a serum bactericidal assay using human serum as source of complement (hSBA) was performed on FA1090 and MS11 strains, selected based on the Luminex and WB results. If the mAbs are able to bind the bacterial surface, they could be able to activate the classical complement pathway cascade leading to the formation of the Membrane Attach Complex (MAC) thus killing the bacteria by lysis (Heesterbeek et al., 2018). The results reported in figure 4.6.6 showed that both mAbs were highly bactericidal against the homologous strain FA1090: mAb1 was able to induce >50% killing at a concentration up to 0.1 µg/ml whilst mAb2 at a concentration minor than 0.1 µg/ml. However, with the heterologous strain MS11 no bactericidal activity was observed.

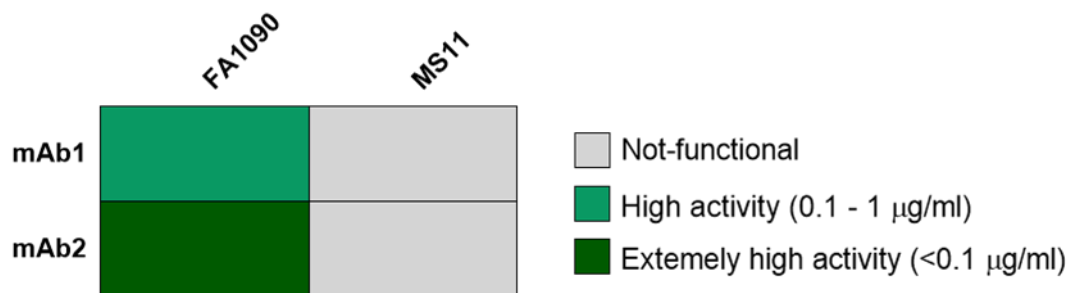


**Figure 4.6.6:** Serum bactericidal activity using human serum as source of complement to test the functional activity of the anti-PorB mAb1 and mAb2.

## Protein microarray technology

Protein microarray technology has made enormous progress in the last decade, increasingly becoming an important research tool for the study and detection of proteins, protein-protein interactions, and numerous other biotechnological applications (Berrade et al., 2011). It is also a powerful technique to identify the specific targets of monoclonal antibodies, since its high sensitivity allows to screen many constructs simultaneously using a very low amount of antibodies. The protein Porin B has 8 extracellular surface-exposed loops that are the part more antigenically variable and potentially immunogenic (Chen and Seifert., 2018). To better characterize the epitopes recognized by mAb1 and mAb2, an *in house* produced protein microarray was used. Different constructs of PorB have been spotted on the protein chip, to allow the analysis of mAbs reactivity toward different protein epitopes and conformations. In particular, the 8 extracellular loops were singularly extrapolated and inserted by genetic fusion into a soluble protein scaffold, the D3 domain (see Fig. 4.6.7A). The Domain 3 (D3) from Group B Streptococcus (GBS) pilus 2a backbone protein has been identified and engineered to be used as a scaffold for the display of extracellular loops (Cappelli L. et al. 2024). On the protein array we also spotted the two full length isoforms of the protein, PorB1a and PorB1b, expressed in *E. coli* and purified as his-tagged recombinant proteins after resolubilization of the inclusion bodies in urea and refolding of the protein as reported in literature (Weiyang Zhu et al., 2018). Given the insoluble nature of PorB, we also successfully expressed PorB1b on *E.coli* OMVs (as reported in Viviani et al., 2023) to preserve the Porin native conformation. Both mAbs were probed on this microarray to confirm their specificity for the PorB1b protein and to assess if they can recognize one of the extracellular loops. The mAb1 gave a positive signal only on the *E.coli* OMVs expressing the PorB1b, suggesting that it is able to recognize the protein only when it is displayed in its native conformation. In line with this assumption, mAb1 was not able to

recognize the refolded recombinant protein nor any of the linear loops fused on the D3 domain, suggesting that it might recognize a conformational epitope. Moreover, the discrepancy between Luminex and microarray results of the mAb1 observed for the PorB1b can be due to a lower sensitivity of the array technology. On the other side, the mAb2 was confirmed to be highly specific for PorB1b by strongly reacting with both, the recombinant protein and the protein displayed in *E.coli* OMVs. Moreover, mAb2 was highly reactive to the loop5 of the protein, indicating that the mAb2 recognize a linear epitope within the loop 5 of PorB1b (figure 4.6.7B).

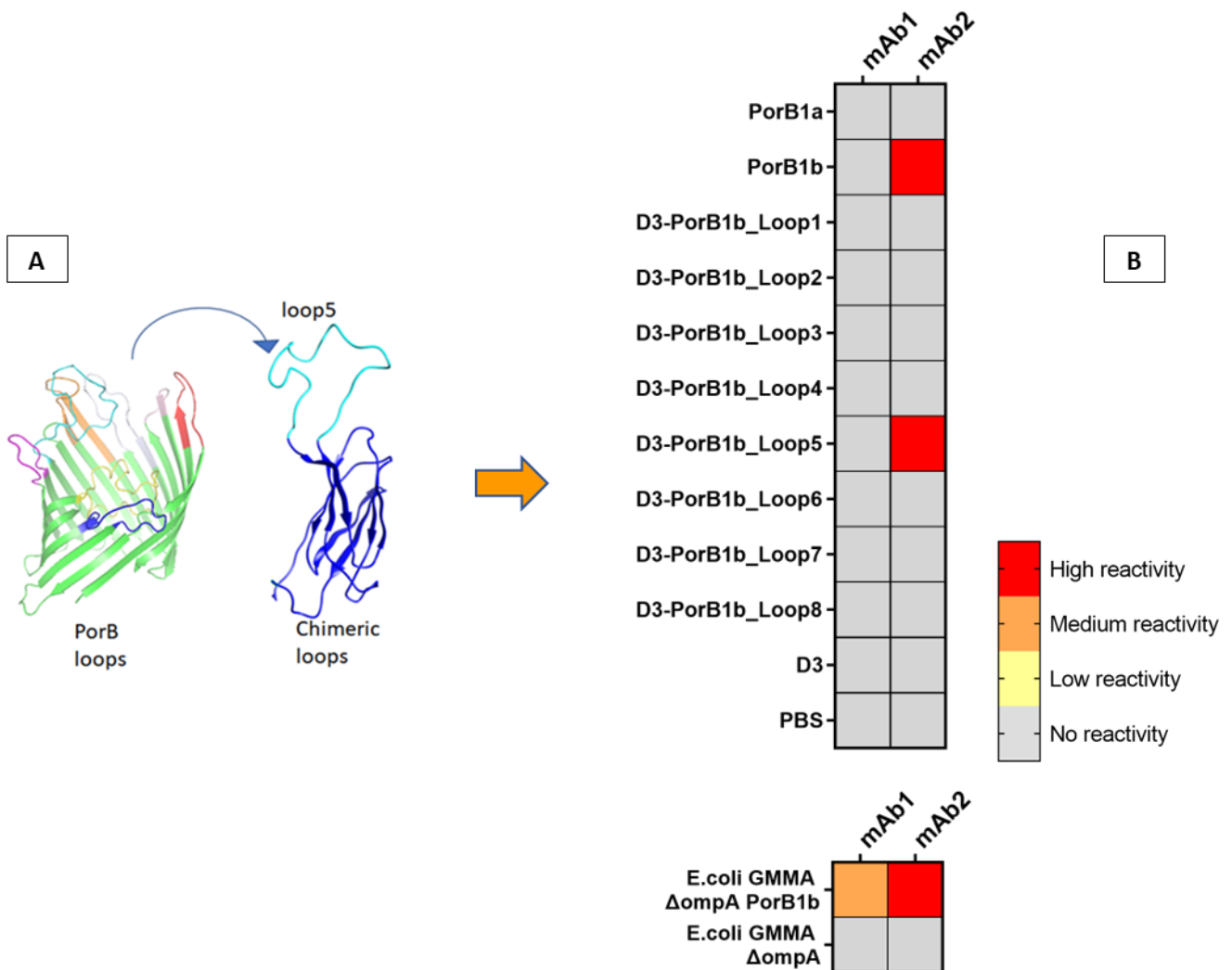


**Figure 4.6.7:** A) On the left side is represented the monomer of the PorinB 1b, in blue is highlighted the loop5 of the protein and the chimeric scaffold carrying the single PorB loop. On the right side (B) is represented the heatmap generated with the results of protein chip microarray. MFI: Mean Fluorescence Intensity. All obtained MFI scores were then ranked in four categories: (1) high reactivity;  $MFI \geq 30,000$ ; (2) medium reactivity;  $15,000 \leq MFI \leq 29,999$ ; (3) low reactivity;  $6000 \leq MFI \leq 14,999$ ; (4) no reactivity;  $MFI \leq 5,999$ . Model generated with alphaphold2; image elaborated with pymol.

In order to evaluate the cross-coverage of the two mAbs on a panel of Ng circulant strains, a second analysis was conducted with an *ad hoc* developed OMVs microarray (Troisi et al., under submission). In this case we spotted on the chip the OMVs naturally released by the selected Ng strains, as surrogate of the bacterial outer membrane for a high throughput binding analysis. The strains selected were a panel of 18 circulating strains and 5 laboratory strains. In Figure 4.6.8 it is reported the heatmap representing qualitative differences in immunofluorescence signals and representing the Mean Fluorescence Intensity (MFI) after detection with fluorescent-labeled secondary antibody. Both mAbs tested recognized the OMVs from the homologous strain FA1090, as expected, and reacted also with additional strains. We observed that the mAb2 has more intense and widespread recognition, with respect to the mAb1, among the panel of the various gonococcal strains tested, highlighting more cross-coverage.

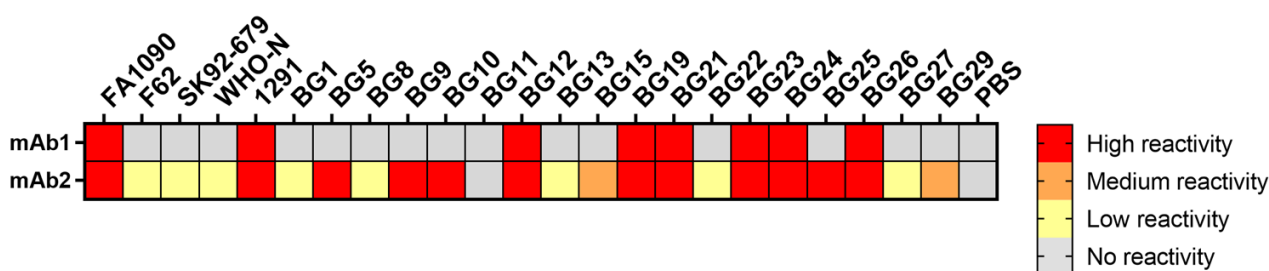


**Figure 4.6.8:** Heatmap generated from the OMVs array generating using OMVs derived from a panel of NG strains reported on the top of the figure. All obtained MFI (Mean Fluorescence Intensity) scores were then ranked in four categories: (1) high reactivity;  $MFI \geq 30,000$ ; (2) medium reactivity;  $15,000 \leq MFI \leq 29,999$ ; (3) low reactivity;  $6000 \leq MFI \leq 14,999$ ; (4) no reactivity;  $MFI \leq 5,999$ .

Previous data indicated that the epitope of mAb2 is localized in loop5 of PorB1b of FA1090 strain. We wanted to verify whether the cross-reactivity of this mAb on different strains was consistent with the sequence conservation of the loop5. With this aim, we aligned the aminoacidic sequences of PorB-loop5 of all the strains (with the exception of BG1 and BG10 strains, for which the sequences were not available). As shown in Figure 4.6.9, the strains carrying a loop 5 with an aminoacidic sequence more similar to the one present on the reference strain FA1090 (i.e. BG5, BG9, BG12, BG19, BG24, BG21, BG23, BG26, BG25, 1291) are recognized by mAb2 with a similar fluorescence in the array experiments, while in the other strains (F62, SK92, WHO-N, BG1, BG8, BG11, BG13, BG22, BG27) the aminoacidic sequence has very low degree of homology and the strains resulted poorly recognized by mAb2 in the array.

In the table 4.6.1, we see that although identity percentage treats all amino acid substitutions in the same way, it correlates well with reactivity observed with the array, demonstrating that reactivity is greatest when the sequence of loop5 have high identity with the same loop from FA1090 and decreases when the homology is lower. This tells us that it is probably loop5 that drives this recognition.

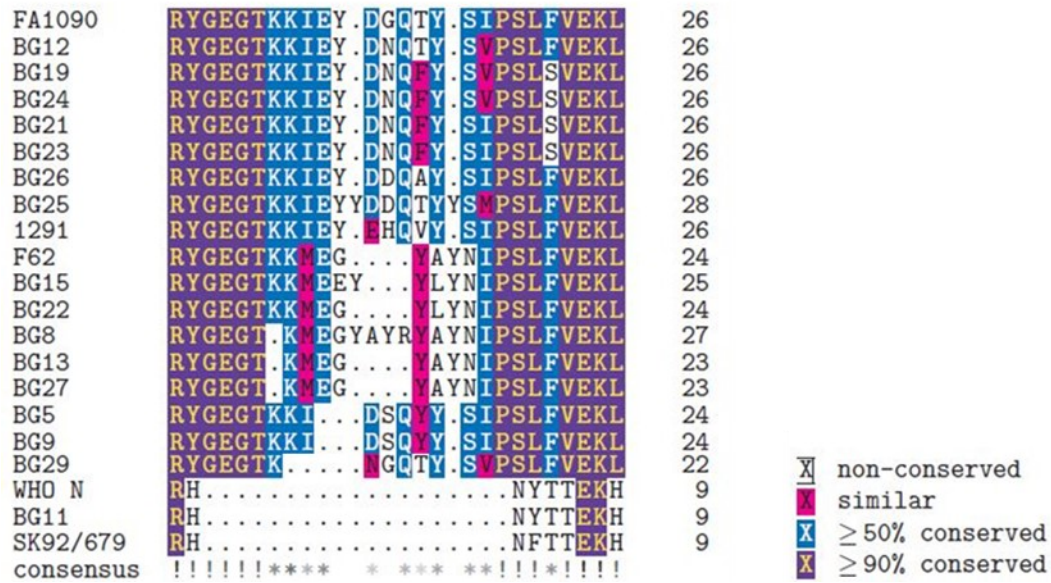


**Figure 4.6.9: Multiple sequence alignment of loop 5 of the PorB protein.** The alignment is done at the amino acid level for all the strains for which we had the PorB sequence available. Background colors refer, as stated in the legend, to the degree of conservation of each amino acid in the alignment. Consensus line is gray shaded, with darker color reflecting higher similarity and lighter color reflecting lower similarity, for each position. Left column: strain name, central column: aa sequence of loop5, right column: aa length of loop5.

strain	identity percentage	Reactivity	Porin isoform
FA1090	100,0%	High	1b
BG12	92,9%	High	1b
BG26	92,9%	High	1b
BG21	89,3%	High	1b
BG23	89,3%	High	1b
1291	89,3%	High	1b
BG19	85,7%	High	1b
BG24	85,7%	High	1b
BG25	85,7%	High	1b
BG5	85,7%	High	1b
BG9	85,7%	High	1b
BG29	78,6%	Medium	1b
F62	67,9%	Low	1b
BG22	67,9%	Low	1b
BG15	64,3%	Medium	1b
BG13	64,3%	Low	1b
BG27	64,3%	Low	1b
BG8	60,7%	Low	1b
WHO-N	17,9%	Low	1a
BG11	17,9%	No reactivity	1a
SK92/679	17,9%	Low	1a

**Table 4.6.1:** the identity percentage obtained comparing each amino acid sequence to the PorB loop 5 of FA1090 (Identity) and the reactivity measured in the protein array is reported and categorized in 4 levels. The 4<sup>th</sup> column represent which Porin isoform has each strain. The Pearson's correlation coefficient calculated for the identity and the Reactivity, transformed in values from 0 (no reactivity) to 3 (high) is 0.84.

## Characterization of murine recombinant IgG2a mAbs anti-OpaB

Opacity-associated proteins are abundant family of adhesins found in Ng outer membrane. Ng genome contains approximately 11 *opa* loci, encoding 8-11 unique, antigenically distinct Opa proteins (Cole J.G & Jerse A.E., 2009). Opa proteins share a conserved  $\beta$ -barrel structure but differ in the sequence of extracellular loops, which dictate Opa receptor specificity (Figure 4.6.10) (Sadarangani et al., 2011). Any given neisserial population should be composed of a mixture of individual bacteria expressing either none, one or multiple Opa proteins (Sadarangani et al., 2011).

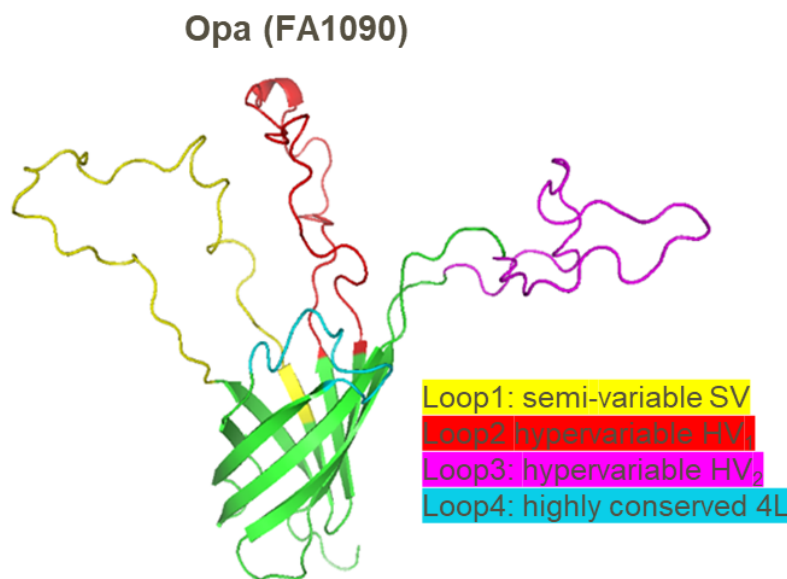


**Figure 4.6.10:** Model structure of the Opa on the homologous strain FA1090, sequence variation is observed predominantly within loop2 and loop3. OpaB is one of the proteins encoded by the FA1090 genome (Cole J.G & Jerse A.E., 2009). Model generated with alphaphold2; image elaborated with pymol.

### Luminex binding assay

A Luminex multiplex binding assay was carried out, as for the anti-PorB mAbs, to verify the specificity and the cross-binding of the two anti-OpaB recombinant mAbs, coupling the Luminex beads with the recombinant protein rOpaB, FA1090 OMVs as positive control and a panel of Ng laboratory strains derived OMVs ( SK92-679, WHO-F, WHO-N, BG27, MS11, F62): as shown in figure 4.6.11, the two mAbs recognize the protein rOpaB and the OMVs of FA1090, while it was not observed any cross-reactivity with the OMVs of the additional strains tested.

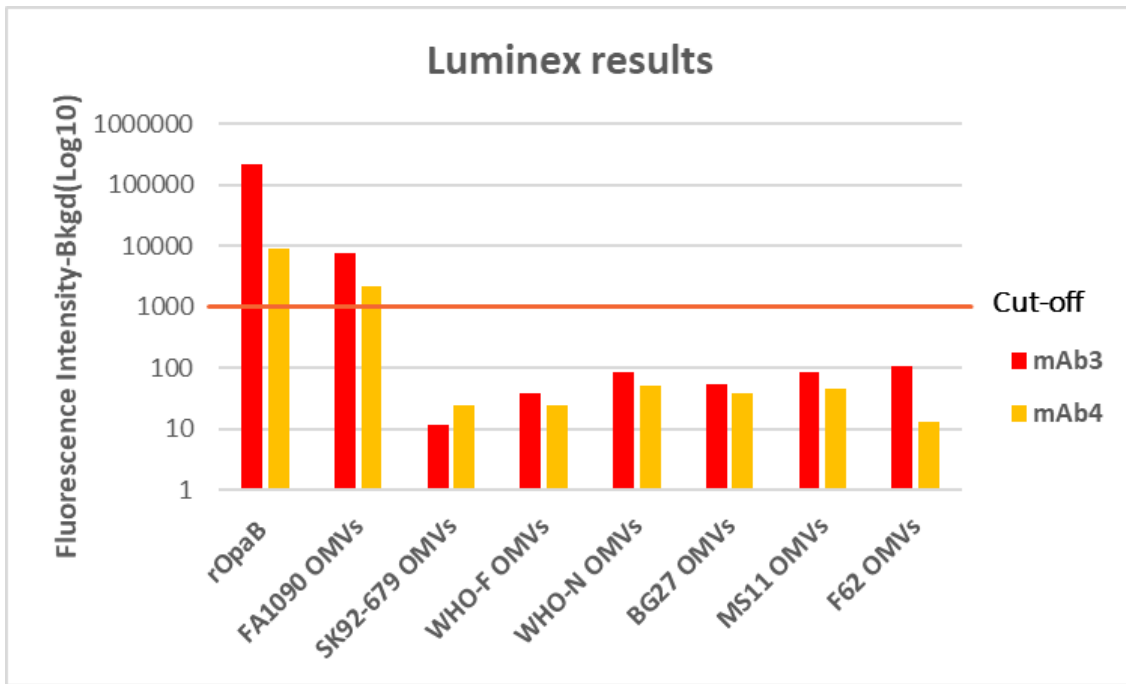


**Figure 4.6.11:** On the left axis it is reported the mean fluorescence intensity (FI) measured with the Luminex, subtracted of the background in Log10 scale. A 1000 MFI was fixed as threshold to consider positive the binding of the mAbs above this value. The FI value reported correspond to a mAb concentration of 100 ng/ $\mu$ l.

The two mAbs anti-OpaB were then tested in WB to evaluate protein recognition in a total Ng bacterial extract using the homologous bacterial strain FA1090 and a panel of laboratory heterologous Ng strains WHO-M, MS11, WHO-N, SK92-679, F62, BG27 (Figure 4.6.12). As positive control we used an FA1090 strain over expressing OpaB and an FA1090  $\Delta opa$  strain, deleted of all the 11 Opa genes, as negative control. The mAb3 recognizes a band at the expected OpaB size (~27 kDa) in the lysate of the strain FA1090 and is cross-reactive with WHO-M and F62. This mAb3 is also positive with the strain that overexpress OpaB and is negative against the strain  $\Delta opa$  confirming its specificity for OpaB protein. On the contrary, mAb4 do not show any reactivity at least in these experimental conditions.

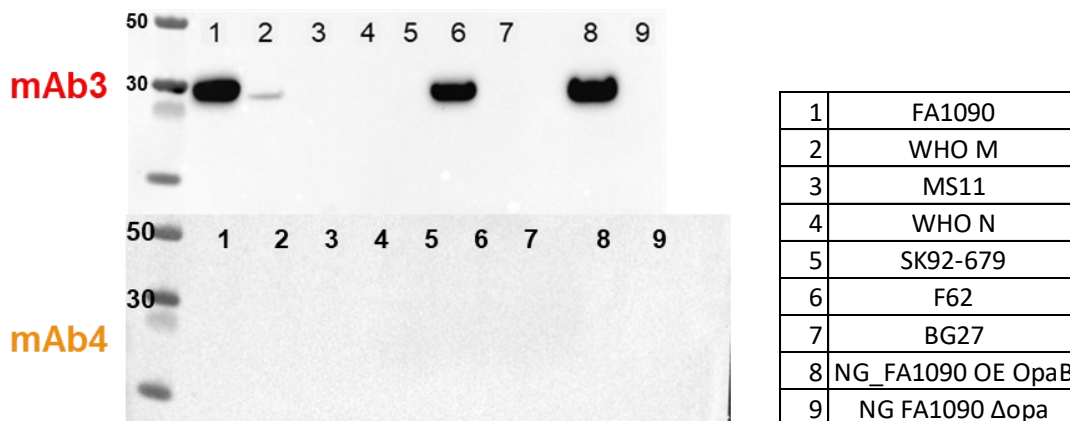


**Figure 4.6.12:** WB using total bacterial extract of a panel of Ng laboratory strains.

## Serum bactericidal activity (hSBA)

In order to investigate the functional activity of the selected OpaB-positive mAbs, bactericidal assay, using human serum as source of complement, was performed on FA1090, MS11 and F62 strains selected based on their positivity in the WB. The results reported in figure 4.6.13 showed that mAb3 was highly bactericidal against both the homologous strain FA1090, and the heterologous strain WHO-M while mAb4 was not functional against none of the strains. mAb3 was able to induce >50% killing at a concentration lower than 0.1  $\mu\text{g/ml}$  against FA1090, and at a concentration between 0.1 and 1  $\mu\text{g/ml}$  against WHO-M. No killing was observed on F62 strain despite the high recognition/reactivity observed in WB (Figure 4.6.12).

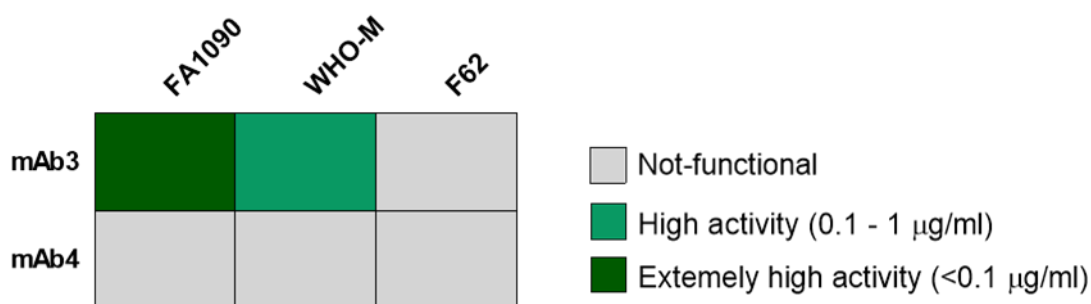


**Figure 4.6.13:** Serum bactericidal activity using human serum as source of complement to test the functional activity of the the anti-OpaB mAb3 and mAb4.

## Protein microarray technology

Opa proteins share a conserved  $\beta$ -barrel structure but differ in the sequence of the extracellular loops, which dictate Opa receptor specificity (Sadarangani et al., 2011). To better characterize the epitope recognized by mAb3 and mAb4, an *in house* produced protein microarray was used. As already described for PorB, we included in the analysis the extracellular loops extrapolated and inserted into a protein soluble scaffold (Cappelli L. et al., 2024). We were able to spot singularly the loops 1, 2 and 4 of OpaB. The construct containing the entire loop3 was obtained only after array printing and therefore analyzed only in dot blot. The strategy used for the loops cloning is reported in figure 4.6.14. The full length OpaB protein, purified as his-tagged recombinant protein from *E. coli* inclusion bodies, was spotted on the same chip. Both purified recombinant mAbs were used to probe this microarray to assess the specificity for the Opa protein and to investigate if they can recognize the extrapolated surface-exposed extracellular loops. In the figure 4.6.15 are reported the results obtained: the mAb3 was confirmed to be OpaB specific but did not recognize any of the extracellular loops tested, loop 1, 2 and 4. Based on these results we could hypothesize that mAb3 recognizes the hypervariable loop3 (HV-loop3), not included in the analysis. The mAb4 did not show any specificity, in line with all the previous observations done with the recombinant version of this monoclonal antibody (WB and hSBA), but in contrast with the low-level specificity measured by Luminex.

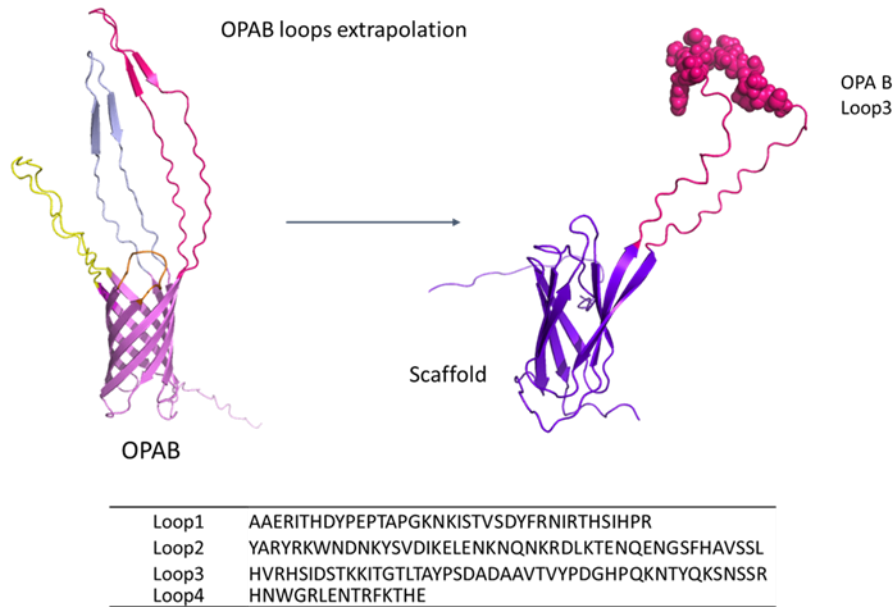


**Figure 4.6.14:** The left panel represents the OpaB 3D structure predicted with Alphafold2, with individual loops coloured in yellow (loop-1), purple (loop-2), magenta (loop-3) and orange (loop-4). The right panel represents the 3D structure of the protein scaffold carrying the heterologous OpaB loop, predicted with Alphafold2. Aminoacidic sequence of 4 OpaB loops extrapolated and cloned into the protein scaffold to obtain recombinant chimeric proteins carrying one single loop to investigate OpaB loops binding.

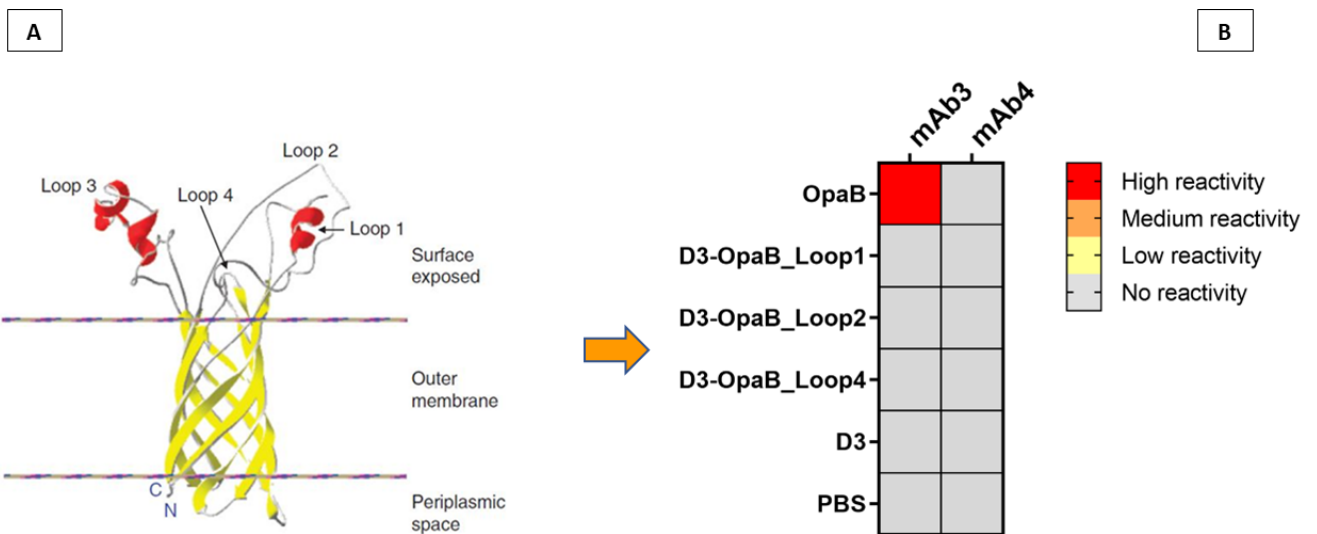


**Figure 4.6.15:** On the left side (A) is reported the structure of the Opa protein in which are clearly visible the loops surface exposed (Sadarangani et al., 2011, authorization copyright n°5587080549656). The heat map generated from the protein chip results is reported on the right side (B). All obtained MFI (Mean Fluorescence Intensity) scores were then ranked in four categories: (1) high reactivity; MFI  $\geq 30,000$ ; (2) medium reactivity;  $15,000 \leq \text{MFI} \leq 29,999$ ; (3) low reactivity;  $6000 \leq \text{MFI} \leq 14,999$ ; (4) no reactivity; MFI  $\leq 5,999$ .

The native mAb4 showed specificity (i.e., positive to rOpaB and FA1090 OMVs) only in Luminex but neither in WB, nor in protein array. One possible explanation for this different behavior could be that mAb4 has low affinity for OpaB and the binding could be detected only in Luminex, an approach with higher sensitivity when compared to protein array. To investigate if the mAb3 could recognize the OpaB-loop3, the entire Loop3 was extrapolated from OpaB protein and inserted into the same protein scaffold previously used for Loops 1, 2 and 4. The recombinant Loop3 was produced in *E. coli* and purified as a soluble protein. A Dot blot analysis was performed using all four single OpaB loops extrapolated from the protein and OpaB full length purified from *E. coli* inclusion bodies and resolubilized in presence of detergents.

The ponceau staining of the membrane confirmed the successful spotting of the four single loops as well of the entire OpaB. After probing the membrane with mAb3, only the single OpaB-loop3 and full length OpaB are recognized, revealing that mAb3 binds to an epitope localized in OpaB-loop3 (Figure 4.6.16)

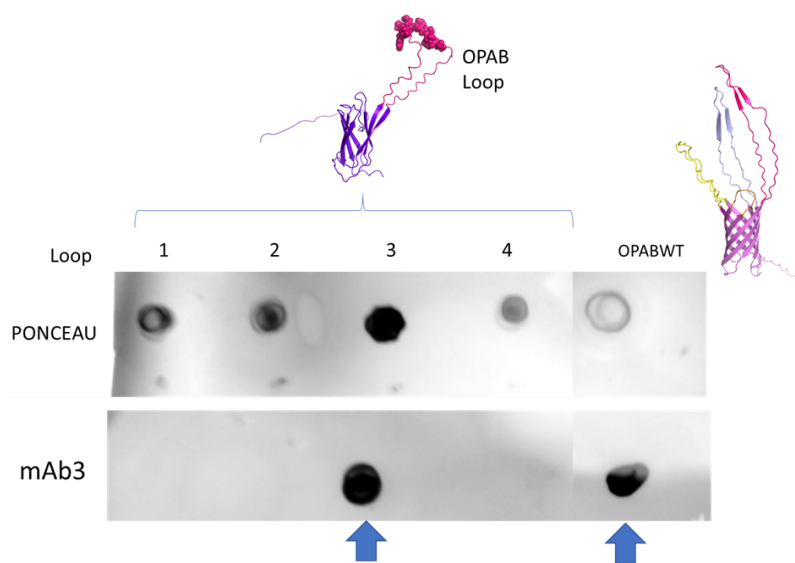


**Figure 4.6.16:** Dot Blot using the single loops separated and the OpaB wt: the mAb3 clearly recognize the loop3 of the protein and the OpaB wt.

A second analysis with the same Protein microarray used to test the cross-reactivity of PorB-specific mAbs was conducted, to evaluate the cross-coverage of the two mAbs on a panel of Ng circulating strains. mAb3 recognized the OMV of FA1090 and resulted cross reactive with low reactivity against some Ng circulating strains, while mAb4 showed again no reactivity at all (Figure 4.6.17)

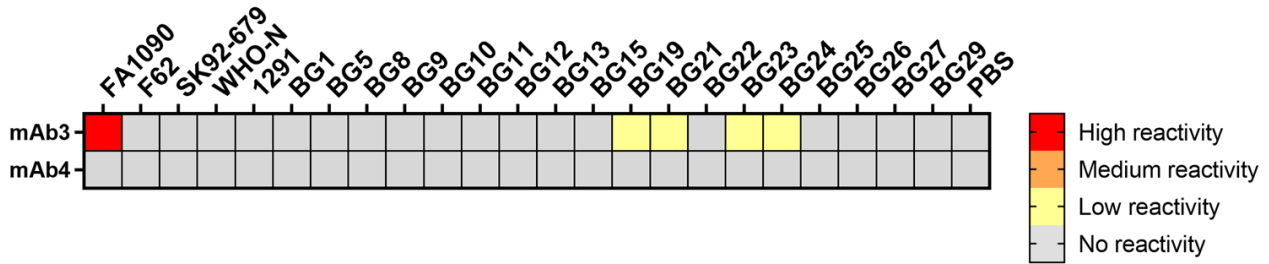


**Figure 4.6.17:** Heatmap generated from the OMVs array generating using nOMVs derived from a panel of Ng strains reported on the top of the figure. All obtained MFI (Mean Fluorescence Intensity) scores were then ranked in four categories: (1) high reactivity; MFI  $\geq 30,000$ ; (2) medium reactivity;  $15,000 \leq \text{MFI} \leq 29,999$ ; (3) low reactivity;  $6000 \leq \text{MFI} \leq 14,999$ ; (4) no reactivity;  $\text{MFI} \leq 5,999$ . MFI: Middle Fluorescence Intensity

### Characterization of murine recombinant IgG2a mAbs with Unknown target antigen

This category of mAbs was identified based on a lack of recognition against the two major surface exposed antigens on Ng membrane, PorB and OpaB, coupled with positivity against FA1090 OMVs: these mAbs are supposed to recognize other unknown minor antigens expressed on gonococcal surface. Our goal was to identify the unknown target antigen recognized by the two mAbs.

### Luminex binding assay

A Luminex multiplex binding assay was carried out with the recombinant form of mAb5 and mAb6, to confirm the lack of recognition against PorB and OpaB and to verify the cross-binding of the two mAbs against a panel of Ng strains, coupling the Luminex beads with the protein rPorB, rOpaB, FA1090 OMVs as positive control and a panel of Ng laboratory strains derived OMVs (WHO-F, WHO-N, F62, BG27 and MS11). In Luminex, both mAbs showed low Fluorescence Intensity signal on the strains tested: mAb5 and mAb6 show low recognition for FA1090, mAb6 has low signal ( $1000 < \text{FI} < 10000$ ) also on the other strains tested (Figure 4.6.18). Both mAbs do not show binding against PorB and OpaB proteins as expected. To understand which the target might be a WB was carried out.

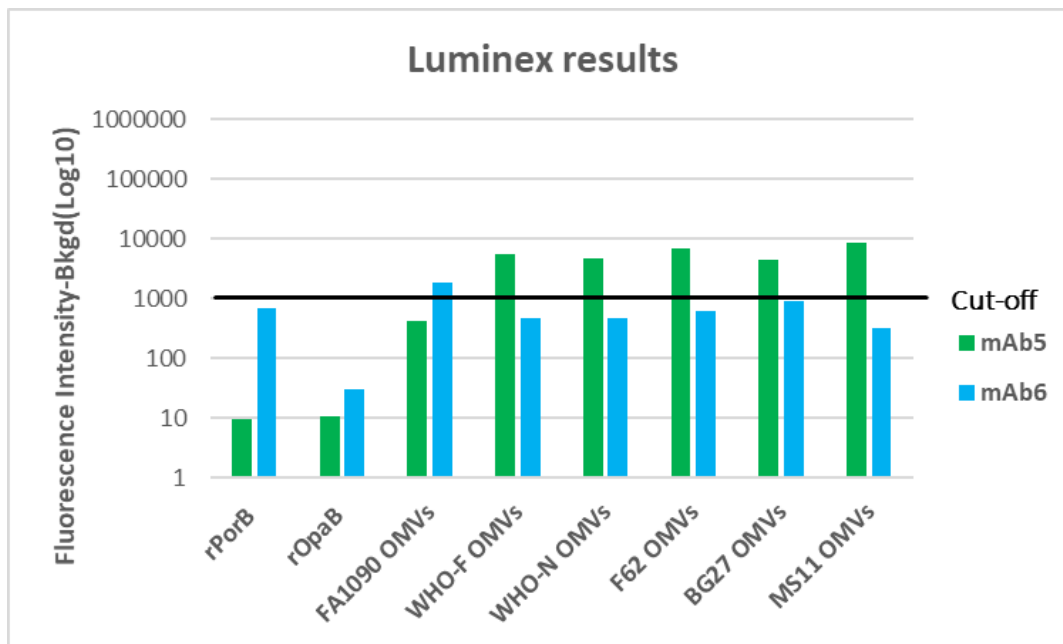


**Figure 4.6.18:** On the left axis is reported the mean fluorescence intensity (FI) measured with the Luminex, subtracted of the background in Log10 scale. A 1000 MFI was fixed as threshold to consider positive the binding of the mAbs above this value.

To reveal the protein recognized by the two mAbs with unknown target, a WB with bacterial lysates was carried out as previously described, using FA1090 as positive control and a panel of Ng laboratory strains: WHO-M, WHO-N, SK92-679, F62, MS11 and BG27. As shown in Figure 4.6.19, the mAb5 recognized a band with variable Molecular Weight (MW), ranging between 18 and 25 kDa in all the strains, while mAb6 recognized a band with MW of 55 kDa in all the tested strains. Both unknown target antigens seem well expressed and conserved in the different strains.

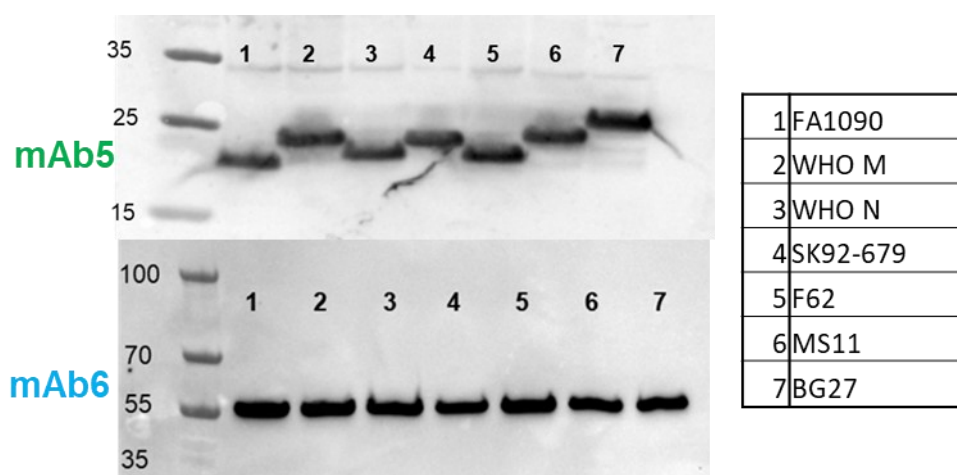


**Figure 4.6.19:** WB using Ng bacterial lysates with unknown target mAb5 and mAb6

## Protein microarray technology

To try to identify specific targets of the mAbs, protein microarray was needed to have a high throughput screening on the targets. Protein microarray satisfies the requirements of such screening: low quantity of mAbs and a screen on hundreds of different antigens. An in-house protein microarray was used, containing 79 different recombinant proteins, purified as his-tagged recombinant proteins. To cover a broad range of antigens and to evaluate interspecies cross-reactivity, the proteins spotted in the array were derived from *Neisseria meningitidis* and *Neisseria gonorrhoeae*. Both purified recombinant mAbs were used to probe this microarray. According to protein array (Figure 4.6.20.), mAb5 is specific for the meningococcal OmpH.8 antigen, a conserved, immunogenic surface exposed lipoprotein, that in strain FA1090 is composed entirely of 13 AAEAP repeats with an expected MW ~20 kDa (Woods et al., 1989). The peculiar MW pattern observed in WB is in line with what reported in literature for OmpH.8, in which they observe that electrophoretic mobility varies slightly between strains (diffuse bands ranging from 18 to 30 kDa) despite it is a highly conserved protein with similar molecular weight. Differences in migration may be due to its lipid modification or its uncommon aminoacidic composition and repeating structure (Shaughnessy J., Sanjay R., & Peter A.R., 2019), (Cannon et al., 1984). Unfortunately, the mAb6 did not react with any of the proteins present on the protein array (data not shown), therefore the target antigen of this mAb remains still unknown.

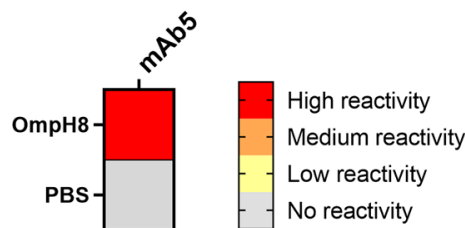


**Figure 4.6.20:** Heatmap generated from the protein microarray results: the target of mAb5 is the Omp.H8 protein. All obtained MFI (Mean Fluorescence Intensity) scores were then ranked in four categories: (1) high reactivity;  $MFI \geq 30,000$ ; (2) medium reactivity;  $15,000 \leq MFI \leq 29,999$ ; (3) low reactivity;  $6000 \leq MFI \leq 14,999$ ; (4) no reactivity;  $MFI \leq 5,999$ .

## Serum bactericidal activity (hSBA)

To test the functionality of the mAb5 targeting Omp.H.8, and mAb6 targeting an unknown protein, an SBA using human serum as source of complement was performed. hSBA was conducted on a panel of five Ng strains FA1090, WHO-M, WHO-N, F62 and MS11. In the figure below the results obtained are reported: both mAbs do not show bactericidal activity in our experimental conditions (Figure 4.6.21).

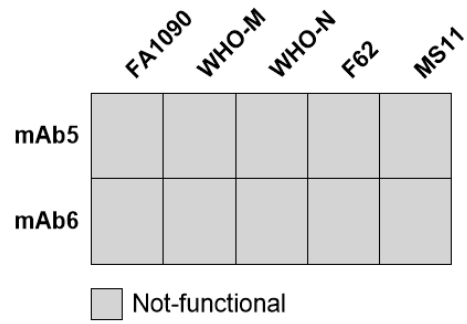


**Figure 4.6.21:** Serum bactericidal activity using human serum as source of complement with a panel of five Ng strains

## 5 DISCUSSION

Monoclonal antibodies are essential tools for many diagnostic applications and research investigations. mAbs have become crucial therapeutic drugs for many diseases and are well used in the treatment of cancer, autoimmune disorders, and infectious diseases (Marasco et al., 2007).

The hybridoma technology is the best-known immortalization technique of mouse B cells and since its development (Kohler and Milstein in 1975) it has revolutionized the use of mAbs. The technique is inefficient due to its dependence on a fusion event (immortalized short-lived antibody secreting cells (ASCs) fused with myeloma cells generating immortal clones, whose supernatant can be analyzed for the antigen-specific antibody). Through this technique many B cells do not get sampled and the diversity of an immune repertoire is not interrogated (Starkie et al., 2016), (Pedrioli and Oxenius., 2021).

In recent years, there has been an emergence of a number of single B cell technologies that allow a direct sampling of the immune repertoire. Developed platforms allow to retain the natural heavy and light chain pairing, leading to an efficient mining of B cell populations, allowing the discovery of rare antibodies with an attractive affinity, specificity, and stability profile (Tiller., 2011).

The mAbs against the surface exposed antigens of the pathogen *Neisseria gonorrhoeae* are very few, and only obtained through the hybridoma technology and ascitic fluid methodology (Nachamin et al., 1981), (Virji et al., 1985), (Virji et Heckles., 1988), (Paz et al., 1995).

Many studies on the components of bacterial surface of the pathogenic *Neisseria* species have been performed, especially on Outer Membrane Proteins (OMPs), lipopolysaccharide, and pili. It has been demonstrated that the composition of the surface of pathogenic *Neisseria spp.* is highly variable. Differences in particular surface components can be appreciated between different strains and also within a specific strain (Cannon et al., 1983).

Aim of this work was to develop an efficient mouse single B cell cloning and expression platform for the isolation and characterization of mAbs specific for bacterial surface antigens, with a particular focus on the isolation of murine mAbs against *N. gonorrhoeae* to deconvolute the immunogenicity of the surface exposed antigens, using the Outer Membrane Vesicles (OMVs) as representative of the bacterial membrane.

To do so, we single cell sorted 816 mice Memory B cells derived from the spleens of 3 mice immunized with Ng OMVs derived from the strain FA1090 and sorted with the target antigen Ng FA1090 OMVs in 384 well plates. After two weeks of clonal expansion on feeder cells in the presence of IL-2 and IL-21, the natural mAbs released in the supernatants were analyzed through Luminex assay for IgG detection and binding specificity against the target antigens of interest. Positive selected clones were selected to retrieve through NGS approach the VH and VL regions of the immunoglobulins encoded by the isolated cells, then the corresponding recombinant mAbs were expressed in raw supernatants of transfected mammalian cells.

This approach was partially derived from the work of Starkie, in which Antigen-specific recombinant mAbs were generated from single IgG+ Memory B cells isolated from immunized mice through multi-parameter flow cytometry. The main modification we introduced is that the immunization and the sorting was previously performed against one single recombinant antigen, while in this work the immunization and the sorting occur against OMVs, that are spherical portions of the outer membrane of gram-negative bacteria, containing outer-membrane lipids and proteins, and soluble periplasmic content. OMVs display a composite mixture of antigens and may comprise more than 300 different protein components, up to 80% of which are Outer Membrane Proteins (OMPs)

(Scwechheimer and Kuehn., 2015), (Van Der Pol et al., 2015). Therefore, OMVs can be used as a surrogate of the bacterial membrane.

Looking at the IgG content and binding specificity of the raw supernatants, we observed that 69% of isolated MBCs generated IgG, according to Luminex results, and intriguingly 83% of them showed binding specificity against the target antigen with which the cells were sorted. This means that we have obtained optimal recovery from the multiparameter Flow Cytometry FACS-sorting technique. With the aim to determine the binding specificity of the raw mouse supernatants against the surface exposed antigens of the OMVs, a Luminex multiplex binding assay was carried out coupling the beads with the major surface exposed antigen Porin (PorB1b) and the OpaB abundant family of adhesins, FA1090-derived OMVs were used as positive control.

After this analysis, we were able to divide the mAbs into categories based on their specific pattern recognition: as not surprisingly, 68% of them were specific for the Porin PorB1b, the major integral outer membrane protein on the surface of gonococci (Zhu et al., 2005), confirming this as the immunodominant protein present in the bacterial membrane. The second category identified included mAbs against the OpaB: 8.7% of them were specific for this adhesin protein. Quite interestingly, we have also identified a group of mAbs (8.9% of mAbs) that cross-recognized both PorB1b and OpaB antigens. In the last group classified as Others (14.4% of mAbs) were included mAbs that do not recognize neither PorB nor OpaB but do recognize the positive control Ng OMVs. These group represents a category of mAbs that recognize either the LOS or other unknown protein antigens not included in our Luminex assay but present at the gonococcal surface.

Based on this result, we selected a subgroup of 230 OMV-positive samples and coupling Retro-transcription using Gene Specific Primers (GSPs) with nested PCRs we were able to successfully recover 177 paired amplicons encoding the variable regions of the mAbs, VH-VL. Through NGS Miseq Illumina platform we retrieved 87 unique and paired VH-VL sequences that were then inserted into expression plasmids to transfect Expi293 mammalian cells, in order to obtain the full length recombinant murine gonococcus mAbs.

We expressed and purified 66 mAbs and in this work we selected a panel of 6 mAbs to be further analyzed for specificity and functionality: 2 anti PorB (mAb1 and mAb2), 2 anti OpaB (mAb3 and mAb4) and 2 against unknown target antigens (mAb5, mAb6).

The panel of recombinant mAbs was evaluated through four different assays: Luminex multiplex assay to confirm mAbs specificity for the known targets (PorB and OpaB) and to characterize cross-binding on different gonococcal strains, Western Blot to assess protein recognition in a total of bacterial extract, human Serum Bactericidal Assay (hSBA) to evaluate complement-mediated functional activity of mAbs and Protein microarray technology to evaluate mAb specificity and cross-reactivity.

The first category analyzed were the two mAbs against the PorB: to evaluate the ability of cross-binding of the two mAbs, we developed an *ad hoc* multiplex Luminex assay coupling the beads with the rPorB, the OMVs of FA1090 as positive control, and an additional panel of six Ng laboratory strains derived OMVs: WHO-F, SK92-679, WHO-N, BG27, MS11 and F62 to evaluate the possible cross-binding. The use of OMVs derived from the various strains allowed the maintenance of the protein structures likely in their native conformation. Both mAbs recognized with high affinity the rPorB and the OMVs of FA1090 meaning that the two mAbs are specific for the target antigen and moreover a slightly recognition was observed against the heterologous strain MS11, a strain that like FA1090 express PorB.1B variant (Jones et al., 2023).

Based on these results we performed a WB using a total bacterial extract to evaluate mAbs protein recognition from bacterial lysates; the strains used were FA1090 and the heterologous strains WHO-M, MS11, WHO-N, SK92-679, F62 and BG27. In line with Luminex results (recognition from the OMVs of the strains), both mAbs recognized a band at the expected PorB size (~35 kDa) in the homologous strain FA1090 and interestingly mAb2 showed recognition against the heterologous strain MS11. The purified mAbs, were analyzed in terms of functionality evaluating them in hSBA based on the strains recognized by the WB results. The mAb1 and mAb2 show bactericidal activity against the homologous strain FA1090 but not for the heterologous strain MS11. These results could be due to different expression level of PorB on the surface of the bacterial strain. To investigate this aspect, a FACS technique could be useful to look further on the binding of these mAbs on the bacterial surface.

PorB has 8 extracellular surface- exposed loops that are the part more antigenically variable and potentially immunogenic (Chen and Seifert., 2018). To better characterize the epitope recognized by mAb1 and mAb2, an in house produced protein microarray was used. On the protein chip different constructs of PorB have been spotted. In particular, the 8 single extracellular loops (each one has been extrapolated and inserted into a soluble protein scaffold) (Cappelli L. et al. 2024), the two full length isoforms PorB1a and PorB1b (purified as his-tagged recombinant proteins), and *E. coli* OMVs displaying Ng PorB likely in its native conformation (Viviani et al., 2023). The exposure on OMVs was explored as the PorB hydrophobic nature posed a challenge on its expression and correct folding outside the membrane context. Since proper folding of this protein is necessary to conserve the exposed epitope in their native conformation (a mandatory quality to mediate mAb recognition of conformational epitopes), the OMV approach was selected to present this protein, as it already proved successful on presenting bacterial antigens (Bartolini et al., 2013).

mAb1 recognize PorB only when it is expressed on *E.coli* GMMA, so when it is displayed in its native conformation meaning that this mAb is likely recognizing a conformational epitope of the protein in which aminoacid residues that are discontinuous in the protein sequence come within close proximity to form an antigenic surface on the protein 3D structure recognized by the mAb.

Intriguingly, mAb2 was confirmed to be specific for Porin1b and moreover it is able to recognize with high reactivity the loop5 of the protein and also the protein when it is displayed on GMMA. These data indicate that the epitope of mAb2 is localized in the loop5 of the PorB. Further analysis like epitope-mapping could be carried to identify the specific portion of the loop5 recognized by mAb2. Intriguingly, extracellular loop5, together with loop7, has been reported to mediate C4BP binding to PorB1b on the surface of Ng (Chen and Seifert., 2013). The protein C4bp is a regulatory protein of the classical complement pathway that inhibits classical pathway activation and mediates bacterial resistance to complement (Ram et al., 2001). The mAb2, by binding its epitope on loop5, is probably able to compete with C4BP binding on the surface of the bacteria thus increasing its bactericidal activity.

A second analysis with an *ad hoc* developed protein microarray was conducted to analyze the binding of mAbs on OMVs derived from a panel of Ng strains to assess the degree of coverage of the two mAbs. mAb2 is more cross-reactive and has more intense and widespread recognition with respect to mAb1 across the strains. mAb1 recognizes a less conserved epitope with respect to mAb2 and an epitope mapping could help clarify the region recognized by the mAb. To better understand if the loop5-PorB recognized by mAb2 is conserved among the strains tested, an aminoacidic alignment was carried out and compared to the degree of reactivity that mAb2 has in protein chip.

The cross-reactivity of mAb2 in protein array is in line with the isoform of the Porin present in the strains and with the aminoacidic conservation within the loop5 sequence with respect to the reference FA1090. Not surprisingly, mAb2 has low or absent reactivity in the strains that express the isoform PorB1a (WHO-N, BG11 and SK92-679) given the low degree of conservation between the loop5 of the two isoforms. Indeed, mAb2 is more cross-reactive with strains that express the PorB1b and that have more than 80 % of similarity in the loop5 (e.g. BG5, BG9, BG12, BG19, BG24, BG21, BG23, BG26, BG25, 1291). The strains that have the PorB1b isoform and similarity lower than 80 % are poorly recognized by mAb2 in the OMVs array.

The analysis of OpaB-specific mAbs has been conducted with the same rationale discussed for PorB-specific mAbs. Luminex assay was exploited to understand their cross-binding between different Ng strains. An *ad hoc* panel was utilized coupling the Luminex beads with the rOpaB, the OMVs of FA1090 as positive control and a panel of Ng laboratory strains, the same used for the PorB mAbs (OMVs derived from SK92-679, WHO-F, WHO-N, BG27, MS11 and F62). The two mAbs characterized (mAb3 and mAb4) confirmed their specificity for the rOpaB and positivity to the OMVs of the homologous strain FA1090, while we did not observe any cross-reactivity with the OMVs of the selected strains. This could be explained by the fact that the bacteria can express 8-11 antigenically distinct Opa proteins that are encoded by distinct *opa* genes. Each gene undergoes phase variation through a frame-shift mechanism, and a single gonococcus can express no Opa proteins, one Opa protein, or multiple Opa proteins simultaneously (Cole and Jerse., 2009).

In order to evaluate the mAb recognition on a total bacterial extract, WB analysis was done using the same Ng lab strains previously discussed for the PorB mAbs (FA1090, WHO-M, MS11, WHO-N, SK92-679, F62 and BG27) plus two additional strains used as control: a strain OpaB locked that overexpresses the protein on its surface for positive control and a strain depleted of all the 11 loci (or  $\Delta opa$ ) strain for negative control. mAb3 recognizes the strain FA1090 and is cross-reactive with two heterologous strains (WHO-M and F62), it also recognizes the positive control: all the bands are at expected OpaB size (~27 kDa). The mAb4 did not show any recognition in WB. Afterwards, hSBA using human serum as source of complement was evaluated on the three strains recognized in WB: FA1090, WHO-M and F62. The mAb3 resulted bactericidal against the homologous FA1090 strain and the heterologous strain WHO-M, but not strain F62.

A FACS strategy or confocal microscopy could be applied in this case to have a better visualization of the mAb recognition on bacterial surface, especially for F62 strain, that despite a good reactivity in WB is not killed by this mAb in our experimental conditions. A possible explanation for this behavior could be linked to protein and/or epitope accessibility on the bacterial surface for the mAb3 in this strain. The mAb4 instead does not show any killing activity for the strains tested.

The peculiarity of the Opa proteins is that they share a conserved  $\beta$ -barrel structure but differ in the sequence of the extracellular loops, which dictate Opa receptor specificity. Sequence variation is mostly observed within loop2 and loop3, which have also been named hypervariable region 1 (HV1) and hypervariable region 2 (HV2) respectively (Sadarangani et al., 2011). To better characterize the epitope recognized by mAb3 and mAb4, an in house produced protein microarray was used. The extracellular sequences of loop 1, 2 and 4, each one extrapolated and inserted into a soluble protein scaffold (Cappelli L. et al., 2024), were spotted singularly on the array, together with the full length OpaB protein, purified as his-tagged recombinant protein from *E. coli* inclusion bodies. Loop3 fused in the same soluble scaffold was tested in ELISA. Our analysis confirmed that mAb3 binds

recombinant rOpaB protein with high reactivity and is able to recognize the single OpaB-loop3 fused in the soluble scaffold, revealing that mAb3 binds to a linear epitope included into OpaB-loop3.

mAb4 anti-OpaB resulted positive only in Luminex, where it recognized the recombinant rOpaB and OMVs of FA1090. The mAb resulted negative in WB and in protein chip in our experimental conditions, suggesting that it could likely recognize a conformational epitope in the 3D protein structure that is not reconstituted in the recombinant protein purified from inclusion bodies.

We then used the OMVs microarray to evaluate the cross-coverage on a panel of different Ng strains. The mAb3 recognized the OMVs derived from the homologous strain FA1090 but showed very low reactivity on few heterologous strains. This could be due on one side to the already discussed high sequence variability of Opa proteins within and among each strain, but also to the different expression level that the protein can have in different growth phases. In line with this hypothesis, F62 OpaB is recognized in WB (where bacteria are grown in exponential phase) but not in the Luminex nor in the OMV array, where we tested mAbs on nOMV released by bacteria in stationary phase. On the other side, mAb4 does not show any reactivity except on the Luminex, despite we used the same nOMVs both for Luminex and OMV array. The positivity of mAb4 on the OMVs of strain FA1090 only in Luminex assay could be explained by the higher sensitivity of this method with respect to the array.

The third category of characterized mAbs was those of antibodies with unknown target antigen. We performed Luminex assay on the panel of Ng laboratory strains already evaluated for the other mAbs (FA1090, WHO-F, WHO-N, F62, BG27 and MS11) to evaluate eventual cross-binding on different strains. Moreover, we tested the mAbs on beads conjugated with PorB and OpaB, to confirm the lack of recognition for these antigens observed in the initial screening with nativa mAbs in raw supernatant. The results confirmed lack of binding for the two proteins, slight recognition of FA1090 OMVs and very low to medium recognition on the different strains. WB analysis on bacterial lysates using, as for the other categories the laboratory strains FA1090, WHO-M, WHO-N, SK92-679, F62, MS11 and BG27, revealed two different band patterns generated by the two mAbs. The mAb5 recognize a peculiar band ranging from 18 kDa and 30 kDa in all the strains while the mAb6 shows a uniform protein recognition at 55 kDa in all the strains tested. To try to identify the target of the two mAbs a protein chip array was exploited, to have a high-throughput screening on the targets. mAbs were probed on a protein microarray containing 79 different recombinant proteins, purified as his-tagged recombinant proteins. Proteins were selected based on their expression level on the surface on bacterial OMV (Viviani et al.,2023). To have a broad range of antigens at disposal and to evaluate interspecies cross-reactivity, the proteins spotted in the membrane were from *Neisseria meningitidis* and *Neisseria gonorrhoeae*. We were able to identify the target of the mAb5, that recognizes the OmpH.8 protein, which is a highly conserved surface-exposed lipoprotein found in both *N. gonorrhoeae* and *N. meningitidis*. This protein has been already described and a conserved epitope recognized by the mAb5 has been previously observed by Cannon and coworkers (Cannon et al., 1983). The OmpH8 is composed entirely of repeats of the pentapeptide sequence Ala-Ala-Glu-Ala-Pro (AAEAP), whose number can change among strains and be responsible of the different migration pattern observed in SDS-page. The epitope binding of the mAb H.8 is within the AAEP repeat domain and probably this is also the case of the mAb5, that is able to recognize the protein in WB in all the tested strains. OmpH.8 protein is present predominantly in the pathogenic *Neisseria* species, suggesting that it could be involved in pathogenesis, and it is potentially immunogenic. In

strain FA1090, the predicted protein has 71 aa in length, and it is composed entirely of 12 AAEP repeats (Woods et al., 1989), (Shaughnessy et al., 2019).

Woods et al, performed WB and SDS page on this protein and they observed diffuse band ranging from 18 to 30 KDa, in line with our data on WB in which we observed this peculiar ranging band pattern. The mAb6 on the contrary still remains without a specific target, since in the protein array it did not recognize any of the proteins present. We concluded that its target is probably a protein not included in the protein array due to its low abundance in the OMVs. Further investigations will be done to try to elucidate the target of this mAb. The minor antigens present on the bacterial surface could contribute, altogether with the most abundant surface-exposed antigens to the immunogenicity of the OMVs.

Finally, we want to evaluate if the mAbs are able to kill the bacteria using hSBA approach; given the lack of recognition on the strains, the SBA was carried out with an extended panel of 5 strains (FA1090, WHO-M, WHO-N, F62, MS11). Both mAbs are not bactericidal in our experimental conditions; this could be due to a low accessibility of the epitope on the bacterial surface or to a very low abundance of the antigen on the bacterial membrane, not sufficient to initiate the complement cascade and cause bacterial lysis. The surface exposure of the antigens recognized by these two mAbs could be evaluated through FACS analysis.

In conclusion, a protocol for isolation, sequencing, and recombinant production of murine mAbs derived from mouse MBCs has been developed. This method could be easily exploited for the generation of libraries of antibodies against diverse proteins of any pathogen.

By using OMVs as surrogate of bacterial surface, we were able to deconvolute the immune response to Ng surface antigens in mice: not surprisingly, we mainly identified mAbs specific for the two major surface protein antigens, PorB1b and OpaB, while a small percentage of mAbs recognize other unknown antigens present on gonococcal surface.

Characterization analysis performed on six mAbs representative of three different binding profiles showed that the anti-PorB and one anti-OpaB mAbs are specific, cross-reactive between different Ng strains and bactericidal at least against the homologous strain FA1090.

Moreover, we were able to identify a new immunogenic target, the lipoprotein OmpH.8, recognized by mAb5. Further analysis should be focused on the expansion of the panel of mAbs at disposal for characterization in specificity and functionality, moreover further studies could be to combine the mAbs with different target antigens together in hSBA functional assay to evaluate their synergistic effect. Finally, mAbs could also be tested *in vivo* to evaluate protective efficacy in mice.

## DECLARATION OF INTERESTS:

This work was sponsored by GlaxoSmithKline Biologicals SA. The author has declared the following interest: Francesca Papi is a PhD student at the University of Siena and participates to a post graduate studentship program at GSK.

## BIBLIOGRAPHY:

- 1) Alcott, A. M., Werner, L. M., Baiocco, C. M., Belcher Dufrisne, M., Columbus, L., & Criss, A. K. (2022). Variable expression of opa proteins by *Neisseria gonorrhoeae* influences bacterial association and phagocytic killing by human neutrophils. *Journal of Bacteriology*, 204(4), e00035-22.
- 2) Amanna, I. J., & Slifka, M. K. (2006). Quantitation of rare memory B cell populations by two independent and complementary approaches. *Journal of immunological methods*, 317(1-2), 175-185.
- 3) Apicella, M. A., Mandrell, R. E., Shero, M., Wilson, M. E., Griffiss, J. M., Brooks, G. F., ... & Rice, P. A. (1990). Modification by sialic acid of *Neisseria gonorrhoeae* lipooligosaccharide epitope expression in human urethral exudates: an immunoelectron microscopic analysis. *Journal of Infectious Diseases*, 162(2), 506-512.
- 4) Ayers, M., Howell, P. L., & Burrows, L. L. (2010). Architecture of the type II secretion and type IV pilus machineries. *Future microbiology*, 5(8), 1203-1218.
- 5) Bartolini, E., Ianni, E., Frigimelica, E., Petracca, R., Galli, G., Berlanda Scorza, F., ... & Grifantini, R. (2013). Recombinant outer membrane vesicles carrying *Chlamydia muridarum* HtrA induce antibodies that neutralize chlamydial infection in vitro. *Journal of extracellular vesicles*, 2(1), 20181.
- 6) Belland, R. J., Morrison, S. G., Carlson, J. H., & Hogan, D. M. (1997). Promoter strength influences phase variation of neisserial opa genes. *Molecular microbiology*, 23(1), 123-135.
- 7) Berrade, L., Garcia, A. E., & Camarero, J. A. (2011). Protein microarrays: novel developments and applications. *Pharmaceutical research*, 28, 1480-1499.
- 8) Bjercknes, Robert, et al. "Neisserial porins inhibit human neutrophil actin polymerization, degranulation, opsonin receptor expression, and phagocytosis but prime the neutrophils to increase their oxidative burst." *Infection and immunity* 63.1 (1995): 160-167.
- 9) Bos, M. P., Grunert, F., & Belland, R. J. (1997). Differential recognition of members of the carcinoembryonic antigen family by Opa variants of *Neisseria gonorrhoeae*. *Infection and immunity*, 65(6), 2353-2361.
- 10) Bos, M. P., Kao, D., Hogan, D. M., Grant, C. C., & Belland, R. J. (2002). Carcinoembryonic antigen family receptor recognition by gonococcal Opa proteins requires distinct combinations of hypervariable Opa protein domains. *Infection and immunity*, 70(4), 1715-1723.
- 11) Bhat, K. S., Gibbs, C. P., Barrera, O., Morrison, S. G., Jähnig, F., Stern, A., ... & Swanson, J. (1991). The opacity proteins of *Neisseria gonorrhoeae* strain MS11 are encoded by a family of 11 complete genes. *Molecular microbiology*, 5(8), 1889-1901.
- 12) Cannon, J. G., Buchanan, T. M., & Sparling, P. F. (1983). Confirmation of association of protein I serotype of *Neisseria gonorrhoeae* with ability to cause disseminated infection. *Infection and immunity*, 40(2), 816-819.
- 13) Cannon, Janne G., William J. Black, Irving Nachamkin, and Patricia W. Stewart. "Monoclonal antibody that recognizes an outer membrane antigen common to the pathogenic *Neisseria* species but not to most nonpathogenic *Neisseria* species." *Infection and immunity* 43, no. 3 (1984): 994-999.
- 14) Cappelli, L., Cinelli, P., Perrotta, A., Veggi, D., Audagnotto, M., Tuscano, G., ... & Cozzi, R. (2024). Computational structure-based approach to study chimeric antigens using a new protein scaffold displaying foreign epitopes. *The FASEB Journal*, 38(1), e23326.

- 15) Château, A., & Seifert, H. S. (2016). *Neisseria gonorrhoeae* survives within and modulates apoptosis and inflammatory cytokine production of human macrophages. *Cellular microbiology*, 18(4), 546-560.
- 16) Chen, T., Grunert, F., Medina-Marino, A., & Gotschlich, E. C. (1997). Several carcinoembryonic antigens (CD66) serve as receptors for gonococcal opacity proteins. *The Journal of experimental medicine*, 185(9), 1557-1564.
- 17) Chen, A., & Seifert, H. S. (2013). Structure-function studies of the *Neisseria gonorrhoeae* major outer membrane porin. *Infection and immunity*, 81(12), 4383-4391.
- 18) Cho, C., Teghanemt, A., Apicella, M. A., & Nauseef, W. M. (2020). Modulation of phagocytosis-induced cell death of human neutrophils by *Neisseria gonorrhoeae*. *Journal of Leucocyte Biology*, 108(5), 1543-1553.
- 19) Clargo, A. M., Hudson, A. R., Ndlovu, W., Wootton, R. J., Cremin, L. A., O'Dowd, V. L., ... & Lightwood, D. J. (2014, January). The rapid generation of recombinant functional monoclonal antibodies from individual, antigen-specific bone marrow-derived plasma cells isolated using a novel fluorescence-based method. In *MABs* (Vol. 6, No. 1, pp. 143-159). Taylor & Francis.
- 20) Cole, J. A. (2012). Legless pathogens: how bacterial physiology provides the key to understanding pathogenicity. *Microbiology*, 158(6), 1402-1413.
- 21) Cole, J. G., & Jerse, A. E. (2009). Functional characterization of antibodies against *Neisseria gonorrhoeae* opacity protein loops. *PloS one*, 4(12), e8108.
- 22) Corbett, A., Exley, R., Bourdoulous, S., & Tang, C. M. (2004). Interactions between *Neisseria meningitidis* and human cells that promote colonisation and disease. *Expert reviews in molecular medicine*, 6(14), 1-14.
- 23) Craig, L., Forest, K. T., & Maier, B. (2019). Type IV pili: dynamics, biophysics and functional consequences. *Nature reviews microbiology*, 17(7), 429-440.
- 24) Craig, L., Pique, M. E., & Tainer, J. A. (2004). Type IV pilus structure and bacterial pathogenicity. *Nature Reviews Microbiology*, 2(5), 363-378.
- 25) Criss, A. K., & Seifert, H. S. (2008). *Neisseria gonorrhoeae* suppresses the oxidative burst of human polymorphonuclear leukocytes. *Cellular microbiology*, 10(11), 2257-2270.
- 26) Criss, A. K., Katz, B. Z., & Seifert, H. S. (2009). Resistance of *Neisseria gonorrhoeae* to non-oxidative killing by adherent human polymorphonuclear leucocytes. *Cellular microbiology*, 11(7), 1074-1087.
- 27) Danaher, R. J., Levin, J. C., Arking, D., Burch, C. L., Sandlin, R., & Stein, D. C. (1995). Genetic basis of *Neisseria gonorrhoeae* lipooligosaccharide antigenic variation. *Journal of bacteriology*, 177(24), 7275-7279.
- 28) Deo, P., Chow, S. H., Hay, I. D., Kleifeld, O., Costin, A., Elgass, K. D., ... & Naderer, T. (2018). Outer membrane vesicles from *Neisseria gonorrhoeae* target PorB to mitochondria and induce apoptosis. *PLoS pathogens*, 14(3), e1006945.
- 29) Edwards, J. L., Brown, E. J., Uk-Nham, S., Cannon, J. G., Blake, M. S., & Apicella, M. A. (2002). A co-operative interaction between *Neisseria gonorrhoeae* and complement receptor 3 mediates infection of primary cervical epithelial cells. *Cellular microbiology*, 4(9), 571-5848
- 30) Edwards, J. L., & Apicella, M. A. (2004). The molecular mechanisms used by *Neisseria gonorrhoeae* to initiate infection differ between men and women. *Clinical microbiology reviews*, 17(4), 965-981.
- 31) Edwards, J. L., & Apicella, M. A. (2005). I-domain-containing integrins serve as pilus receptors for *Neisseria gonorrhoeae* adherence to human epithelial cells. *Cellular microbiology*, 7(8), 1197-1211.

- 32) Elias, J. F. & Vogel, U. in *Manual of Clinical Microbiology* 12th edn Vol. 1(eds Carroll, C. C. et al.) 640–655 (American Society for Microbiology, 2019).
- 33) Farkas, A. E., Capaldo, C. T., & Nusrat, A. (2012). Regulation of epithelial proliferation by tight junction proteins. *Annals of the New York Academy of Sciences*, 1258(1), 115-124.
- 34) Fudyk, T. C., Maclean, I. W., Simonsen, J. N., Njagi, E. N., Kimani, J., Brunham, R. C., & Plummer, F. A. (1999). Genetic diversity and mosaicism at the por locus of *Neisseria gonorrhoeae*. *Journal of bacteriology*, 181(18), 5591-5599.
- 35) Giardina, P. C., Williams, R., Lubaroff, D., & Apicella, M. A. (1998). *Neisseria gonorrhoeae* induces focal polymerization of actin in primary human urethral epithelium. *Infection and immunity*, 66(7), 3416-3419.
- 36) Gill, D. B., Spitzer, D., Koomey, M., Heuser, J. E., & Atkinson, J. P. (2005). Release of host-derived membrane vesicles following pilus-mediated adhesion of *Neisseria gonorrhoeae*. *Cellular microbiology*, 7(11), 1672-1683.
- 37) Golparian, D., & Unemo, M. (2022). Antimicrobial resistance prediction in *Neisseria gonorrhoeae*: current status and future prospects. *Expert Review of Molecular Diagnostics*, 22(1), 29-48.
- 38) Gómez-Duarte, O. G., Dehio, M., Guzman, C. A., Chhatwal, G. S., Dehio, C., & Meyer, T. F. (1997). Binding of vitronectin to opa-expressing *Neisseria gonorrhoeae* mediates invasion of HeLa cells. *Infection and immunity*, 65(9), 3857-3866.
- 39) Gotschlich, E. C. (1994). Genetic locus for the biosynthesis of the variable portion of *Neisseria gonorrhoeae* lipooligosaccharide. *The Journal of experimental medicine*, 180(6), 2181-2190.
- 40) Grant, C. C., Bos, M. P., & Belland, R. J. (1999). Proteoglycan receptor binding by *Neisseria gonorrhoeae* MS11 is determined by the HV-1 region of OpaA. *Molecular microbiology*, 32(2), 233-242.
- 41) Grassmé H, Gulbins E, Brenner B, et al. Acidic sphingomyelinase mediates entry of *N. gonorrhoeae* into nonphagocytic cells. *Cell*. 1997 Nov;91(5):605-615. DOI: 10.1016/s0092-8674(00)80448-1. PMID: 9393854.
- 42) Gray-Owen, S. D., & Blumberg, R. S. (2006). CEACAM1: contact-dependent control of immunity. *Nature Reviews Immunology*, 6(6), 433-446.
- 43) Griffiss, J. M., Lammel, C. J., Wang, J., Dekker, N. P., & Brooks, G. F. (1999). *Neisseria gonorrhoeae* coordinately uses Pili and Opa to activate HEC-1-B cell microvilli, which causes engulfment of the gonococci. *Infection and immunity*, 67(7), 3469-3480.
- 44) Guerrant, R. L., Walker, D. H., & Weller, P. F. (2011). *Tropical infectious diseases: Principles, pathogens and practice e-book*. Elsevier Health Sciences.
- 45) Gulati, S., Shaughnessy, J., Ram, S., & Rice, P. A. (2019). Targeting lipooligosaccharide (LOS) for a gonococcal vaccine. *Frontiers in immunology*, 10, 321.
- 46) Haas, R., & Meyer, T. F. (1986). The repertoire of silent pilus genes in *Neisseria gonorrhoeae*: evidence for gene conversion. *Cell*, 44(1), 107-115.
- 47) Hafez, E. S., & Kenemans, P. (2012). *Atlas of Human Reproduction: By Scanning Electron Microscopy*. Springer Science & Business Media.
- 48) Hagblom, P., Segal, E., Billyard, E., & So, M. (1985). Intragenic recombination leads to pilus antigenic variation in *Neisseria gonorrhoeae*. *Nature*, 315(6015), 156-158.

- 49) Harris, R. L., Van Den Berg, C. W., & Bowen, D. J. (2012). ASGR1 and ASGR2, the genes that encode the asialoglycoprotein receptor (Ashwell receptor), are expressed in peripheral blood monocytes and show interindividual differences in transcript profile. *Molecular biology international*, 2012.
- 50) Harvey, H. A., Jennings, M. P., Campbell, C. A., Williams, R., & Apicella, M. A. (2001). Receptor-mediated endocytosis of *Neisseria gonorrhoeae* into primary human urethral epithelial cells: the role of the asialoglycoprotein receptor. *Molecular microbiology*, 42(3), 659-672.
- 51) Harvey, H. A., Ketterer, M. R., Preston, A., Lubaroff, D., Williams, R., & Apicella, M. A. (1997). Ultrastructural analysis of primary human urethral epithelial cell cultures infected with *Neisseria gonorrhoeae*. *Infection and immunity*, 65(6), 2420-2427.
- 52) Harvey, H. A., Post, D. M., & Apicella, M. A. (2002). Immortalization of human urethral epithelial cells: a model for the study of the pathogenesis of and the inflammatory cytokine response to *Neisseria gonorrhoeae* infection. *Infection and immunity*, 70(10), 5808-5815.
- 53) Hauck, C. R., & Meyer, T. F. (2003). 'Small' talk: Opa proteins as mediators of *Neisseria*-host-cell communication. *Current opinion in microbiology*, 6(1), 43-49.
- 54) Heesterbeek, D. A., Angelier, M. L., Harrison, R. A., & Rooijackers, S. H. (2018). Complement and bacterial infections: from molecular mechanisms to therapeutic applications. *Journal of Innate Immunity*, 10(5-6), 455-464.
- 55) Hung, M. C., & Christodoulides, M. (2013). The biology of *Neisseria* adhesins. *Biology*, 2(3), 1054-1109.
- 56) Islam, E. A., Anipindi, V. C., Francis, I., Shaik-Dasthagirisahab, Y., Xu, S., Leung, N., ... & Gray-Owen, S. D. (2018). Specific binding to differentially expressed human carcinoembryonic antigen-related cell adhesion molecules determines the outcome of *Neisseria gonorrhoeae* infections along the female reproductive tract. *Infection and immunity*, 86(8), 10-1128.
- 57) Jiang, X., Suzuki, H., Hanai, Y., Wada, F., Hitomi, K., Yamane, T., & Nakano, H. (2006). A novel strategy for generation of monoclonal antibodies from single B cells using RT-PCR technique and in vitro expression. *Biotechnology progress*, 22(4), 979-988.
- 58) Jin, A., Ozawa, T., Tajiri, K., Obata, T., Kondo, S., Kinoshita, K., ... & Muraguchi, A. (2009). A rapid and efficient single-cell manipulation method for screening antigen-specific antibody-secreting cells from human peripheral blood. *Nature medicine*, 15(9), 1088-1092.
- 59) Jones, R. A., Jerse, A. E., & Tang, C. M. (2023). Gonococcal PorB: a multifaceted modulator of host immune responses. *Trends in Microbiology*.
- 60) Jonsson, A. B., Nyberg, G., & Normark, S. (1991). Phase variation of gonococcal pili by frameshift mutation in pilC, a novel gene for pilus assembly. *The EMBO journal*, 10(2), 477-488.
- 61) Johnson, A. P. The pathogenic potential of commensal species of *Neisseria*. *J. Clin. Pathol.* **36**, 213–223 (1983).
- 62) Kawasaki, T., & Kawai, T. (2014). Toll-like receptor signaling pathways. *Frontiers in immunology*, 5, 461
- 63) Keenan, C., & Kelleher, D. (1998). Protein kinase C and the cytoskeleton. *Cellular signalling*, 10(4), 225-232.
- 64) Kehl-Fie, T. E., & Skaar, E. P. (2010). Nutritional immunity beyond iron: a role for manganese and zinc. *Current opinion in chemical biology*, 14(2), 218-224.

- 65) Kuespert, K., Pils, S., & Hauck, C. R. (2006). CEACAMs: their role in physiology and pathophysiology. *Current opinion in cell biology*, 18(5), 565-571.
- 66) Kuespert, K., Weibel, S., & Hauck, C. R. (2007). Profiling of bacterial adhesin—host receptor recognition by soluble immunoglobulin superfamily domains. *Journal of microbiological methods*, 68(3), 478-485.
- 67) Kurita, T. (2011). Normal and abnormal epithelial differentiation in the female reproductive tract. *Differentiation*, 82(3), 117-126.
- 68) Lee, H. S., Ostrowski, M. A., & Gray-Owen, S. D. (2008). CEACAM1 dynamics during *Neisseria gonorrhoeae* suppression of CD4+ T lymphocyte activation. *The Journal of Immunology*, 180(10), 6827-6835.
- 69) Lorenzen, D. R., Günther, D., Pandit, J., Rudel, T., Brandt, E., & Meyer, T. F. (2000). *Neisseria gonorrhoeae* porin modifies the oxidative burst of human professional phagocytes. *Infection and immunity*, 68(11), 6215-6222.
- 70) Love, J. C., Ronan, J. L., Grotenbreg, G. M., van der Veen, A. G., & Ploegh, H. L. (2006). A microengraving method for rapid selection of single cells producing antigen-specific antibodies. *Nature biotechnology*, 24(6), 703-707.
- 71) Ma, H., & O’Kennedy, R. (2015). The structure of natural and recombinant antibodies. *Peptide Antibodies: Methods and Protocols*, 7-11.
- 72) Malorny, B., Morelli, G., Kusecek, B., Kolberg, J., & Achtman, M. (1998). Sequence diversity, predicted two-dimensional protein structure, and epitope mapping of neisserial Opa proteins. *Journal of bacteriology*, 180(5), 1323-1330.
- 73) Mandrell, R. E., Lesse, A. J., Sugai, J. V., Shero, M., Griffiss, J. M., Cole, J. A., ... & Apicella, M. A. (1990). In vitro and in vivo modification of *Neisseria gonorrhoeae* lipooligosaccharide epitope structure by sialylation. *The Journal of experimental medicine*, 171(5), 1649-1664.
- 74) Mandrell, R. E., Griffiss, J. M., & Macher, B. A. (1988). Lipooligosaccharides (LOS) of *Neisseria gonorrhoeae* and *Neisseria meningitidis* have components that are immunochemically similar to precursors of human blood group antigens. Carbohydrate sequence specificity of the mouse monoclonal antibodies that recognize crossreacting antigens on LOS and human erythrocytes. *The Journal of experimental medicine*, 168(1), 107-126.
- 75) Marasco, W. A., & Sui, J. (2007). The growth and potential of human antiviral monoclonal antibody therapeutics. *Nature biotechnology*, 25(12), 1421-1434.
- 76) McCaw, Shannon E., Jutta Schneider, Edward H. Liao, Wolfgang Zimmermann, and Scott D. Gray-Owen. "Immunoreceptor tyrosine-based activation motif phosphorylation during engulfment of *Neisseria gonorrhoeae* by the neutrophil-restricted CEACAM3 (CD66d) receptor." *Molecular microbiology* 49, no. 3 (2003): 623-637.
- 77) Meijer, P. J., Andersen, P. S., Hansen, M. H., Steinaa, L., Jensen, A., Lantto, J., ... & Nielsen, L. S. (2006). Isolation of human antibody repertoires with preservation of the natural heavy and light chain pairing. *Journal of molecular biology*, 358(3), 764-772.
- 78) Meyer, L., López, T., Espinosa, R., Arias, C. F., Vollmers, C., & DuBois, R. M. (2019). A simplified workflow for monoclonal antibody sequencing. *PLoS one*, 14(6), e0218717.
- 79) Morand, P. C., Bille, E., Morelle, S., Eugene, E., Beretti, J. L., Wolfgang, M., ... & Nassif, X. (2004). Type IV pilus retraction in pathogenic *Neisseria* is regulated by the PilC proteins. *The EMBO journal*, 23(9), 2009-2017.

- 80) MORSE, S. A. (1979). *Neisseria gonorrhoeae*: physiology and metabolism. *Sexually transmitted diseases*, 6(1), 28-37.
- 81) Muenzner, P., Bachmann, V., Zimmermann, W., Hentschel, J., & Hauck, C. R. (2010). Human-restricted bacterial pathogens block shedding of epithelial cells by stimulating integrin activation. *Science*, 329(5996), 1197-1201.
- 82) Muenzner, P., Rohde, M., Kneitz, S., & Hauck, C. R. (2005). CEACAM engagement by human pathogens enhances cell adhesion and counteracts bacteria-induced detachment of epithelial cells. *The Journal of cell biology*, 170(5), 825-836.
- 83) Nachamkin, I., Cannon, J. G., & Mittler, R. S. (1981). Monoclonal antibodies against *Neisseria gonorrhoeae*: production of antibodies directed against a strain-specific cell surface antigen. *Infection and Immunity*, 32(2), 641-648.
- 84) Ngampasutadol, J., Ram, S., Blom, A. M., Jarva, H., Jerse, A. E., Lien, E., ... & Rice, P. A. (2005). Human C4b-binding protein selectively interacts with *Neisseria gonorrhoeae* and results in species-specific infection. *Proceedings of the National Academy of Sciences*, 102(47), 17142-17147.
- 85) Palmer, A., & Criss, A. K. (2018). Gonococcal defenses against antimicrobial activities of neutrophils. *Trends in microbiology*, 26(12), 1022-1034.
- 86) Parray, H. A., Shukla, S., Samal, S., Shrivastava, T., Ahmed, S., Sharma, C., & Kumar, R. (2020). Hybridoma technology a versatile method for isolation of monoclonal antibodies, its applicability across species, limitations, advancement and future perspectives. *International immunopharmacology*, 85, 106639.
- 87) Paz, H. D. L., Cooke, S. J., & Heckels, J. E. (1995). Effect of sialylation of lipopolysaccharide of *Neisseria gonorrhoeae* on recognition and complement-mediated killing by monoclonal antibodies directed against different outer-membrane antigens. *Microbiology*, 141(4), 913-920.
- 88) Pedrioli, A., & Oxenius, A. (2021). Single B cell technologies for monoclonal antibody discovery. *Trends in immunology*, 42(12), 1143-1158.
- 90) Popp, A., Dehio, C., Grunert, F., Meyer, T. F., & Gray-Owen, S. D. (1999). Molecular analysis of neisserial Opa protein interactions with the CEA family of receptors: identification of determinants contributing to the differential specificities of binding. *Cellular microbiology*, 1(2), 169-181.
- 91) Pujol, C., Eugène, E., Marceau, M., & Nassif, X. (1999). The meningococcal PilT protein is required for induction of intimate attachment to epithelial cells following pilus-mediated adhesion. *Proceedings of the National Academy of Sciences*, 96(7), 4017-4022.
- 92) Quillin, S. J., & Seifert, H. S. (2018). *Neisseria gonorrhoeae* host adaptation and pathogenesis. *Nature Reviews Microbiology*, 16(4), 226-240.
- 93) Rajasekariah, G. R., Edward, S. I. M. O. N. E., Shapira, D. E. B. O. R. A. H., Tapsall, J. O. H. N., Walsh, J. O. H. N., Ho, J. U. L. I. E., ... & Pucci, A. L. E. S. S. A. N. D. R. A. (1989). Direct detection of *Neisseria gonorrhoeae* with monoclonal antibodies characterized by serotyping reagents. *Journal of clinical microbiology*, 27(7), 1700-1703.
- 94) Ram, S., Cullinane, M., Blom, A. M., Gulati, S., McQuillen, D. P., Monks, B. G., ... & Rice, P. A. (2001). Binding of C4b-binding protein to porin: a molecular mechanism of serum resistance of *Neisseria gonorrhoeae*. *The Journal of experimental medicine*, 193(3), 281-296.

- 95) Ramsey, K. H., Schneider, H., Cross, A. S., Boslego, J. W., Hoover, D. L., Staley, T. L., ... & Deal, C. D. (1995). Inflammatory cytokines produced in response to experimental human gonorrhoea. *Journal of Infectious Diseases*, 172(1), 186-191.
- 96) Rohatgi, S., Ganju, P., & Sehgal, D. (2008). Systematic design and testing of nested (RT-) PCR primers for specific amplification of mouse rearranged/expressed immunoglobulin variable region genes from small number of B cells. *Journal of immunological methods*, 339(2), 205-219.
- 97) Robertson, B. D., & Meyer, T. F. (1992). Genetic variation in pathogenic bacteria. *Trends in Genetics*, 8(12), 422-427.
- 98) Rohde, K. H., & Dyer, D. W. (2003). Mechanisms of iron acquisition by the human pathogens *Neisseria meningitidis* and *Neisseria gonorrhoeae*. *Frontiers in Bioscience-Landmark*, 8(4), 1186-1218.
- 99) Rowley, J., Vander Hoorn, S., Korenromp, E., Low, N., Unemo, M., Abu-Raddad, L. J., ... & Taylor, M. M. (2019). Chlamydia, gonorrhoea, trichomoniasis and syphilis: global prevalence and incidence estimates, 2016. *Bulletin of the World Health Organization*, 97(8), 548.
- 100) Rudel, T., Scheuerpflug, I., & Meyer, T. F. (1995). *Neisseria* PilC protein identified as type-4 pilus tip-located adhesin. *Nature*, 373(6512), 357-359.
- 101) Sadarangani, M., Pollard, A. J., & Gray-Owen, S. D. (2011). Opa proteins and CEACAMs: pathways of immune engagement for pathogenic *Neisseria*. *FEMS microbiology reviews*, 35(3), 498-514.
- 102) Sarantis, H., & Gray-Owen, S. D. (2012). Defining the roles of human carcinoembryonic antigen-related cellular adhesion molecules during neutrophil responses to *Neisseria gonorrhoeae*. *Infection and immunity*, 80(1), 345-358.
- 103) Shaughnessy, J., Gulati, S., Agarwal, S., Unemo, M., Ohnishi, M., Su, X. H., ... & Ram, S. (2016). A novel factor H-Fc chimeric immunotherapeutic molecule against *Neisseria gonorrhoeae*. *The Journal of Immunology*, 196(4), 1732-1740.
- 104) Shaughnessy, J., Ram, S., & Rice, P. A. (2019). Biology of the gonococcus: disease and pathogenesis. *Neisseria gonorrhoeae: Methods and Protocols*, 1-27.
- 105) Schmitter, T., Agerer, F., Peterson, L., Münzner, P., & Hauck, C. R. (2004). Granulocyte CEACAM3 is a phagocytic receptor of the innate immune system that mediates recognition and elimination of human-specific pathogens. *The Journal of experimental medicine*, 199(1), 35-46.
- 106) Schneider, H., Griffiss, J. M., Boslego, J. W., Hitchcock, P. J., Zahos, K. M., & Apicella, M. A. (1991). Expression of paragloboside-like lipooligosaccharides may be a necessary component of gonococcal pathogenesis in men. *The Journal of experimental medicine*, 174(6), 1601-1605.
- 107) Schneider, H., Hammack, C. A., Apicella, M. A., & Griffiss, J. M. (1988). Instability of expression of lipooligosaccharides and their epitopes in *Neisseria gonorrhoeae*. *Infection and immunity*, 56(4), 942-946.
- 108) Schneider, H., Cross, A. S., Kuschner, R. A., Taylor, D. N., Sadoff, J. C., Boslego, J. W., & Deal, C. D. (1995). Experimental human gonococcal urethritis: 250 *Neisseria gonorrhoeae* MS11mkC are infective. *Journal of Infectious Diseases*, 172(1), 180-185.
- 109) Sheehan, J., & Marasco, W. A. (2015). Phage and yeast display. *Antibodies for Infectious Diseases*, 103-127.
- 110) Schwechheimer, C., & Kuehn, M. J. (2015). Outer-membrane vesicles from Gram-negative bacteria: biogenesis and functions. *Nature reviews microbiology*, 13(10), 605-619.

- 111) Sintsova, A., Wong, H., MacDonald, K. S., Kaul, R., Virji, M., & Gray-Owen, S. D. (2015). Selection for a CEACAM receptor-specific binding phenotype during *Neisseria gonorrhoeae* infection of the human genital tract. *Infection and immunity*, *83*(4), 1372-1383.
- 112) Sintsova, A., Sarantis, H., Islam, E. A., Sun, C. X., Amin, M., Chan, C. H., ... & Gray-Owen, S. D. (2014). Global analysis of neutrophil responses to *Neisseria gonorrhoeae* reveals a self-propagating inflammatory program. *PLoS pathogens*, *10*(9), e1004341.
- 113) Song, W., Yu, Q., Wang, L. C., & Stein, D. C. (2020). Adaptation of *Neisseria gonorrhoeae* to the Female Reproductive Tract. *Microbiology insights*, *13*, 1178636120947077.  
<https://doi.org/10.1177/1178636120947077>
- 114) Spiegel, S., Foster, D., & Kolesnick, R. (1996). Signal transduction through lipid second messengers. *Current opinion in cell biology*, *8*(2), 159-167.
- 115) Stanley, M. (2010). Potential mechanisms for HPV vaccine-induced long-term protection. *Gynecologic oncology*, *118*(1), S2-S7.
- 116) Starkie, D. O., Compson, J. E., Rapecki, S., & Lightwood, D. J. (2016). Generation of recombinant monoclonal antibodies from immunised mice and rabbits via flow cytometry and sorting of antigen-specific IgG+ memory B cells. *PLoS One*, *11*(3), e0152282.
- 117) Stern, A., & Meyer, T. F. (1987). Common mechanism controlling phase and antigenic variation in pathogenic neisseriae. *Molecular microbiology*, *1*(3), 5-12.
- 118) Tønjum, T. & van Putten, J. in *Infectious Diseases* 4th edn (eds Cohen, J., Powderly, W. G. & Steven M. Opal) 1553-1564 (Elsevier, 2016).
- 119) Troisi, M., Fabbrini, M., Stazzoni, S., Viviani, V., Carboni, F., Abbiento, V., ... & Rappuoli, R. (2023). Human monoclonal antibodies reveal subdominant gonococcal and meningococcal cross-protective antigens. *bioRxiv*, 2023-12.
- 120) Tsevat, D. G., Wiesenfeld, H. C., Parks, C., & Peipert, J. F. (2017). Sexually transmitted diseases and infertility. *American journal of obstetrics and gynecology*, *216*(1), 1-9.
- 121) Unemo, M., Seifert, H. S., Hook III, E. W., Hawkes, S., Ndowa, F., & Dillon, J. A. R. (2019). Gonorrhoea. *Nature Reviews Disease Primers*, *5*(1), 79.
- 122) Unemo, M., & Shafer, W. M. (2011). Antibiotic resistance in *Neisseria gonorrhoeae*: origin, evolution, and lessons learned for the future. *Annals of the New York Academy of Sciences*, *1230*(1), E19-E28.
- 123) Unemo, M., & Shafer, W. M. (2014). Antimicrobial resistance in *Neisseria gonorrhoeae* in the 21st century: past, evolution, and future. *Clinical microbiology reviews*, *27*(3), 587-613.
- 124) Unemo, M., Ross, J. D. C., Serwin, A. B., Gomberg, M., Cusini, M., & Jensen, J. S. (2020). 2020 European guideline for the diagnosis and treatment of gonorrhoea in adults. *International journal of STD & AIDS*, 0956462420949126.
- 125) Unemo, M., & Shafer, W. M. (2011). Antibiotic resistance in *Neisseria gonorrhoeae*: origin, evolution, and lessons learned for the future. *Annals of the New York Academy of Sciences*, *1230*(1), E19-E28.
- 126) Warner, D. M., Shafer, W. M., & Jerse, A. E. (2008). Clinically relevant mutations that cause derepression of the *Neisseria gonorrhoeae* MtrC-MtrD-MtrE efflux pump system confer different levels of antimicrobial resistance and in vivo fitness. *Molecular microbiology*, *70*(2), 462-478.127) Valenta, T.,

- Hausmann, G., & Basler, K. (2012). The many faces and functions of  $\beta$ -catenin. *The EMBO journal*, 31(12), 2714–2736. <https://doi.org/10.1038/emboj.2012.150>
- 128) Van Der Pol, L., Stork, M., & van der Ley, P. (2015). Outer membrane vesicles as platform vaccine technology. *Biotechnology journal*, 10(11), 1689-1706.
- 129) Van der Woude, M. W. (2011). Phase variation: how to create and coordinate population diversity. *Current opinion in microbiology*, 14(2), 205-211.
- 130) Van Putten, J. P., & Paul, S. M. (1995). Binding of syndecan-like cell surface proteoglycan receptors is required for *Neisseria gonorrhoeae* entry into human mucosal cells. *The EMBO journal*, 14(10), 2144-2154.
- 131) van Putten, J. P., Duensing, T. D., & Carlson, J. (1998). Gonococcal invasion of epithelial cells driven by P. IA, a bacterial ion channel with GTP binding properties. *The Journal of experimental medicine*, 188(5), 941-952.
- 132) Virji, M., Makepeace, K., Ferguson, D. J., & Watt, S. M. (1996). Carcinoembryonic antigens (CD66) on epithelial cells and neutrophils are receptors for Opa proteins of pathogenic neisseriae. *Molecular microbiology*, 22(5), 941-950.
- 133) Virji, M., & Heckels, J. E. (1988). Nonbactericidal antibodies against *Neisseria gonorrhoeae*: evaluation of their blocking effect on bactericidal antibodies directed against outer membrane antigens. *Microbiology*, 134(10), 2703-2711.
- 134) Virji, M., Zak, K., & Heckels, J. E. (1986). Monoclonal antibodies to gonococcal outer membrane protein IB: use in investigation of the potential protective effect of antibodies directed against conserved and type-specific epitopes. *Microbiology*, 132(6), 1621-1629.
- 135) Viviani, V., Fantoni, A., Tomei, S., Marchi, S., Luzzi, E., Bodini, M., ... & Bartolini, E. (2023). OpcA and PorB are novel bactericidal antigens of the 4CMenB vaccine in mice and humans. *npj Vaccines*, 8(1), 54.
- 136) von Boehmer, L., Liu, C., Ackerman, S., Gitlin, A. D., Wang, Q., Gazumyan, A., & Nussenzweig, M. C. (2016). Sequencing and cloning of antigen-specific antibodies from mouse memory B cells. *Nature protocols*, 11(10), 1908-1923.
- 137) Wang, J., Gray-Owen, S. D., Knorre, A., Meyer, T. F., & Dehio, C. (1998). Opa binding to cellular CD66 receptors mediates the transcellular traversal of *Neisseria gonorrhoeae* across polarized T84 epithelial cell monolayers. *Molecular microbiology*, 30(3), 657-671.
- 138) Werner, L. M., Alcott, A., Mohlin, F., Ray, J. C., Belcher Dufresne, M., Smirnov, A., ... & Criss, A. K. (2023). *Neisseria gonorrhoeae* co-opts C4b-binding protein to enhance complement-independent survival from neutrophils. *PLoS pathogens*, 19(3), e1011055.
- 139) Wi, T., Lahra, M. M., Ndowa, F., Bala, M., Dillon, J. A. R., Ramon-Pardo, P., ... & Unemo, M. (2017). Antimicrobial resistance in *Neisseria gonorrhoeae*: global surveillance and a call for international collaborative action. *PLoS medicine*, 14(7), e1002344.
- 140) Woods, J. P., Spinola, S. M., Strobel, S. M., & Cannon, J. G. (1989). Conserved lipoprotein H. 8 of pathogenic *Neisseria* consists entirely of pentapeptide repeats. *Molecular microbiology*, 3(1), 43-48.
- 141) Youssef, A. R., van der Flier, M., Estevao, S., Hartwig, N. G., van der Ley, P., & Virji, M. (2009). Opa+ and Opa- isolates of *Neisseria meningitidis* and *Neisseria gonorrhoeae* induce sustained proliferative responses in human CD4+ T cells. *Infection and immunity*, 77(11), 5170-5180.

- 142) Zaroff, S., & Tan, G. (2019). Hybridoma technology: the preferred method for monoclonal antibody generation for in vivo applications. *Biotechniques*, 67(3), 90-92.
- 143) Zeth, K., Kozjak-Pavlovic, V., Faulstich, M., Fraunholz, M., Hurwitz, R., Kepp, O., & Rudel, T. (2013). Structure and function of the PorB porin from disseminating *Neisseria gonorrhoeae*. *Biochemical Journal*, 449(3), 631-642.
- 144) Zhu, W., Tomberg, J., Knilans, K. J., Anderson, J. E., McKinnon, K. P., Sempowski, G. D., ... & Duncan, J. A. (2018). Properly folded and functional PorB from *Neisseria gonorrhoeae* inhibits dendritic cell stimulation of CD4+ T cell proliferation. *Journal of Biological Chemistry*, 293(28), 11218-11229.
- 145) Zhu, W., Thomas, C. E., Chen, C. J., Van Dam, C. N., Johnston, R. E., Davis, N. L., & Sparling, P. F. (2005). Comparison of immune responses to gonococcal PorB delivered as outer membrane vesicles, recombinant protein, or Venezuelan equine encephalitis virus replicon particles. *Infection and immunity*, 73(11), 7558-7568.